



Out of Amazonia again and again: episodic crossing of the Andes promotes diversification in a lowland forest flycatcher

Matthew J. Miller^{1,2,*}, Eldredge Bermingham¹, John Klicka³,
Patricia Escalante⁴, Fabio S. Raposo do Amaral⁵, Jason T. Weir⁶
and Kevin Winker²

¹University of Alaska Museum, 907 Yukon Drive, Fairbanks, AK 99775, USA

²Smithsonian Tropical Research Institute, Apartado 0843-03092, Balboa, Panama

³Barrick Museum of Natural History, Box 454012, University of Nevada Las Vegas, 4504 Maryland Parkway, Las Vegas, NV 89154-4012, USA

⁴Instituto de Biología, Universidad Nacional Autónoma de México, AP 70-153, 04511 México DF, México

⁵Departamento de Genética e Biologia Evolutiva, Universidade de São Paulo, Rua do Matão, 277, Cidade Universitária, São Paulo, CEP 05508-900, Brazil

⁶Center for Biodiversity Research, University of British Columbia, Vancouver, BC, Canada V6T 1Z4

Most Neotropical lowland forest taxa occur exclusively on one side of the Andes despite the availability of appropriate habitat on both sides. Almost all molecular phylogenies and phylogenetic analyses of species assemblages (i.e. area cladograms) have supported the hypothesis that Andean uplift during the Late Pliocene created a vicariant barrier affecting lowland lineages in the region. However, a few widespread plant and animal species occurring in lowland forests on both sides of the Andes challenge the generality of this hypothesis. To understand the role of the Andes in the history of such organisms, we reconstructed the phylogeographic history of a widespread Neotropical flycatcher (*Mionectes oleagineus*) in the context of the other four species in the genus. A molecular phylogeny based on nuclear and mitochondrial sequences unambiguously showed an early basal split between montane and lowland *Mionectes*. The phylogeographic reconstruction of lowland taxa revealed a complex history, with multiple cases in which geographically proximate populations do not represent sister lineages. Specifically, three populations of *M. oleagineus* west of the Andes do not comprise a monophyletic clade; instead, each represents an independent lineage with origins east of the Andes. Divergence time estimates suggest that at least two cross-Andean dispersal events post-date Andean uplift.

Keywords: Andes; dispersal; area cladograms; ancestral area reconstruction; Neotropical phylogeography

1. INTRODUCTION

The high passes and montane habitats of the Andean cordilleras present a formidable ecological interruption of the Amazonian lowland moist tropical forests and similar habitats found in northwestern South America and most of Middle America. Thus, it is not surprising that when lowland organisms from this region have been analysed in a phylogenetic framework, most researchers have found a basal split between the lowlands east and west of the Andes (arachnids: Zeh *et al.* 2003; birds: Cracraft & Prum 1988, Brumfield & Capparella 1996, Eberhard & Bermingham 2004, 2005, Cheviron *et al.* 2005; primates: Cortes-Ortiz *et al.* 2003; reptiles: Zamudio & Greene 1997; trees: Dick *et al.* 2003). Likewise, when geographical relationships among entire faunal assemblages have been evaluated either phenetically (da Silva & Oren 1996; Bates *et al.* 1998) or cladistically (Prum 1988; Ron 2000),

similar results were obtained. One obvious explanation for these results is that for many widespread species the final uplift of the northern Andes in the Late Pliocene (ca 2.7 Myr ago; Gregory-Wodzicki 2000) split the distributions of organisms found in the lowland forests of the region, an hypothesis advanced nearly a century ago by Chapman (1917). Even in birds, which must be among the most vagile of lowland Neotropical organisms, distributional patterns suggest that the rise of the Andes restricted gene flow and dispersal: of the approximately 3800 bird species found in the Neotropics, only 178 (less than 5%) are encountered in lowland forests both east and west of the Andes (Haffer 1967).

Several observations point to the role that the Andes may play in limiting dispersal of lowland forest birds over or around them. First, even the lowest passes in the northern Andes reach nearly 2000 m higher in elevation than the surrounding lowland forests (Haffer 1967). At these elevations, Andean montane habitats present novel physiological (Janzen 1967) and competitive (Terborgh & Weske 1975) challenges to birds typically found in lowland

* Author for correspondence (millerma@si.edu).

Electronic supplementary material is available at <http://dx.doi.org/10.1098/rspb.2008.0015> or via <http://journals.royalsociety.org>.

forest habitats (Terborgh 1971). Second, the northern extent of the forests of the northwestern Amazon Basin is bordered by the large *llanos* savannah, which itself is bounded by the eastern Andean cordillera, extending northeastward into the Caribbean ocean and terminating with the island of Trinidad. Under current climatic conditions, the shortest low-elevation route around the Andes is interrupted by extensive stretches of ocean, *llanos*, and arid scrublands in the Caribbean lowlands north and east of the Andes (Eva *et al.* 2002).

Thus, for species with populations occurring in lowland forests on both sides of the Andes, three possibilities exist: (i) populations have been isolated too recently for speciation to occur, (ii) gene flow across presumably significant barriers occurs with sufficient regularity to inhibit speciation, or (iii) phenotypic evolution is sufficiently conservative that we fail to recognize species-level differences. We investigated these hypotheses by reconstructing the evolutionary history of *Mionectes oleagineus* (ochre-bellied Flycatcher), which is widespread in lowland forests both east and west of the Andes. Furthermore, we placed our phylogeographic analysis of *M. oleagineus* within the phylogenetic context of the remaining species in the genus. *Mionectes* consists of a pair of montane flycatchers found in the Andes and southern Middle America and three lowland species, including our focal species. *M. oleagineus* is found exclusively in the understorey of lowland tropical forests and woodlands and is replaced by congeners at higher elevations, suggesting that dispersal across the Andes should be unlikely in this species. Furthermore, because morphological evolution is very conservative among *Mionectes* species (Capparella & Lanyon 1985), it is possible that cross-Andean populations have been isolated since before Andean uplift yet remain sufficiently similar phenotypically to be classified as conspecific.

2. MATERIAL AND METHODS

The genus *Mionectes* consists of five species of drab, principally frugivorous flycatchers found in the understorey of most Neotropical forests. Two species are found in montane forests: *Mionectes olivaceus* inhabits premontane and lower montane forests in the Andes and southern Middle America (north to Costa Rica); in higher elevations in the Andes, this species is replaced by *Mionectes striaticollis*. There are three lowland species in the genus. The most widespread, *M. oleagineus*, ranges throughout tropical Middle America, Amazonia, and the lowland forests of the Guiana Shield and also includes two disjunct populations in the western Ecuador and the Atlantic Forest of Brazil (figure 1b). In the field, it is often difficult to separate *M. oleagineus* from the two other lowland *Mionectes* species (*Mionectes macconnelli* and *Mionectes rufiventris*), both of which are partially sympatric with *M. oleagineus*. *M. macconnelli* has a disjunct distribution in southwestern Amazonia and the Guiana Shield (figure 1b). In both regions, it is almost entirely sympatric with *M. oleagineus*. *M. rufiventris* is restricted to forest and woodland habitats in coastal southeastern South America, where it narrowly overlaps with *M. oleagineus* (figure 1b).

(a) Phylogenetic tree reconstruction

We generated three different molecular datasets to establish phylogenetic relationships among *Mionectes* species and

populations. Because earlier classifications (e.g. Todd 1921; Meyer de Schauensee 1970) placed lowland *Mionectes* in their own genus (*Pipromorpha*), we wanted to confirm the sister relationship between montane and lowland *Mionectes* and to place a root for the latter. To do this, we generated a dataset using a portion of the cytochrome *b* mitochondrial gene (999 basepairs (bp)) and fragments of two nuclear single-copy protein-coding genes: *RAG-1* (930 bp) and *c-myc* (477 bp). We sequenced a single individual of both montane and all three lowland *Mionectes* species; for out-groups, we used several taxa available from GenBank (Johansson *et al.* 2002). We generated phylogenetic trees from this dataset using two methods: Bayesian inference (implemented in MrBAYES v. 3.1.2; Ronquist & Huelsenbeck 2003) and branch-and-bound maximum-likelihood phylogeny (implemented in PAUP* v. 4.0b10; Swofford 2002). To further resolve phylogenetic and phylogeographic variation within lowland *Mionectes*, we obtained the entire mitochondrial *ND2* gene for 153 additional lowland *Mionectes* and 5 additional montane *Mionectes* from widespread geographical origins within their respective ranges, focusing on the widespread *M. oleagineus* (see table 1 in the electronic supplementary material for details about locality and other voucher specimen data). Similar to the first dataset, we generated a Bayesian inference phylogeny using MrBAYES for this second dataset. Although this analysis showed strong support for *M. oleagineus* nodes near the tips of the phylogeny, some interior nodes were not strongly supported. To test the validity of these nodes, we selected one individual from each major lowland *Mionectes* clade recovered in the second phylogenetic tree ($n=14$) as well as one each of the two montane species and sequenced the entire cytochrome *b* mitochondrial gene to create a new mtDNA dataset that combined this gene with the *ND2* sequence from the previous analysis. For the clade comprising individuals from eastern Panama and northern South America, we included one individual from each side of the Andes. We generated a Bayesian inference phylogeny using MrBAYES from this new dataset as well. Details of laboratory sequencing techniques and phylogenetic tree reconstruction can be found in the electronic supplementary material.

(b) Ancestral area analysis and molecular clock techniques

Using the consensus phylogram from the combined *ND2* and *cyt b* dataset, we reconstructed the ancestral areas of lowland *Mionectes* using maximum parsimony and maximum-likelihood ancestral state simulations in MESQUITE v. 1.06 (Maddison & Maddison 2005) with the default maximum-likelihood model for character-state reconstruction. Terminal taxa were coded as either west or east of the Andes. A likelihood ratio test failed to reject the assumption of a molecular clock ($-2\Delta \ln L = 9.37$, d.f. = 12, $p = 0.67$), so we modified the consensus topology to conform to a molecular clock as implemented in PAUP*.

Because the widely used $2\% \text{ Myr}^{-1}$ mtDNA molecular clock rate calibration has not been critically examined in suboscines, following Ribas *et al.* (2007) we calibrated a relaxed molecular clock (non-parametric rate smoothing, NPPS; Sanderson 1997) topology for a dataset consisting of the *Mionectes RAG-1* sequences and a variety of *RAG-1* sequences obtained from GenBank. This provided an independent estimate for the age of the split between montane and lowland *Mionectes* and thus an alternative calibration for the clock-enforced *cyt b/ND2* tree. Uncertainty in this

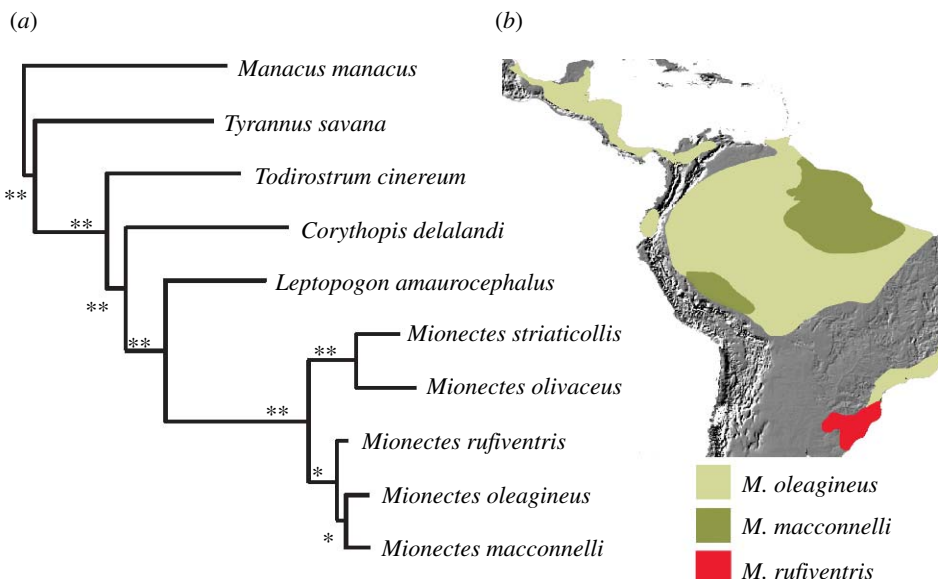


Figure 1. (a) Relationship of *Mionectes* and related genera determined by Bayesian inference using partial sequences of the mtDNA cytochrome *b* gene (999 bp) and the nuclear exons *RAG-1* (930 bp) and *c-myc* (477 bp). The monophyly of *Mionectes* and a basal split between montane and lowland clades are strongly supported. (b) Distribution map for the three lowland *Mionectes* species; two additional species, *M. olivaceus* and *M. striaticollis*, are found in montane habitats in the Andes and southern Middle America and are not depicted. Posterior probabilities: double asterisk, 100%; single asterisk 95%.

alternative calibration was evaluated by bootstrapping the expanded *RAG-1* data matrix. The NPPS molecular dating analysis is described in further detail in the electronic supplementary material.

(c) Cross-Andes gene flow

The lack of reciprocal monophyly found between *M. oleagineus* populations in eastern Panama and northern South America, which are bisected by the Andes (figures 2 and 4), can be due to incomplete lineage sorting or to continued gene flow. To estimate the extent of post-separation gene flow between populations, we fitted a population genetic model of divergence with gene flow using Metropolis-coupled Markov Chain Monte Carlo simulations of the coalescent in IM (Hey & Nielsen 2004). This analysis determined whether the more complex model including post-separation gene flow was a better fit to the data than a model without gene flow, as evaluated by a likelihood ratio test (per Vollmer & Palumbi 2002). Several trial runs assuming unrealistic priors helped determine the range of priors for final runs. Final run conditions included an HKY model of molecular evolution, Metropolis coupling involving geometric heating along 10 chains with 10 chain-swap attempts per step, a burn-in of 500 000 steps, and symmetric gene flow between the two populations, because initial runs showed broad overlap between the 95% highest posterior densities (HPDs) for directional migration estimates. We ran the program four times with unique starting seeds to ensure proper convergence of parameter estimates; all runs lasted over 30×10^6 steps, which ensured that lowest effective sample sizes for all parameter estimates were at least an order of magnitude larger than the value (500) suggested by the authors (Hey & Nielsen 2004). We obtained estimates for θ_E and θ_W , which are equal to two times the effective size of females scaled to the mutation rate (e.g. $2N_{\text{eff}}\mu$) for the populations east and west of the Andes, respectively, and m_E and m_W , which represent the migration rate per generation

into the respective population. Following Peters *et al.* (2005), we calculated the number of females moving across the Andes per generation as: $N_f = (\theta_E + \theta_W) \times (m_E + m_W)/2$. Because the results from all four runs were similar, we present parameter estimates obtained from the longest run. To visualize relationships among this clade of birds that span the Andes (the YELLOW clade using the nomenclature presented in the figures), we used a haplotype network obtained by statistical parsimony using TCS v. 1.21 (Clement *et al.* 2000). The resulting network was redrawn by hand.

3. RESULTS

Our multi-locus phylogeny recovered all five *Mionectes* species as a monophyletic clade with 100% posterior probability (figure 1a). The branch-and-bound ML search recovered an identical topology (not shown) with 100% bootstrap support for a monophyletic *Mionectes*, as did an unpartitioned MRBAYES search (not shown). Among the species sampled, *Leptopogon* and *Corythopis* were the closest out-groups for *Mionectes*. However, these taxa are only distantly related to *Mionectes*: average *cyt b* pairwise model-corrected distance between these two genera and *Mionectes* was 35.9%. Adopting the commonly used avian mitochondrial clock of 2% sequence divergence Myr⁻¹ or related approximations thereof (Fleischer *et al.* 1998; Weir & Schlüter 2004) places the origin of *Mionectes* in the Mid-Miocene. Within *Mionectes*, two clades were recovered with 100% posterior probability (100% ML bootstrap), corresponding to the lowland and montane *Mionectes* clades, respectively (figure 1a). This split is old: average model-corrected *cyt b* distance between the montane and lowland *Mionectes* clades was 14.3%, dating to ca 7 Myr ago.

In the montane species *M. olivaceus*, ND2 sequences revealed two phylogroups in Panama corresponding to an eastern-central clade (including the Darién highlands) and a western clade (Talamanca highlands). The average

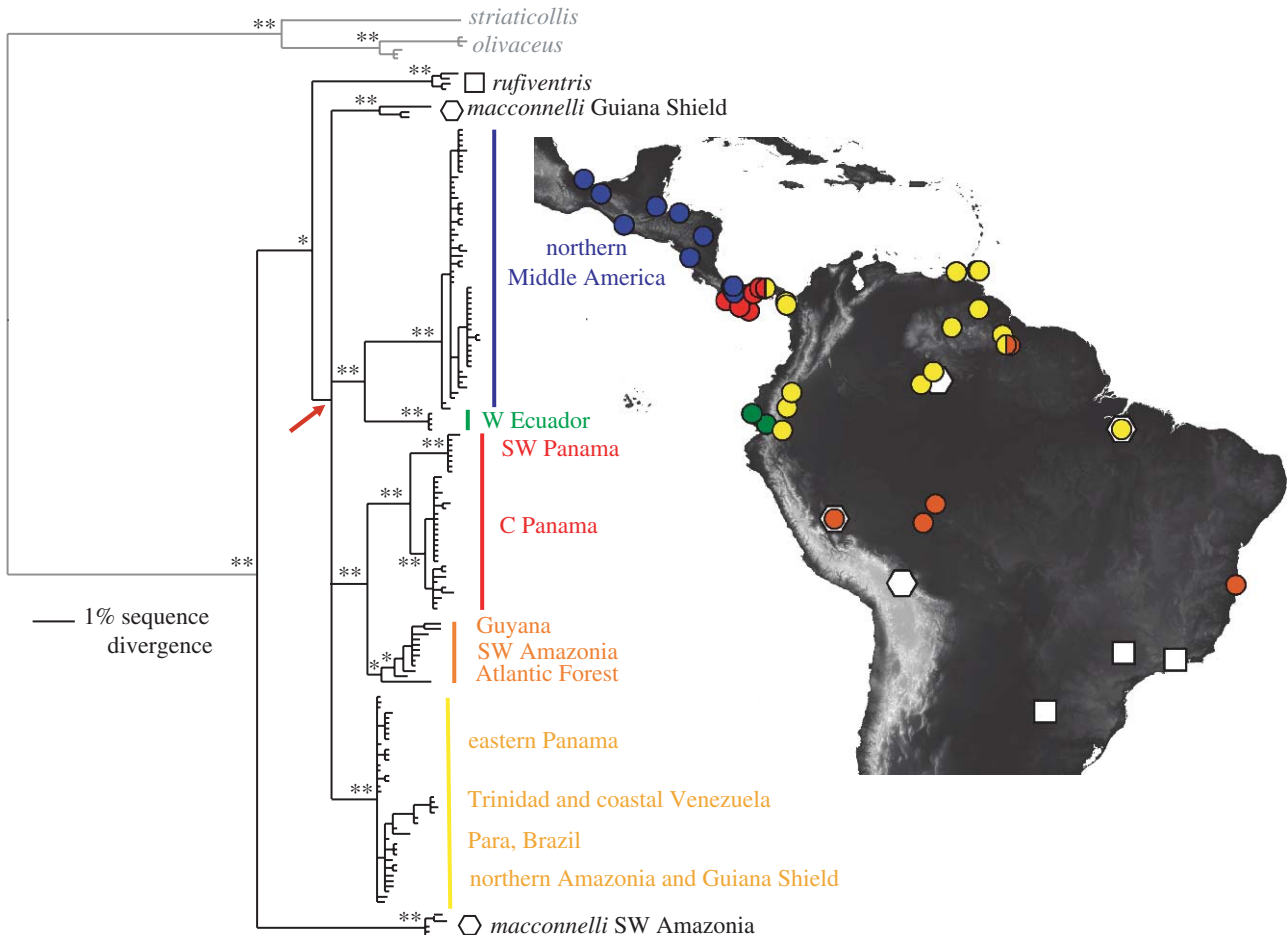


Figure 2. Majority-rule consensus Bayesian inference topology for 163 individuals of *Mionectes* flycatchers (156 lowland and 7 highland birds) based on complete *ND2* sequences. Posterior probabilities for bifurcations indicated at node: double asterisk, 100%; single asterisk, greater than 95% (omitted from the most terminal nodes for clarity). Internal nodes with less than 95% posterior probabilities were collapsed, but terminal nodes with less than 95% pp support were retained. The red arrow shows an unresolved polytomy (see text). The map shows localities for 156 lowland *Mionectes* colour coded to correspond to the major clades at left. Two sites (central Panama and Guyana) are bicoloured to indicate two mtDNA clades at these locations. Circles are *M. oleagineus*, white hexagons *M. macconnelli*, and white squares *M. rufiventris*. Four *M. oleagineus* clades occur west of the Andes: the BLUE clade (northern Middle America), the GREEN clade (western Ecuador), the RED clade (central and southwestern Panama), and the YELLOW clade (eastern Panama). The YELLOW clade also occurs east of the Andes across northern South America. The ORANGE clade occurs exclusively east of the Andes (figure 4).

model-corrected distance between these two clades was 2.0%. Owing to a lack of widespread geographical sampling in *M. striaticollis*, we have no phylogeographic results for this montane species.

Our broad geographical sampling of *ND2* sequences from birds collected throughout the range of the three lowland *Mionectes* species identified a series of strongly supported clades (figure 2) with posterior probability nodal support greater than 95% (figure 2). *Mionectes rufiventris* was represented by a single mtDNA haplotype clade, whereas the other two, more widespread, lowland taxa showed phylogeographic complexity. *Mionectes macconnelli* was represented by two clades, corresponding to geographically disjunct populations in southwestern Amazonia and the Guiana Shield. Within *M. oleagineus*, we recovered five clades: three exclusively west of the Andes (BLUE, RED, and GREEN clades; figure 2), one found east and west of the Andes (YELLOW; figure 2), and one exclusively east of the Andes (ORANGE; figure 2). For heuristic purposes, we refer to each clade by its colour in figure 2, because mtDNA clades do not

correlate well with currently recognized subspecific limits (see below). West of the Andes, the BLUE clade ranged from southeastern Mexico to the northwestern corner of Panama. The RED clade occupied points throughout central Panama, and the GREEN clade was found in the Pacific lowlands of western Ecuador. West of the Andes, the YELLOW clade was found only in eastern Panama, whereas east of the Andes it had a broad distribution north of the Amazon River (Ecuador, Venezuela, Guyana, Trinidad, and northern Brazil). The ORANGE clade was the only *M. oleagineus* clade found exclusively east of the Andes, where it was widespread: southwestern Amazonia, Guyana, and the Atlantic Forest of southeastern Brazil.

For *M. oleagineus*, the current subspecies do not correlate well with the recovered mtDNA clades. Based on a recent revision of *oleagineus* subspecies (Fitzpatrick 2004), our clades represent the following subspecies: BLUE: *assimilis*; RED: *parcus*; YELLOW: *parcus*, *abdominalis*, *pallidiventris* and *oleagineus*; GREEN: *pacificus*, and ORANGE: *oleagineus*. Furthermore, in two instances,

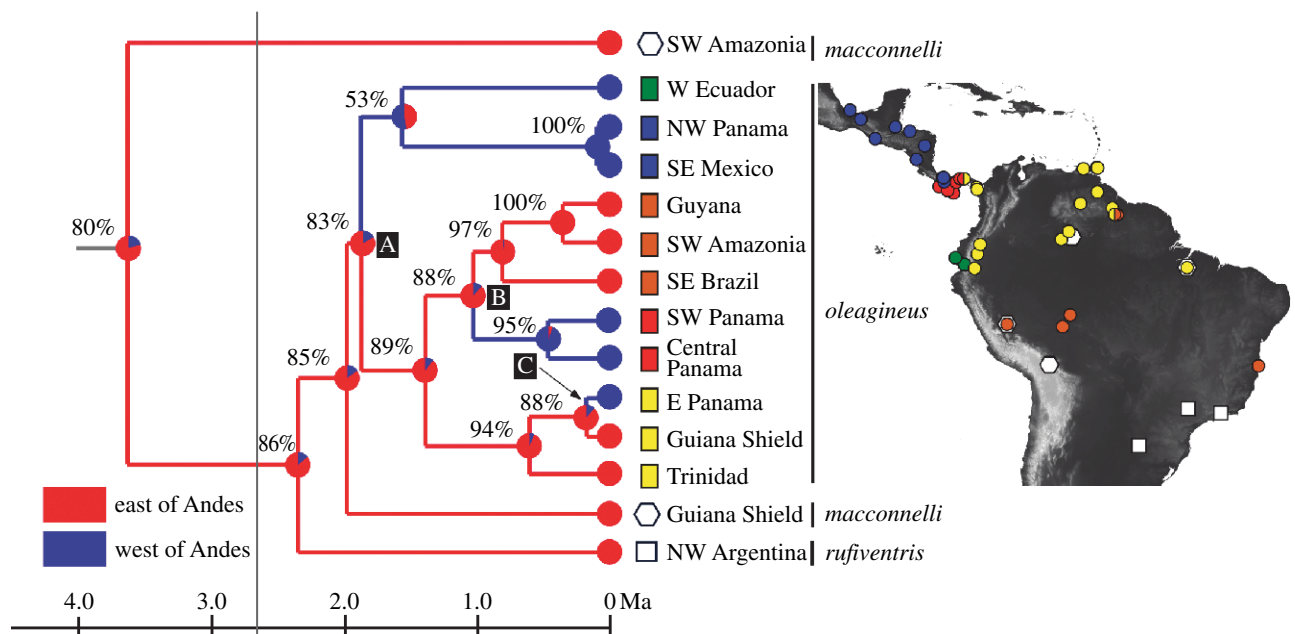


Figure 3. Ancestral area reconstruction for lowland *Mionectes* flycatchers. The phylogenetic tree represents the consensus Bayesian inference topology obtained from cytochrome *b* and *ND2* sequences (2184 bp) modified to conform to an enforced molecular clock (see text). Posterior probabilities of all nodes were 100% except node A (98%). Branch colour reflects the most parsimonious state (east or west of the Andes) for that branch, while coloured circles at nodes represent relative likelihoods of each state. For *M. oleagineus*, colour coding follows figure 2 (see also inset map). Both parsimony and likelihood reconstructions indicate three cross-Andean biogeographic events at nodes A, B, and C. Scale bar represents millions of years BP assuming a rate of mtDNA diversification of 2.0% Myr⁻¹ (Fleischer et al. 1998). The vertical grey line at 2.7 Myr BP indicates completion of uplift in the northern Andes (Gregory-Wodzicki 2000).

sampling locations included individuals from more than a single clade. In Panama province (central Panama), we recovered five RED haplotypes and one YELLOW haplotype, while in Iwokrama Reserve (Guyana), we recovered three ORANGE haplotypes and one YELLOW haplotype (figure 2). This broad sampling of *ND2* sequences from *M. oleagineus* did not resolve sister relationships among clades in every instance (figure 2).

The addition of *cyt b* sequences to a subsample of birds provided a phylogeny with greatly improved nodal support throughout the tree (figure 3), with all bifurcations supported by at least 95% posterior probabilities. Based on this phylogeny, geographically proximate clades were not one another's closest phylogenetic neighbour, and several sister relationships among clades were bisected by the Andes. All of the lineages west of the Andes had a sister lineage found to the east. Both maximum-likelihood and maximum-parsimony analyses indicated that the ancestral area for lowland *Mionectes* taxa was east of the Andes, requiring a minimum of three cross-Andean biogeographic events. In the clock-enforced maximum-likelihood tree, the earliest divergence across the Andes occurred at node A (figure 3), roughly 1.9 Myr ago assuming a 2% pairwise divergence rate (Fleischer et al. 1998; Weir & Schlüter 2004). The other two nodes corresponding to cross-Andean events date to 1.0 and 0.2 Myr ago, respectively. For either of these latter events to be coincident with the final uplift of the Andes, the single lineage rate of mtDNA evolution in *Mionectes* for node B (the second crossing of the Andes) would have to be less than 0.38% Myr⁻¹, and for node C (the third crossing) slower than 0.06% Myr⁻¹. The former is slower than any reported rate for birds and less than half of the typical result for passerines such as *Mionectes* (Lovette

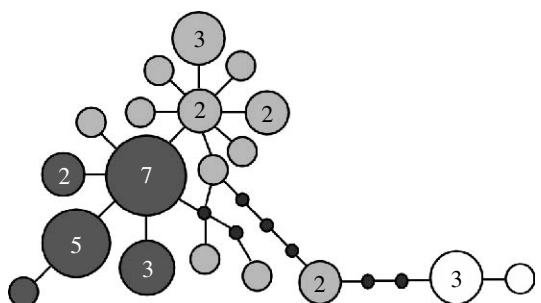


Figure 4. Statistical parsimony-based haplotype network for the YELLOW clade (see figure 2) of *M. oleagineus* showing incomplete lineage sorting between populations east and west of the Andes. Dark grey, eastern Panama; light grey, Amazon Basin and Guiana Shield; white, coastal South America. Black dots (smallest circles) indicate unobserved haplotypes; larger circle sizes indicate haplotype frequencies. Birds from eastern Panama (west of the Andes) are more closely related to birds from the Amazon Basin and the Guiana Shield than from coastal South America, which provides some evidence for dispersal over rather than around the Andes.

2004), while the latter is nearly an order of magnitude slower than the reported rate of mtDNA evolution for any vertebrate. Dates for these nodes obtained using NPPS and a *RAG-1* calibration (see §2 and the electronic supplementary material) were similar (node A, 1.5 ± 0.4 Myr ago; node B, 0.8 ± 0.2 Myr ago and node C 0.5 ± 0.1 Myr ago) and give support to the 2% Myr⁻¹ mtDNA calibration henceforth used in this paper.

Individuals from the YELLOW clade were found on both sides of the Andes and were not reciprocally monophyletic with respect to the mountains (figure 4). Parameter estimates for θ east and west of the Andes and the average migration rate since separation of the eastern

Panama and northern South American populations (i.e. θ_E , θ_W and m) were highly unimodal and similar in all four runs. Posterior distributions peaked at 2.0 (95% HPD: 0.5–6.6) for θ_E and 50.2 (95% HPD: 16.4–265.2) for θ_W , whereas the posterior distribution of estimates of the scaled migration parameter (m) peaked at 0.5 (95% HPD: 0.1–1.7). These parameters yielded a peak value of 6.2 females per generation (N_f) migrating across the Andes, with a range of 0.3–115.3 assuming extreme 95% HPD values. Our model, which included cross-Andean migration, was a significantly better fit to the data than a model without post-divergence gene flow across the Andes ($-2\Delta \ln L = 8.65$, d.f. = 1, $p = 0.003$).

4. DISCUSSION

Evidence from nuclear and mitochondrial DNA supported the monophyly of the five flycatcher species currently placed in the genus *Mionectes* relative to allied genera (figure 1a), consistent with recent classifications (Sibley & Monroe 1990; American Ornithologists' Union 1998; Fitzpatrick 2004; Remsen *et al.* 2007). Genetic distances between these taxa and putative out-groups are considerable, again in agreement with earlier studies of genetic relationships among *Mionectes* and its allies (Sibley & Monroe 1990; Bates & Zink 1994; Chesser 2004). Within the genus, both mitochondrial and nuclear gene sequences identified a basal phylogenetic split between montane and lowland *Mionectes* species, providing support for earlier classifications that placed the three lowland species in the genus *Pipromorpha* (e.g. Traylor 1977). The model-corrected *cyt b* mtDNA distance between montane *Mionectes* and lowland *Mionectes* was 14.3%, dating the split between these forms to the Late Miocene, or *ca* 7 Myr ago.

The montane *Mionectes* group consists of two species that inhabit higher-elevation habitats in South America and southern Middle America: *M. olivaceus* can be found in premontane and montane forests, and in the Andes it is replaced at even higher elevations by *M. striaticollis*. Our evidence indicates that the two montane species last shared a common ancestor in the Late Miocene or Early Pliocene.

Despite only modest geographical sampling of montane *Mionectes* (table 1 found in electronic supplementary material), some comparisons to phylogeographic patterns in other Neotropical montane bird taxa are possible. The model-corrected *ND2* distance between the Darien (eastern Panama) and Talamanca (western Panama) clades of *M. olivaceus* was 2.0%. Across this same geographical span, *Myadestes* solitaires showed identical mtDNA divergence (Miller *et al.* 2007). If we assume a constant rate of mtDNA divergence of *ca* 2.0% Myr⁻¹, then both montane *Mionectes* and *Myadestes* in southern Middle America began to differentiate across the Isthmus of Panama *ca* 1.0 Myr ago, well after its Pliocene formation. However, in the *Chlorospingus* bush-tanagers species complex, average pairwise distance between Darien and Talamanca mtDNA clades was nearly three times that of montane *Mionectes* and *Myadestes* (approx. 5–6%; Weir *et al.* *in press*). These comparisons identify central Panama as an important barrier to gene flow of montane Neotropical birds but also suggest that avian lineages have responded differently to regional changes in

the Pliocene and Pleistocene landscapes of lower Middle America as the Isthmus of Panama developed (see also Bermingham & Martin 1998).

The lowland and montane *Mionectes* clades are elevational replacements, and where they meet the zones of overlap are narrow. It is worth noting that despite roughly 7 Myr of independent evolution, the montane clade has not diversified to exploit lowland habitats, nor has the lowland clade diversified to exploit montane habitats. We posit that this long history of habitat segregation between montane and lowland *Mionectes* probably arises from ecological interactions between individuals of the two clades. Our hypothesis is supported by the observation that in the Pacific lowlands of Colombia and Ecuador, where lowland *M. oleagineus* is absent, *M. olivaceus*, one of the montane species, ranges down to sea level. Likewise, in areas such as Bolivia and southern Venezuela, where montane *Mionectes* are absent, lowland *M. macconnelli* populations reach elevations above 2000 m (Ridgely & Tudor 1994).

Lowland *Mionectes* are currently classified as three species. However, our mtDNA phylogeny suggests that evolutionary relationships among populations of these three species are more complex than predicted by current taxonomy (figure 3). *Mionectes macconnelli*, which has a disjunct distribution in southwestern Amazonia and the Guiana Shield (figure 1b), is polyphyletic: specimens from southern Amazonia form a clade that is sister to all other lowland *Mionectes*, including *M. macconnelli* specimens from the Guiana Shield and the Atlantic Forest endemic, *M. rufiventris* (figure 3). Also, *M. oleagineus* was recovered as a monophyletic clade with pronounced phylogeographic structure among mtDNA haplotypes (figure 3).

The geographical pattern of diversification in lowland *Mionectes* differs from previously published area cladograms for the region and other studies of the diversification of widespread Neotropical organisms (references given in §1). Most strikingly, the overwhelming majority of these studies found a basal split across the Andes, whereas lowland *Mionectes* show three cross-Andean divergences near the tips of the phylogeny. When only areas east of the Andes are considered, most studies have found that the deepest divergences split the Atlantic Forest from the Amazon Basin and the Guiana Shield (e.g. Ron 2000). In contrast, the basal split among lowland *Mionectes* separates the southern Amazonian *M. macconnelli* from the rest of the region including the Atlantic Forest (figure 3), a pattern most similar to that observed for howler monkeys (*Alouatta* spp.; Cortes-Ortiz *et al.* 2003). Finally, nearly all previous studies have shown a sister relationship between northern and southern clades in western Amazonia (e.g. Cracraft & Prum 1988; Ron 2000). This was not the case in lowland *Mionectes* for either *M. macconnelli* or *M. oleagineus* (figure 3).

The *Mionectes* mtDNA phylogeny (figure 3) provides strong inference that *M. oleagineus* has diversified across the Andes at least three times over the course of its evolutionary history. The earliest separation of *M. oleagineus* populations on either side of the Andes (node A, figure 3) might represent vicariance associated with the final uplift of the northern Andes. Assuming typical rates of passerine mtDNA evolution, these populations split *ca* 1.9 Myr ago, about the same time the northern Andes reached their current elevation (Gregory-Wodzicki 2000). The

other two splits within *M. oleagineus* occurred at more recent nodes on the clock-enforced phylogram (nodes B and C, figure 3). Forcing the date of the splits represented by nodes B and C to be coincident with the northern Andean uplift would imply unreasonably slow rates of mtDNA evolution (see §3). Thus, the two later splits between *M. oleagineus* populations on either side of the Andes must necessarily represent dispersal over or around the mountains.

Haffer (1967) proposed two alternative mechanisms for gene flow across the Andes following their final uplift. The first was via dispersal over low passes in the northern Andes (first suggested by Chapman 1917), and the second was through ephemeral forest corridors during Quaternary interglacials along the northern coast of South America. These hypothetical forest corridors passed through regions currently characterized by grassland and savannah ecosystems and might have facilitated the dispersal of forest-dwelling organisms between lowland populations east and west of the Andes. Although our mtDNA phylogenies cannot rule out either scenario, several observations suggest dispersal over Andean passes rather than around the northern cordilleras for the splits represented by nodes B and C (figure 3).

As noted, the upper elevational limit for lowland *Mionectes* in the Andes may be due to competition with montane *Mionectes* rather than to physiological limits. Where highland congeners are absent, lowland *M. oleagineus* reach over 2000 m elevation, which is nearly the elevation of the lowest Andean passes. In the split at node B (figure 3), ancestral area analysis suggests that birds from southwestern Amazonia or the Guiana Shield colonized lowlands west of the Andes (figure 3). One possible route for this colonization is through the Marañon Valley in northern Peru, which is the lowest Andean pass between Venezuela and Bolivia (2140 m), and which was previously suggested as a dispersal corridor for many Amazonian taxa into a semi-humid area of endemism west of the Andes in northern Peru (Chapman 1917). While this would be the most direct route between southwestern Amazonia and the lowlands west of the Andes, this hypothesis requires the RED clade to have moved through regions along the Pacific slope of South America that are currently occupied by representatives of the GREEN clade (figure 2). In the most recent split (node C, figure 3), it is more difficult to determine whether *M. oleagineus* dispersed around or over the Andes. Tissues from northern Colombia and northwestern Venezuela were unavailable for this study, but the subspecies there is *Mionectes oleagineus parcus*, the same that occurs in eastern Panama (Fitzpatrick 2004). This alone provides little evidence to discern between the two routes, because the ranges of many bird species extend from Panama into this region without occurring in the Amazon Basin (Chapman 1917). Furthermore, individuals from northwestern Amazonia are genetically more similar to birds from eastern Panama than to those from the coast of north-central Venezuela and Trinidad (figure 4). Finally, the shortest dispersal route between northwestern Amazonia and eastern Panama is the Andalucia Pass into central Colombia (Chapman 1917), providing additional evidence that the most recent dispersal event also occurred over rather than around the Andes.

However, several observations suggest that dispersal around the Andes is a reasonable alternative. Under current climatic conditions, the shortest low-elevation route around the Andes is interrupted by extensive stretches of ocean, *llanos*, and arid scrublands in the Caribbean lowlands north and east of the Andes (Eva *et al.* 2002). But habitats during the Pleistocene in northern South America probably differed from current conditions. Conditions in the South American lowlands east of the Andes during the Pleistocene were generally cooler (Colinvaux *et al.* 2000) and wetter (Baker *et al.* 2001) than at present. Pollen records from the Colombian *llanos* suggest that savannah persisted as far back as the last glacial maximum (LGM), but no earlier data exist (Behling & Hooghiemstra 1999). However, pollen evidence from the Gran Sabana, a grassland east of the Colombian *llanos*, indicates that trees typical of contemporary premontane cloud forests were replaced by expanding savannah coincident with the onset of the Holocene (Rull 2007). If mesic forest occurred in currently arid areas, dispersal around the tip of the northern Andes would be facilitated by relatively low passes in the northern cordillera.

Our coalescent simulations indicate that gene flow between the most recently separated populations of *M. oleagineus* in eastern Panama and northern South America may be ongoing or episodic. Estimates indicate that the rate of female dispersal across the Andes between these populations is at least 0.3 individuals per generation (95% HPD: 0.3–115 females per generation). Furthermore, a coalescent model including post-dispersal gene flow across the Andes was a significantly better fit to the data than a model without migration. Because no lowland forest corridor currently connects Amazonia and Middle America, the coalescent simulations argue for some gene flow across the Andes.

How common is cross-Andean dispersal? Several studies of lowland birds have provided phylogenetic hypotheses discounting its importance (Cracraft & Prum 1988; Prum 1988; Brumfield & Capparella 1996; Bates *et al.* 1998; Ron 2000; Brumfield *et al.* 2001). An exception occurs in the lowland forest woodcreeper *Glyptorhynchus spirurus*, in which Middle American populations nest phylogeographically within a northern Amazonian clade, perhaps due to Quaternary dispersal around the Andes (Marks *et al.* 2002). Two studies of bats have also shown lack of reciprocal monophyly in DNA lineages on either side of the Andes, which the authors attributed to post-uplift gene flow across the Andes (Ditchfield 2000; Hoffman & Baker 2003). Finally, Dick *et al.* (2004) reported phylogenetic evidence of recent cross-Andean dispersal in two groups of euglossine bees. In sum, these studies indicate that cross-Andean movement by lowland species may be more frequent than previously assumed. However, *M. oleagineus* stands out in the repeated role that the Andes have played in its phylogeographic differentiation.

The evolutionary history of *M. oleagineus* is also striking in the geographical pattern of populations west of the Andes. Descendants of the first cross-Andean split (figures 2 and 3; the BLUE and GREEN clades) show the broadest distribution, extending from southeastern Mexico to western Panama and western Ecuador. The

second cross-Andean split, which must be a dispersal event, is evident in a population that is currently found only in central and parts of western Panama (the RED clade), where it abuts the range of the BLUE clade (**figure 2**). Whether the RED clade has displaced the BLUE clade or has simply colonized a region unoccupied by BLUE clade conspecifics cannot be discerned from our data. One presumes that the ancestor of the BLUE and GREEN clades was once continuously distributed in the lowlands west of the Andes, but the level of phylogeographic divergence between the western Ecuador (GREEN) and northern Middle America (BLUE) haplotypes suggests their separation, and perhaps local extinction on the Isthmus of Panama might have predated colonization by the RED clade. The most recent colonization episode by *M. oleagineus* west of the Andes ushered in the YELLOW mtDNA clade, which has the narrowest trans-Andean distribution of the three western clades, being restricted to eastern Panama (and probably part of northern Colombia).

In both eastern and western Panama, our data suggest relatively narrow zones of transition between mtDNA lineages. Approximately 125 km separate our eight specimens (100% RED haplotypes) from Santa Fe, Veraguas and our 22 specimens (100% BLUE haplotypes) from Bocas del Toro. Likewise, less than 250 km separate our sampling sites from eastern Darien province (18 individuals, 100% YELLOW haplotypes) and our easternmost site in central Panama (five of six specimens had RED haplotypes). We found no evidence of mixing of BLUE and RED mtDNA haplotypes, despite the fact that the numbers of *M. oleagineus* collected near the zone of contact (22 and 11 individuals, respectively) between the two mtDNA haplotype clades was sufficient to provide an 82% probability of observing mixing occurring at a frequency of 5% or greater ($p=1-[0.05^{(22+11)}]=0.82$). However, on the other hand, we did collect one YELLOW clade bird near the eastern edge of the range of RED haplotypes. It is worth noting that the Caribbean slope of Panama in the region of both of these putative contact zones is continuously forested.

The apparently parapatric distributions of three mtDNA clades of *M. oleagineus* in Panama evoke several unanswered questions: what explains the lack of geographical overlap? Is secondary contact recent, or has demographic inertia retarded replacement of one clade by another (Reeves & Bermingham 2006)? Is Haldane's rule operating to retard female-mediated gene flow (females are the heterogametic sex in birds)? Finally, are the mtDNA clades cryptic species, with parapatry enforced through competitive exclusion? Only further study will resolve these issues.

The phylogeographic relationships in *M. oleagineus* provide an alternative model for the role of the Andes in the biogeography of lowland Neotropical animals. The area cladogram approach to Neotropical biogeography has suggested that the Andes was an early barrier to lowland taxa, and rarely, if ever, transgressed by descendants on either side. Our data showing episodic dispersal across (or around) the Andes suggest that these mountains can play a more persistent role in Neotropical biogeography and diversification.

We thank P. Sweet and the American Museum of Natural History, R. Brumfield and the Louisiana State University Natural History Museum, and L. Silveira and the Museu de Zoologia da Universidade de São Paulo for providing specimens. S. Vollmer and J. Maley gave advice on running IM. This work was supported by the University of Alaska Museum, a University of Alaska Fairbanks EPSCoR graduate fellowship and a grant from the AMNH Chapman Fund to M.J.M.; F.S.R.A. received financial support from FAPES, CAPES and CNPq.

REFERENCES

- American Ornithologists' Union 1998 *Check-list of North American birds*, 7th edn. Washington, DC: American Ornithologists' Union.
- Baker, P. A., Seltzer, G. O., Fritz, S. C., Dunbar, R. B., Grove, M. J., Tapia, P. M., Cross, S. L., Rowe, H. D. & Broda, J. P. 2001 The history of South American tropical precipitation for the past 25,000 years. *Science* **291**, 640–643. ([doi:10.1126/science.291.5504.640](https://doi.org/10.1126/science.291.5504.640))
- Bates, J. M. & Zink, R. M. 1994 Evolution into the Andes: molecular evidence for species relationships in the genus *Leptopogon*. *Auk* **111**, 507–515.
- Bates, J. M., Hackett, S. J. & Cracraft, J. 1998 Area relationships in the Neotropical lowlands: an hypothesis based on raw distributions of birds. *J. Biogeogr.* **25**, 783–793. ([doi:10.1046/j.1365-2699.1998.2540783.x](https://doi.org/10.1046/j.1365-2699.1998.2540783.x))
- Behling, H. & Hooghiemstra, H. 1999 Environmental history of the Colombian savannas of the Llanos Orientales since the Last Glacial Maximum from lake records El Pinal and Carimagua. *J. Paleolimnol.* **21**, 461–476. ([doi:10.1023/A:1008051720473](https://doi.org/10.1023/A:1008051720473))
- Bermingham, E. & Martin, A. P. 1998 Comparative mtDNA phylogeography of Neotropical freshwater fishes: testing shared history to infer the evolutionary landscape of lower Central America. *Mol. Ecol.* **7**, 499–517. ([doi:10.1046/j.1365-294x.1998.00358.x](https://doi.org/10.1046/j.1365-294x.1998.00358.x))
- Brumfield, R. T. & Capparella, A. P. 1996 Historical diversification of birds in northwestern South America: a molecular perspective on the role of vicariant events. *Evolution* **50**, 1607–1624. ([doi:10.2307/2410897](https://doi.org/10.2307/2410897))
- Brumfield, R. B., Jernigan, R. W., McDonald, D. B. & Braun, M. J. 2001 Evolutionary implications of divergent clines in an avian (*Manacus*: Aves) hybrid zone. *Evolution* **55**, 2070–2087.
- Capparella, A. P. & Lanyon, S. M. 1985 Biochemical and morphometric analyses of the sympatric, Neotropical sibling species, *Mionectes macconnelli* and *M. oleagineus*. In *Neotropical ornithology* (eds P. A. Buckley, M. S. Foster, E. S. Morton, R. S. Ridgely & F. G. Buckley), pp. 347–355. Ornithological Monographs, no. 36. Washington, DC: The American Ornithologists' Union.
- Chapman, F. M. 1917 The distribution of bird-life in Colombia. *Bull. Am. Mus. Nat. Hist.* **36**, 347–355.
- Chesser, R. T. 2004 Molecular systematics of New World suboscine birds. *Mol. Phylogenet. Evol.* **32**, 11–24. ([doi:10.1016/j.ympev.2003.11.015](https://doi.org/10.1016/j.ympev.2003.11.015))
- Cheviron, Z. A., Hackett, S. J. & Capparella, A. P. 2005 Complex evolutionary history of a Neotropical lowland forest bird (*Lepidothrix coronata*) and its implications for historical hypotheses of the origin of Neotropical avian diversity. *Mol. Phylogenet. Evol.* **36**, 338–357. ([doi:10.1016/j.ympev.2005.01.015](https://doi.org/10.1016/j.ympev.2005.01.015))
- Clement, M., Posada, D. & Crandall, K. 2000 TCS: a computer program to estimate gene genealogies. *Mol. Ecol.* **9**, 1657–1660. ([doi:10.1046/j.1365-294x.2000.01020.x](https://doi.org/10.1046/j.1365-294x.2000.01020.x))
- Colinvaux, P. A., De Oliveira, P. E. & Bush, M. B. 2000 Amazonian and Neotropical plant communities on glacial

- time-scales: the failure of the aridity and refuge hypotheses. *Quat. Sci. Rev.* **19**, 141–169. (doi:10.1016/S0277-3791(99)00059-1)
- Cortes-Ortiz, L., Bermingham, E., Rico, C., Rodriguez-Luna, E., Sampaio, I. & Ruiz-Garcia, M. 2003 Molecular systematics and biogeography of the Neotropical monkey genus, *Alouatta*. *Mol. Phylogenetic Evol.* **26**, 64–81. (doi:10.1016/S1055-7903(02)00308-1)
- Cracraft, J. & Prum, R. O. 1988 Patterns and processes of diversification: speciation and historical congruence in some Neotropical birds. *Evolution* **42**, 603–620. (doi:10.2307/2409043)
- da Silva, J. M. C. & Oren, D. C. 1996 Application of parsimony analysis of endemism in Amazonian biogeography: an example with primates. *Biol. J. Linn. Soc.* **59**, 427–437. (doi:10.1111/j.1095-8312.1996.tb01475.x)
- Dick, C. W., Abdul-Salim, K. A. & Bermingham, E. 2003 Molecular systematic analysis reveals cryptic tertiary diversification of a widespread tropical rain forest tree. *Am. Nat.* **160**, 691–703. (doi:10.1086/379795)
- Dick, C. W., Roubik, D. W., Gruber, K. F. & Bermingham, E. 2004 Long-distance gene flow and cross-Andean dispersal of lowland rainforest bees (Apidae: Euglossini) revealed by comparative mitochondrial DNA phyogeography. *Mol. Ecol.* **13**, 3775–3785. (doi:10.1111/j.1365-294X.2004.02374.x)
- Ditchfield, A. D. 2000 The comparative phylogeography of Neotropical mammals: patterns of intraspecific mitochondrial DNA variation among bats contrasted to nonvolant small mammals. *Mol. Ecol.* **9**, 1307–1318. (doi:10.1046/j.1365-294x.2000.01013.x)
- Eberhard, J. R. & Bermingham, E. 2004 Phylogeny and biogeography of the *Amazona ochrocephala* (Aves: Psittacidae) complex. *Auk* **121**, 318–332. (doi:10.1642/0004-8038(2004)121[0318:PABOTA]2.0.CO;2)
- Eberhard, J. R. & Bermingham, E. 2005 Phylogeny and comparative biogeography of *Pionopsitta* parrots and *Pteroglossus* toucans. *Mol. Phylogenetic Evol.* **36**, 288–304. (doi:10.1016/j.ympev.2005.01.022)
- Eva, H. D. et al. 2002 *A vegetation map of South America*. Brussels, Belgium: European Commission, Joint Research Centre.
- Fitzpatrick, J. W. 2004 Family Tyrannidae. In *Handbook of the birds of the world* (eds J. del Hoyo, A. Elliot & D. A. Christie). Cotingas to pipits and wagtails, pp. 170–463. Barcelona, Spain: Lynx Edicions.
- Fleischer, R. C., McIntosh, C. E. & Tarr, C. L. 1998 Evolution on a volcanic conveyor belt: using phyogeographic reconstructions and K-Ar-based ages of the Hawaiian Islands to estimate molecular evolutionary rates. *Mol. Ecol.* **7**, 533–545. (doi:10.1046/j.1365-294x.1998.00364.x)
- Gregory-Wodzicki, K. M. 2000 Uplift history of the central and northern Andes: a review. *GSA Bull.* **112**, 1091–1105.
- Haffer, J. 1967 Speciation in Colombian forest birds west of the Andes. *Am. Mus. Novitat.* **2294**, 1–57.
- Hey, J. & Nielsen, R. 2004 Multilocus methods for estimating population sizes, migration rates and divergence time, with applications to the divergence of *Drosophila pseudoobscura* and *D. persimilis*. *Genetics* **167**, 747–760. (doi:10.1534/genetics.103.024182)
- Hoffman, F. G. & Baker, R. J. 2003 Comparative phyogeography of short-tailed bats (Carollia: Phyllostomidae). *Mol. Ecol.* **12**, 3402–3414.
- Janzen, D. H. 1967 Why mountain passes are higher in the tropics. *Am. Nat.* **101**, 233–249. (doi:10.1086/282487)
- Johansson, U. S., Irestedt, M., Parsons, T. J. & Ericson, P. G. P. 2002 Basal phylogeny of the Tyrannoidea based on comparisons of cytochrome *b* and exons of nuclear *c-myc* and *RAG-1* genes. *Auk* **119**, 984–995. (doi:10.1642/0004-8038(2002)119[0984:BPOTTB]2.0.CO;2)
- Lovette, I. J. 2004 Mitochondrial dating and mixed support for the “2% rule” in birds. *Auk* **121**, 1–6. (doi:10.1642/0004-8038(2004)121[0001:MDAMSF]2.0.CO;2)
- Maddison, W. P. & Maddison, D. R. 2005 MESQUITE: a modular system for evolutionary analysis, version 1.06. See <http://mesquiteproject.org>.
- Marks, B. D., Hackett, S. J. & Capparella, A. P. 2002 Historical relationships among Neotropical lowland forest areas of endemism as determined by mitochondrial DNA sequence variation within the wedge-billed woodcreeper (Aves: Dendrocopatidae: *Glyphorynchus spirurus*). *Mol. Phylogenetic Evol.* **24**, 153–167. (doi:10.1016/S1055-7903(02)00233-6)
- Meyer de Schauensee, R. 1970 *A guide to the birds of South America*. Wynnewood, PA: Livingston Publishing Company.
- Miller, M. J., Bermingham, E. & Ricklefs, R. E. 2007 Historical biogeography of the New World solitaires (*Myadestes* spp.). *Auk* **124**, 868–885. (doi:10.1642/0004-8038(2007)124[868:HBOTNW]2.0.CO;2)
- Peters, J. L., Gretes, W. & Omland, K. E. 2005 Late Pleistocene divergence between eastern and western populations of wood ducks (*Aix sponsa*) inferred by the ‘isolation with migration’ coalescent method. *Mol. Ecol.* **14**, 3407–3418. (doi:10.1111/j.1365-294X.2005.02618.x)
- Prum, R. O. 1988 Historical relationships among avian forest areas of endemism in the Neotropics. *Acta Congr. Int. Ornithol.* **19**, 2563–2572.
- Reeves, R. G. & Bermingham, E. 2006 Colonization, population expansion, and lineage turnover: phyogeography of Mesoamerica characiform fish. *Biol. J. Linn. Soc.* **88**, 235–255. (doi:10.1111/j.1095-8312.2006.00619.x)
- Remsen Jr, J. V. et al. 2007 Version 27 July, 2007. A classification of the bird species of South America. Washington, DC: American Ornithologists’ Union. See <http://www.museum.lsu.edu/~Remsen/SACCBaseline.html>.
- Ribas, C. C., Moyle, R. G., Miyaki, C. Y. & Cracraft, J. 2007 The assembly of montane biotas: linking Andean tectonics and climatic oscillations to independent regimes of diversification in *Pionus* parrots. *Proc. R. Soc. B* **274**, 2399–2408. (doi:10.1098/rspb.2007.0613)
- Ridgely, R. S. & Tudor, G. 1994 *The birds of South America*, vol. 2, *the suboscines*. Austin, TX: University of Texas Press.
- Ron, S. R. 2000 Biogeographic area relationships of lowland Neotropical rainforest based on raw distributions of vertebrate groups. *Biol. J. Linn. Soc.* **71**, 379–402. (doi:10.1111/j.1095-8312.2000.tb01265.x)
- Ronquist, F. & Huelsenbeck, J. P. 2003 MrBayes 3: Bayesian phylogenetic inference under mixed models. *Bioinformatics* **19**, 1572–1574. (doi:10.1093/bioinformatics/btg180)
- Rull, V. 2007 Holocene global warming and the origin of the Neotropical Gran Sabana in the Venezuelan Guayana. *J. Biogeogr.* **34**, 279–288. (doi:10.1111/j.1365-2699.2006.01620.x)
- Sanderson, M. 1997 A nonparametric approach to estimating divergence times in the absence of rate constancy. *Mol. Biol. Evol.* **14**, 1218–1231.
- Sibley, C. G. & Monroe Jr, B. L. 1990 *Distribution and taxonomy of birds of the world*. New Haven, CT: Yale University Press.
- Swofford, D. L. 2002 *PAUP* phylogenetic analysis using parsimony (*and other methods)*, version 4. Sunderland, MA: Sinauer Associates.
- Terborgh, J. 1971 Distribution on environmental gradients: theory and a preliminary interpretation of distributional patterns in the avifauna of the Cordillera Vilcabamba, Peru. *Ecology* **52**, 23–40. (doi:10.2307/1934735)

- Terborgh, J. & Weske, J. S. 1975 The role of competition in the distribution of Andean birds. *Ecology* **56**, 562–576. ([doi:10.2307/1935491](https://doi.org/10.2307/1935491))
- Todd, W. E. C. 1921 Studies in the Tyrannidae I. A revision of the genus *Pipromorpha*. *Proc. Biol. Soc. Washington* **34**, 173–192.
- Traylor Jr, M. A. 1977 A classification of the tyrant flycatchers (Tyrannidae). *Bull. Museum Comp. Zool.* **148**, 129–184.
- Vollmer, S. V. & Palumbi, S. R. 2002 Hybridization and the evolution of reef coral diversity. *Science* **296**, 2023–2025. ([doi:10.1126/science.1069524](https://doi.org/10.1126/science.1069524))
- Weir, J. & Schlüter, D. 2004 Ice sheets promote speciation in boreal birds. *Proc. R. Soc. B* **271**, 1881–1887. ([doi:10.1098/rspb.2004.2803](https://doi.org/10.1098/rspb.2004.2803))
- Weir, J. T., Bermingham, E., Miller, M. J., Klicka, J. & Gonzalez, M. A. In press. Phylogeography of a morphologically diverse Neotropical montane species, the common bush-tanager (*Chlorospingus ophthalmicus*). *Mol. Phylogenetic Evol.*
- Zamudio, K. R. & Greene, H. W. 1997 Phylogeny of the bushmaster (*Lachesis muta*: Viperidae): implications for Neotropical biogeography, systematics, and conservation. *Biol. J. Linn. Soc.* **62**, 421–442.
- Zeh, J. A., Zeh, D. W. & Bonilla, M. M. 2003 Phylogeography of the harlequin beetle-riding pseudoscorpion and the rise of the Isthmus of Panamá. *Mol. Ecol.* **12**, 2759–2769. ([doi:10.1046/j.1365-294X.2003.01914.x](https://doi.org/10.1046/j.1365-294X.2003.01914.x))

LETTER

Neotropical birds show a humped distribution of within-population genetic diversity along a latitudinal transect

Abstract

Matthew J. Miller,^{1,2*} Eldredge Bermingham,² John Klicka,³ Patricia Escalante⁴ and Kevin Winker¹

¹University of Alaska Museum,
907 Yukon Drive, Fairbanks, AK
99775, USA

²Smithsonian Tropical Research
Institute, Apartado 0843-03092,
Balboa, Panama

³Barrick Museum of Natural
History, University of Nevada Las
Vegas, Box 454012, 4504
Maryland Parkway, Las Vegas,
NV 89154–4012, USA

⁴Instituto de Biología, UNAM,
AP 70-153, 04511 México, D.F.,
Mexico

*Correspondence: E-mail:
millerma@si.edu

The latitudinal gradient in species richness is a nearly universal ecological phenomenon. Similarly, conspecific genetic diversity often increases towards the equator – usually explained as the consequence of post-glacial range expansion or due to the shared response of genetic diversity to processes that promote species richness. However, no study has yet examined the relationship between latitude and within-population genetic diversity in exclusively tropical species. We surveyed genetic variation in nine resident bird species co-occurring in tropical lowlands between southern Mexico and western Ecuador, where avian species richness increases with decreasing latitude. Within-population genetic variation was always highest at mid-range latitudes, and not in the most equatorial populations. Differences in demography and gene flow across species' ranges may explain some of our observations; however, much of the pattern may be due simply to geometric constraints. Our findings have implications for conservation planning and for understanding how biodiversity scales from genes to communities.

Keywords

Centre-marginal hypothesis, genetic diversity, gradient, latitude, mid-domain effect, tropics.

Ecology Letters (2010) 13: 576–586

INTRODUCTION

Biogeography, community ecology and population genetics all attempt to describe how biological diversity is spatially distributed, albeit at different scales of geographic and biological organization. Therefore, it is not surprising that researchers from these disciplines seek common patterns in the distribution of diversity. One of the oldest and likely most recognized patterns of biodiversity is the latitudinal gradient of species richness (Rosenzweig 1995). For most taxa, the number of species occurring in an area increases towards the Equator. The regard for the latitudinal gradient in species richness is due to its ubiquity: the pattern holds at both small and large latitudinal spans, for plants and animals, for terrestrial and marine organisms, for taxonomic richness of genera and families in addition to species, and for fossil assemblages (Willig *et al.* 2003).

In a similar vein, several studies have reported latitudinal differences in genetic variation, including two important meta-analyses (Martin & McKay 2004; Hughes & Hughes

2007). Examples include Nearctic and Palearctic fishes (Bernatchez & Wilson 1998), Palearctic mammals (Jaarola & Tegelström 1995), Palearctic frogs (Johansson *et al.* 2006), Nearctic and Palearctic birds (Merilä *et al.* 1997) and South African corals (Ridgway *et al.* 2008). However, as Eckert *et al.* (2008) noted, single-species studies of geographic variation in within-population genetic diversity are disproportionately focused on taxa at their northern limits in the northern temperate zone. Because of the strong historical effect that Pleistocene-era glaciers had on the biogeography of higher latitudes, it is perhaps not surprising that post-glacial expansion is usually considered primarily responsible for the observed genetic diversity patterns (Hewitt 1996). This empirically demonstrated pattern of decreasing within-population genetic diversity with increasing latitude might be termed the ‘poleward model’. Like their temperate zone counterparts, tropical habitats also expanded poleward during the Holocene (Leyden 1984; Hillesheim *et al.* 2005). Thus, as expected by latitudinal diversity hypotheses, it would be reasonable to expect that within-population

genetic diversity should decrease as one samples exclusively tropical taxa poleward along a latitudinal gradient.

Similarly, latitudinal gradients in genetic diversity are also predicted by recently developed theory that relates species richness in a community to the genetic variation of members of that community. Vellend and colleagues (Vellend 2003; Vellend & Geber 2005) noted that the same biogeographic conditions favourable to high species richness within a community (i.e. high immigration rates and low extinction rates) should promote high genetic diversity within the species comprising that community. Empirical support for this model has come from forest tree communities (Wehenkel *et al.* 2006), butterflies (Cleary *et al.* 2006), and over half of the archipelago species surveyed in a meta-analysis (Vellend 2003). Vellend (2003) termed this positive relationship between species richness and genetic diversity the species–genetic diversity correlation; here, we will refer to it simply as the ‘species richness model’. One of the most intriguing aspects of the latitudinal gradient in species richness is that it can be found within exclusively tropical samples (Willig *et al.* 2003). Therefore, a correlation between species richness and within-population genetic variation should result in a latitudinal gradient in within-population genetic diversity of exclusively tropical taxa.

Models predicting a latitudinal gradient in genetic variation can be compared with the central–peripheral model, an important general model for the distribution of abundance across a species’ range. The central–peripheral model has been most frequently applied in macroecology, where it predicts that a species’ abundance peaks in the centre of its range and diminishes towards the range edges (Brown 1984), but it has also been extended to genetic diversity (da Cunha *et al.* 1950; Brussard 1984). This pattern is believed to be caused by diminishing ecological suitability of habitats at range edges, resulting in greater population fluctuations in edge populations compared with central ones (Brown *et al.* 1995). Reduced abundance and greater variance in abundance should increase genetic drift, thus reducing within-population genetic variation (Vucetich & Waite 2003). The combined consequences of reduced effective population size and lower immigration rates in edge populations should cause a reduction in genetic diversity relative to central populations.

Additionally, geometry predicts that central populations should have higher immigration rates than edge populations (Eckert *et al.* 2008), thus minimizing the diversity-reducing effects of genetic drift in central populations. This geometric effect parallels the macroecological observation that the richness of a local species pool is strongly influenced by the regional species pool richness (Terborgh 1973; Rosenzweig 1995) as well as the notion that species richness gradients are driven largely by geometric constraints or ‘mid-domain’ effects (Colwell & Hurtt 1994; Lees *et al.* 1999; Colwell &

Lees 2000). As noted by Eckert *et al.* (2008), in spite of the strong theoretical support for this model, there is a relative lack of empirical evidence. These authors also noted that they were unable to find a single study of tropical taxa that investigated latitudinal variation in genetic diversity among conspecific populations. To our knowledge, no study to date has addressed how within-population genetic diversity varies across a tropical latitudinal gradient.

Here, we measure within-population genetic diversity along a tropical latitudinal gradient, contrasting central–peripheral and latitudinal gradient models against a null model of no relationship between population genetic diversity and latitude. Our empirical data were developed from nine resident Neotropical landbird species, sampled more or less concordantly across their ranges from Middle America to the Pacific lowlands of northwestern South America. Lowland tropical forest occurs in a narrow band from southern Mexico to western Ecuador, and along this transect avian resident species richness increases with decreasing latitude (Fig. 1). Furthermore, the avian community is relatively biogeographically homogeneous, whereas avian assemblages east of the Andes are more heterogeneous across a similar latitudinal span. Relatively few species co-occur on both sides of the Andes, and we expect gene flow to be non-existent or greatly diminished across the Andes in these cases (e.g. Brumfield & Capparella 1996; Miller *et al.* 2008). These factors combine to make this transect a natural laboratory for observing how within-species genetic diversity varies along the latitudinal and species richness gradient.

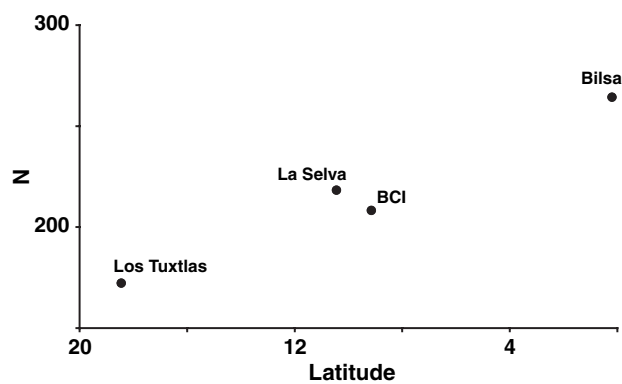


Figure 1 Number of breeding landbirds recorded at four research stations in the Neotropical lowlands from Mexico to Ecuador: (1) Los Tuxtlas (Veracruz, Mexico \approx 18.6° N); (2) La Selva (Heredia, Costa Rica \approx 10.4° N); 3) Barro Colorado Island (BCI: Colon, Panama \approx 9.2° N) and (4) Bilsa (Esmeraldas, Ecuador \approx 0.4° N) (see Appendix S2 for details).

MATERIALS AND METHODS

Tropical evergreen forest is more or less continuously distributed from southern Mexico south through Central America and along the Pacific lowlands of South America until western Ecuador, where a strong moisture gradient results in a relatively abrupt transition to tropical dry forest. Blocked by the continental divide along Central America, this narrow band of forest is restricted to the lowlands of the Middle American Caribbean slope until eastern Panama, where a lower continental ridge and increased Pacific rainfall permit this band to cross the continental divide and continue south along a narrow lowland strip of the Pacific coast of Colombia and northwestern Ecuador. Many tropical forest species have a more or less continuous distribution along this transect: 42% of the resident landbirds from the Los Tuxtlas Biological Station in Veracruz, Mexico, can be found in Bilsa Biological Station in Esmeraldas, Ecuador (see Appendix S2). This transect spans over 18° of latitude separating Veracruz and Esmeraldas, and in most places it is less than 200 km wide.

Based on available tissue samples from vouchered museum specimens, nearly all of which we collected, we identified nine species (Table 1) of resident Neotropical landbirds with suitable sample size at various locations along this transect. In most cases, we sampled these species at six sites: Veracruz, Mexico (*c.* 18.5° N), Toledo District, Belize (*c.* 16.5° N), northern Honduras (*c.* 15.5° N), Bocas del Toro, Panama (*c.* 9.0° N), Darién, Panama (*c.* 7.8° N) and western Ecuador (*c.* 0.0° N). One species, *Euphonia gouldi*, occurs only from southern Mexico to Bocas del Toro, and another species, *Glyphorynchus spirurus*, occurs in our samples northward only to Belize. Additionally, *Myrmeciza exsul* occurs from southern Honduras to western Ecuador; in this case, we included samples from Heredia, Costa Rica (*c.* 10.4° N). In general, for all the nine species, these population samples represent multiple collecting efforts spread over several years at two to four geographic points within a 25-km radius; exact locations are available from the authors and the respective museums. As the range maps in Fig. 3 show, our sampling strategy covered nearly the entire range west of the Andes for these nine species.

As our metric of within-population genetic diversity, we chose nucleotide diversity (π) of the NADH dehydrogenase subunit II (ND2) mitochondrial gene (1041 bp). Nucleotide diversity equals the average number of nucleotide substitutions between all sequences and is a standard measure of DNA polymorphism (Nei 1987). We sequenced the complete ND2 gene following standard protocols as described by Miller *et al.* (2008). In most cases, DNA was extracted from mitochondrially rich muscle tissue; however, a few western Ecuador samples were from feathers. In

addition, we included one sequences from GenBank (a sequence of *Pipra mentalis*, LSUMZ B18078, from Veracruz, Mexico) which is marked with an asterisk in Appendix S1. All other sequence data were generated by the authors in their laboratories, and the first author reviewed all chromatograms. We estimated π in DnaSP 4.2 (Rozas *et al.* 2003).

We aimed to sample at least 10 individuals per population, but sample sizes varied due to the vagaries of field success (Table 1). To explore the effect of sample size on estimates of π , we subsampled three of our largest population samples that also had varying estimates of π (*Mionectes oleagineus*, Bocas del Toro, $n = 18$, $\pi = 0.0010$; *Myrmeciza exsul*, Bocas del Toro, $n = 12$, $\pi = 0.0048$; *Henicorhina leucosticta*, Darién, $n = 13$, $\pi = 0.0029$). For each of these populations, we created 1000 bootstrapped datasets for each possible sample size value from $n = 2$ to $n = 10$. We plotted the mean, median, standard deviation and mean–median of π against bootstrap sample size.

A null model for the distribution of genetic diversity along a cline predicts no relationship between a population's genetic diversity and that of an adjacent population. In contrast, the latitudinal gradient models (poleward and species richness) both predict an increase in genetic diversity with decreasing latitude. We tested for such an increase in π for our nine Neotropical bird species by calculating the value of the expression: $\pi_i - \pi_{i+1}$, where i refers to a given population and $i + 1$ is the next population found at a lower latitude. The latitudinal gradient models predict that this difference should be positive more frequently than negative. The frequency of observed vs. expected positive values was compared with a null hypothesis of equal frequency of positive and negative values using an exact binomial test.

An alternative model to latitudinal models (poleward and species richness, as discussed above) is the central–peripheral model, which would produce a humped distribution, wherein the largest value of π is found in mid-range relative to edge populations. A null hypothesis for this model is that, within a species, the largest value of π is equally likely to be observed in any of the sampled populations. We tested for a humped distribution of π by evaluating whether the frequency of a species' highest value for π occurred in the northernmost or southernmost sampling point (i.e. edge populations) at a lower frequency than predicted by the null hypothesis. Specifically, each of our nine species has two edge populations and two to four mid-range populations, so the probability by chance that the maximum observed value of π occurs in a mid-range population varies from 0.50 to 0.66. We calculated the probability that the observed number of species with maximum π in an edge population was due to chance by computing the joint probabilities of all combinations of

Table 1 Estimated nucleotide diversity for nine species (48 populations) of Neotropical landbirds ranging from SE Mexico to W Ecuador

Scientific name	<i>n</i>	Num Hap	<i>H</i>	π	$\delta\pi$
<i>Phaethornis longirostris</i> (21.7° N – 4.0° S)					
Veracruz, Mexico	10	1	0.000	0.0000	
Toledo, Belize	10	3	0.511	0.0005	0.0005
N Honduras	10	2	0.467	0.0004	-0.0001
Bocas del Toro, Panama	11	4	0.691	0.0016	0.0012
Darién, Panama	12	4	0.455	0.0005	-0.0011
W Ecuador	5	1	0.000	0.0000	-0.0005
<i>Phaethornis strigularis</i> (18.7° N – 0.4° S)					
Veracruz, Mexico	7	1	0.000	0.0000	
Toledo, Belize	10	5	0.756	0.0014	0.0014
N Honduras	6	4	0.867	0.0018	0.0004
Bocas de Toro, Panama	9	5	0.889	0.0033	0.0015
Darién, Panama	10	8	0.956	0.0022	-0.0011
W Ecuador	3	1	0.000	0.0000	-0.0022
<i>Amazilia tzacatl</i> (18.7° N – 3.4° S)					
Veracruz, Mexico	4	3	0.833	0.0010	
Toledo, Belize	10	5	0.667	0.0010	0.0000
N Honduras	4	4	1.000	0.0048	0.0038
Bocas del Toro, Panama	9	6	0.917	0.0021	-0.0027
Darién, Panama	5	2	0.600	0.0087	0.0066
W Ecuador	2	2	1.000	0.0010	-0.0077
<i>Glyptophynchus spirurus</i> (18.0° N – 3.8° S)					
Toledo, Belize	10	2	0.200	0.0002	
N Honduras	9	2	0.389	0.0004	0.0002
Bocas del Toro, Panama	10	7	0.933	0.0061	0.0057
Darién, Panama	10	3	0.378	0.0004	-0.0057
W Ecuador	8	3	0.679	0.0024	0.0020
<i>Myrmeciza exsul</i> (14.2° N – 3.5° S)					
Heredia, Costa Rica	10	3	0.600	0.0008	
Bocas del Toro, Panama	12	6	0.818	0.0048	0.0040
Darién, Panama	11	3	0.564	0.0005	-0.0043
W Ecuador	15	8	0.838	0.0015	0.0010
<i>Pipra mentalis</i> (18.8° N – 0.0° S)					
Veracruz, Mexico	10	2	0.200	0.0002	
Toledo, Belize	12	4	0.561	0.0009	0.0007
N Honduras	10	6	0.889	0.0014	0.0005
Bocas del Toro, Panama	9	3	0.417	0.0004	-0.0010
W Ecuador	2	2	0.100	0.0010	0.0006
<i>Mionectes oleagineus</i> (21.2° N – 4.2° S)					
Veracruz, Mexico	10	5	0.667	0.0014	
Toledo, Belize	10	5	0.822	0.0011	-0.0003
N Honduras	10	5	0.844	0.0015	0.0004
Bocas del Toro, Panama	18	6	0.627	0.0010	-0.0005
Darién, Panama	18	5	0.771	0.0010	0.0000
W Ecuador	5	1	0.000	0.0000	-0.0010
<i>Henicorhina leucosticta</i> (21.0° N – 0.0° S)					
Veracruz, Mexico	7	5	0.905	0.0018	
Toledo, Belize	10	8	0.933	0.0023	0.0005
N Honduras	9	4	0.583	0.0015	-0.0008
Bocas del Toro, Panama	12	7	0.879	0.0016	0.0001
Darién, Panama	13	6	0.859	0.0029	0.0013
W Ecuador	8	3	0.464	0.0007	-0.0022
<i>Euphonia gouldi</i> (18.7° N – 9.0° S)					
Veracruz, Mexico	9	1	0.000	0.0000	

Table 1 continued

Scientific name	<i>n</i>	Num Hap	<i>H</i>	π	$\partial\pi$
Toledo, Belize	9	4	0.806	0.0011	0.0011
N Honduras	10	6	0.889	0.0050	0.0039
Bocas del Toro, Panama	10	8	0.933	0.0029	-0.0021

n = number of individuals sampled; Num Hap: number of haplotypes; *H*: haplotype diversity; π : nucleotide diversity; $\partial\pi = \pi_{i+1} - \pi_i$. Maximum π (per species) in bold. Veracruz, Mexico: ($\sim 18.5^\circ$ N, 95.0° W); Toledo, Belize: ($\sim 16.0^\circ$ N, 89.0° W); N Honduras (Copán & Atlántida): ($\sim 15.5^\circ$ N, 87.5° W); Heredia, Costa Rica: (10.5° N, 84.0° W); Bocas del Toro, Panama: ($\sim 9.0^\circ$ N, 82.5° W); Darién, Panama: ($\sim 7.5^\circ$ N, 78.0° W); W Ecuador (Esmeraldas & Manabí): ($\sim 0.0^\circ$ N, 79.5° W). For each species we have included an estimate of the latitudinal limits of its distribution; see further maps in Figure 3.

observations that equalled or were less frequent than found in our empirical data.

To visualize the collective pattern of genetic diversity among the nine species along this transect (for heuristic purposes only), we did two simple calculations. First, we standardized site-specific values for each species separately by setting the highest value of π observed in that species to 1.0 and calculating the proportion of this value exhibited at other sampled locations. Second, for each site we averaged the values for all species obtained at that location. This was carried out for the six sites along the transect noted above (Veracruz to western Ecuador); the sampled assemblage at each site included seven to nine species. Although each species has a unique range and not all of those included here match that of our transect, among these particular species they are not so different as to obscure the utility of this heuristic visualization approach. Standardizing ranges into quartiles and performing similar calculations resulted in a similar among-species pattern (not shown). We chose to use the former here because spatially shared attributes among co-occurring species (here, community genetics) are more directly applicable to community ecology and conservation biology.

RESULTS

We sequenced ND2 from 48 populations (445 individuals) of the nine species in our study. Among these populations, π varied from 0.0000 to 0.0865 and had a median value of 0.0011. The distribution of values of π was strongly left-skewed and long-tailed (Fig. 2). Values less than 0.001 were most frequent (45%). Only 6% of the populations had π values greater than 0.005.

We found no significant relationship between sample size and the rank of π values within a species (Fig. 2b; $r^2 = 0.02$, $P = 0.31$). Our bootstrap analyses on three of our empirical population datasets did detect a slight downward bias in estimated π in samples of two to three individuals, but this was not observed with sample sizes equal to or greater than 4 (only 3 of our 48 population

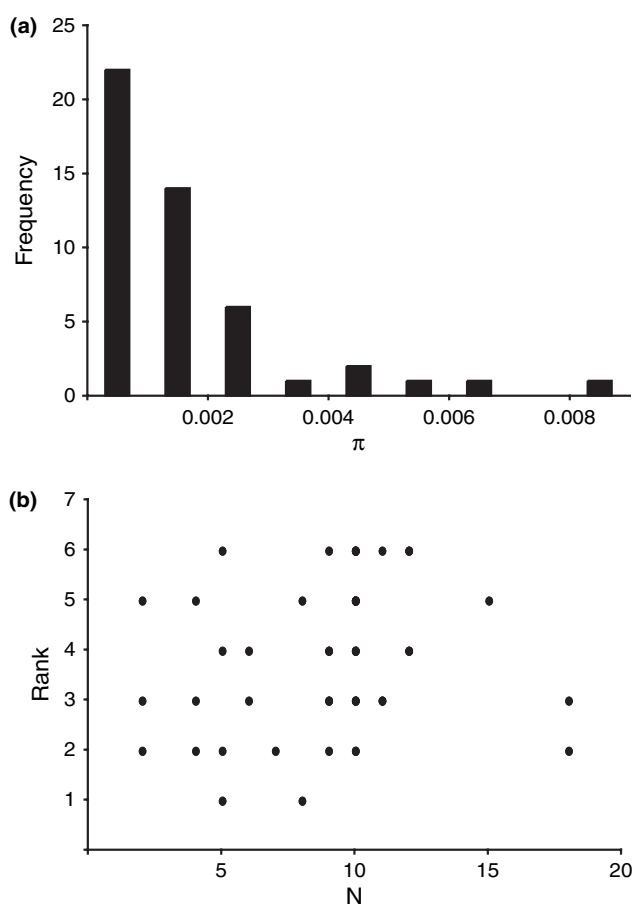


Figure 2 (a) Histogram of estimated nucleotide diversity π from 48 populations (nine species) of Neotropical landbirds. (b) Rank (among populations within species, from largest to smallest) of estimated nucleotide diversity (π) relative to number of individuals sampled, indicating that sample size and π have a non-significant relationship. Note inverted y -axis.

samples had $n = 2$ or 3; see Table 1; Appendix S4 and Table S1 for details). Based on these two findings, we conclude that sample size did not have an undue effect on our estimates of π .

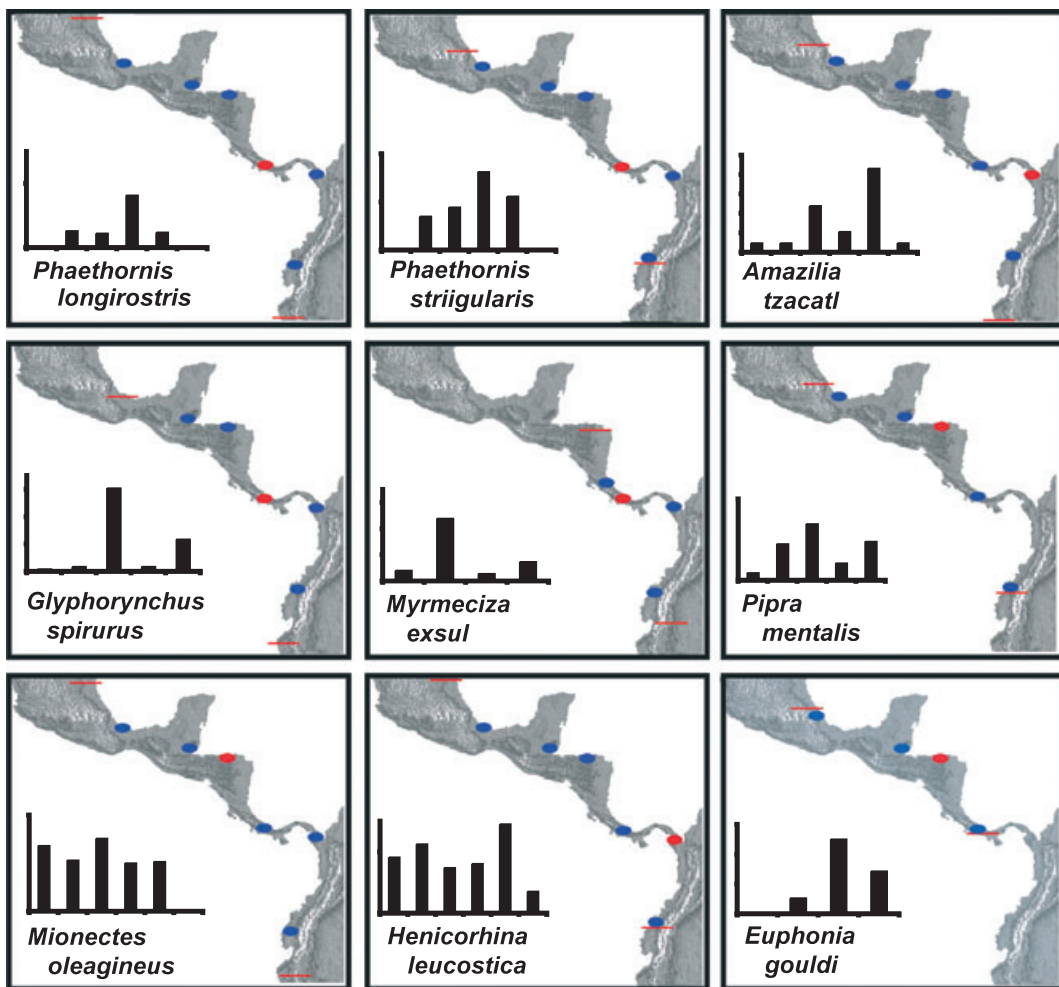


Figure 3 Maps for all nine resident Neotropical landbirds surveyed in this study. For each species, the sampled population with the highest nucleotide diversity (π) is marked in red, other sampled populations are marked in blue. Red lines indicate the species' geographic range latitudinal maximum and minimum (west of the Andes). Inset bar graphs show relative π values for populations, beginning with the northernmost sampled population for each species; data values available in Table 1.

In our comparison of the model of a relationship between genetic diversity and latitude with a null model of uniformity, there were 39 opportunities to evaluate the expression: $\pi_{i+1} - \pi_i$. Of these, 22 were non-negative (frequency = 0.56), which is not significantly different from an expected frequency of 0.5 predicted by a null model of random change with respect to latitude (exact test: $P = 0.26$; Table 1). This finding was consistent even in reduced datasets (i.e. sequentially removing populations with sample sizes below three to eight individuals; range of P -values: 0.10–0.26; see Appendix S4, Table S1 for details). Therefore, there is no evidence for a general trend of increasing within-population genetic diversity with decreasing latitude.

In our comparison of a humped distribution against a null model, we found that zero of the nine species had a maximum π value in an edge population (Fig. 3; see

'Materials and Methods'). The P -value of this result can be calculated analytically as the joint probability of the probability of a mid-range maximum π value for all nine species given a random spatial distribution of maximum values. That result is significant even after a Bonferroni-correction to take into account our previous test of an inverse relationship between latitude and within-population diversity ($\alpha = 0.025$; $P = 0.01$). Likewise, among our reduced datasets (i.e. after sequentially removing populations with sample sizes below three to eight individuals), this probability remained significant in six of seven cases, with the seventh case nearly significant (range of P -values: 0.006–0.065; see Appendix S4, Table S2 for details). We thus reject the null model of no relationship between latitude and within-population genetic variation in favour of a humped distribution model.

We found no evidence of a secondary effect of latitude on estimates of π . Across our nine species, average π calculated from populations north of each species' latitudinal midpoint did not differ from the average π calculated from populations south of that point (Wilcoxon signed-rank test, $W = 16$, $P > 0.2$). Likewise, we found no difference between the average π for each species calculated from populations in the most poleward quartile of the species' range compared with the average π from populations in the most-equatorial quartile (Wilcoxon signed-rank test, $W = 21$, $P > 0.2$).

Heuristic visualization of the distribution of within-population genetic variation among species along the transect also showed a humped distribution; i.e. collectively, the sampled avian assemblages of largely co-distributed species along this transect (seven to nine species per site) exhibited the pattern observed within these species (Fig. 4).

DISCUSSION

Among the nine species of resident Neotropical landbirds, our data reject a null model of no relationship between maximum π and latitude in favour of a humped distribution model in which the highest π for a species was found in mid-latitude populations (Figs 3 and 4). In contrast, a model of increasing mitochondrial DNA nucleotide diversity (π) with decreasing latitude (the poleward or species richness models) was not a better fit to the data than a null model of randomly distributed π . Even after controlling for edge vs. range-centre effects, we found no evidence for a secondary

effect of latitude on within-population genetic variation [note that in Fig. 4, Bocas del Toro, Panama ($\sim 9^\circ$ N) is latitudinally midway between our extreme sampling points Veracruz, Mexico ($\sim 18.5^\circ$ N) and western Ecuador ($\sim 0.0^\circ$ N)].

Although relatively few studies have reported within-population π from mtDNA in Neotropical birds, our results appear consistent with values found by others (Brumfield 2005; Aleixo 2006). And although very small sample size can cause a minor downward bias in the estimate of π (see Appendix S3), our findings remain even after populations of varying thresholds of minimum sample size were removed from the analysis.

Many studies focused on temperate zone organisms (e.g. Jaarola & Tegelström 1995; Merilä *et al.* 1997; Bernatchez & Wilson 1998; Milá *et al.* 2000) have suggested that latitudinal patterns of within-population genetic diversity are most likely due to a history of post-glacial poleward habitat expansion. Could our findings similarly result from post-glacial expansion of tropical species west of the Andes both towards the pole and the equator?

The limits of tropical habitats in northern Middle America have shifted northward since the Pleistocene. Studies show that northern Middle America lacked forest and was instead covered with arid habitats (Leyden 1984; Hillesheim *et al.* 2005). Leyden (1984) has documented regeneration of forest cover through the Holocene. In contrast, Colinvaux (1996) provided strong evidence that lower Middle America and northwestern South America remained continuously forested throughout the late Pleistocene and Holocene. In addition, existing biome models for the Chocó forests of western Colombia (and presumably northwestern Ecuador) indicate that this region was continuously covered by wet evergreen forest since the late Quaternary (Berrio 2002; Marchant *et al.* 2004). Further, although no bioclimatic reconstruction has apparently focused on the Ecuadorian coastal lowlands, at least one continental-scale bioclimatic reconstruction suggests that the vegetation in western Ecuador has remained remarkably stable from the Last Glacial Maximum to the present (Adams 1997). Therefore, although the northern populations in our study may have experienced a reduction in genetic variation as a consequence of tracking northward-expanding forests (Hewitt 1996), habitat shifts since the Last Glacial Maximum are unlikely to explain the lower genetic diversity found at the southern edges of the nine species we examined.

If historic habitat shifts do not explain the humped pattern, then latitudinal variation in the demography of central and range-edge populations may be contributing to lower within-population genetic diversity in edge populations. Among the species included in our study, there is some evidence that edge populations may be less abundant

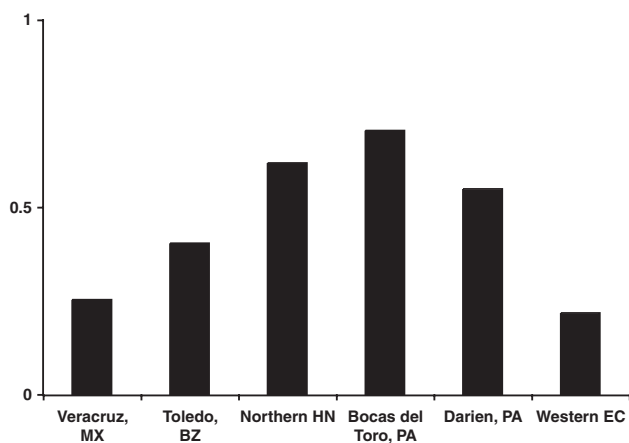


Figure 4 Average nucleotide diversity (π) among nine species of co-distributed resident landbirds across a Neotropical latitudinal gradient showing a humped distribution of π . Values of π are scaled whereby for each species the maximum value of π equals 1. Because our sample points are not evenly spaced across the gradient, the latitudinal midpoint occurs at Bocas del Toro, Panama.

than mid-range populations: of the 18 edge populations, we found abundance estimates for 17 in area checklists. Of these, five (29.4%) were classified as abundant, or common, six as fairly common (35.3%) and the remaining six as uncommon (35.3%), whereas 16 populations surveyed in the centre of the species' ranges were classified as abundant or common 14 times (87.5%) and uncommon twice (12.5%). Paired comparisons among species found that edge populations had lower qualitative rankings for these measures of relative abundance than populations from the range centre (Wilcoxon signed-rank test, $W = 1.5$, $P < 0.05$; see Appendix S3 for details). Thus, mid-range vs. edge variation in relative abundance might be responsible for the observed pattern. If so, this is an interesting observation given that meta-analyses establish that a majority of species do not show a simple pattern of high abundance at mid-range populations and low abundance at range edges (Sagarin & Gaines 2002).

If edge demographics are causing the observed pattern, this would be consistent with models suggesting that reduced abundance and gene flow at range edges may drive central–peripheral models of within-population genetic variation (e.g. Vucetich & Waite 2003; Eckert *et al.* 2008). In fact, while most studies focused on latitudinal variation in genetic diversity in temperate zone species invoke post-glacial expansion to explain reduced genetic variation in poleward populations, at least one study has argued that this factor alone is insufficient: Johansson *et al.* (2006) found a strong latitudinal component to differences in within-population genetic variation among *Rana temporaria* populations. After controlling for latitude, a significant effect of population size on genetic diversity remained, and the authors concluded that demographic patterns in edge populations were principally responsible for their findings. It is important to note if edge effects are responsible for our observation of a humped distribution of genetic variation, they occur on relatively large scales: for six of our nine species at least one 'edge' population occurred greater than 2 latitudinal degrees away from the geographic edge of the species' range.

Lower relative abundance in range-edge populations is not necessary to create the patterns we observed: these patterns can be explained exclusively by the geographical context of contemporary and historical gene flow. On contemporary time scales, immigration counters the loss of genetic diversity caused by genetic drift. For populations that have relatively one-dimensional distributions, such as the birds in this study, range edge populations have functionally half the potential source populations from which to receive immigrants as do mid-range populations. Vucetich & Waite (2003) showed that even in the absence of population size differences, differential migration between central and peripheral populations can diminish

genetic variation in edge populations. Alternatively, the effect of geometry may be historical rather than dependent on contemporary gene flow differences. Haplotypes arise by mutation in a single point in space and then expand to form their current distributions; therefore, they are likely to have a more or less continuous distribution within some portion, or all, of a species' range. The spread of a haplotype across a species' range might be envisioned in purely neutral terms as the spread of a ripple generated from a particular point in a pond. Because these distributions are ultimately bounded by the edges of species' ranges, it is more likely that the majority of haplotypes will overlap in the centre portion of the range. This phenomenon has been coined the 'mid-domain effect' (Colwell & Lees 2000). Proponents of the mid-domain effect (also known as geometric constraints) argue that it is at least partially responsible for other cases in which the geographic distribution of biological diversity is humped, such as latitudinal and altitudinal species-richness gradients (e.g. Jetz & Rahbek 2001; Colwell *et al.* 2004). While controversial (e.g. Colwell *et al.* 2004), geometric constraints can be useful to explain deviations from well-established laws of biodiversity, such as the latitudinal gradient in species richness. For example, Lees *et al.* (1999) argued that geometric constraints explain why, on Madagascar, butterfly species richness peaks at the island's latitudinal midpoint, rather than increasing equatorially as normally occurs with species richness gradients.

We note that six of the nine species examined had a mid-range population comprised of individuals from two clades, one otherwise northward and the second otherwise southward (not shown), consistent with expectations of the mid-domain model. Geometric constraints refer both to the case of secondary contact of two lineages, such as a northern and southern clade in some of the species in our study, or a case in which a single mtDNA lineage is found throughout a species' range. If variants (i.e. mtDNA haplotypes) have relatively continuous distributions and are bound to a discrete area (i.e. a species' range), the greatest number of variants should be found in the middle rather than at the edges of that area, regardless of any particular geographic co-association of variants (i.e. geographic structure). Without finer-scale measurements of contemporary population size and gene flow, we are unable to evaluate the extent to which contemporary vs. historical processes are responsible for the humped mtDNA genetic diversity pattern that we observed. We also note that, as required to compile this dataset, the nine species in this study represent widespread, common birds, and each was reasonably common at our sampling points (which is why they were chosen). Each species does have its own life-history attributes and ecology, but despite their differences they appear to show a common pattern in the distribution of within-population genetic

diversity (e.g. Fig. 4). Future studies will be needed to determine whether the humped distribution found here among common understory forest birds also occurs in rarer or more local taxa.

Differences between the geometric constraints on species and genes may partially explain the decoupling of the gradient in species richness and genetic variation. Haplotypes within our species are geographically bounded by these species' present distributions, which collectively extend from southern Mexico to western Ecuador. However, the processes responsible for the formation of these species have a much wider geographic context. In fact, all of the species included in this study have sister species in regions outside the geographic scope of this study (i.e. northward in Mexico, southward along the Pacific South American coast, into the Andes, or across the Andes into South America), and at these larger geographic scales, Neotropical birds conform to the latitudinal gradient expectation, with highest species richness centred near the Equator (Orme *et al.* 2005). Thus, in cases where the geometry of species formation and genetic variation are coupled, such as island systems, we might expect a coupling between geographic patterns in alpha species richness and within-population genetic variation (e.g. Vellend 2003). However, it seems likely that in most continental cases the geography of conspecific genetic variation will often be decoupled from the geography of the species formation process.

The concept of the 'stable tropics' (Orians 1969; MacArthur 1972) still persists, despite a variety of evidence that tropical populations undergo substantial fluctuations over both contemporary and Quaternary time scales (e.g. Karr & Freemark 1983; Leyden 1984; Phillips *et al.* 1994). Recent reviews continue to posit that effective population sizes of tropical taxa are generally expected to be more stable than those of temperate taxa (e.g. Mallet *et al.* 2005), although the limited genetic evidence for historical stability of tropical populations is mixed (e.g. Schneider & Moritz 1999; Lessa *et al.* 2003; Anthony *et al.* 2007). In contrast, our results suggest that the effective population size (as measured by mtDNA polymorphism) of tropical species is geographically context-dependent: range centres have more genetic diversity than range edges. Because effective population size is proportional to the harmonic mean of the census population size, our results suggest that populations of tropical species near the range centre may have been relatively stable, but that populations on the range edges appear to have been less so.

Our findings have implications for both evolutionary biology and the management of biodiversity, as differences in genetic diversity can have substantial effects on ecological processes (Hughes *et al.* 2008). Further study is needed to determine whether the humped pattern present in mtDNA of

Neotropical birds is also found in potentially adaptive genetic variation. That relationship will be important for conservation and management, because, with respect to the maintenance of genetic diversity, our data predict that consequences of anthropogenic habitat fragmentation and population isolation will likely have differential effects depending on where in a species' range these phenomena occur.

ACKNOWLEDGEMENTS

We thank A. Johnson for collecting many of the Belizean specimens in this study. M. Lelevier and M. Nuñez assisted in the laboratory work. We also thank the people and governments of the five countries who granted scientific collecting permits; research of this scope is only possible with their continued support. This project was partially supported by NIH Fogarty International Center Award Number U01TW006634; the content is solely the responsibility of the authors and does not necessarily represent the official views of the Fogarty International Center or the National Institutes of Health. Additional financial support for this project came from the University of Alaska Museum, the Smithsonian Tropical Research Institute, and University of Alaska Fairbanks EPSCoR graduate, a Smithsonian Pre-doctoral, Angus Gavin Migratory Bird Research, and an AMNH Chapman Fund fellowships/grants to M.J. Miller. We thank A. Crawford, M. Holyoak, K. McCracken, M Olson, and three anonymous referees for comments on earlier drafts.

REFERENCES

- Adams, J.M. (1997). *Global Land Environments Since the Last Interglacial*. Oak Ridge National Laboratory, TN, USA. Available at: <http://www.esd.ornl.gov/ern/qen/nerc.html>.
- Aleixo, A. (2006). Historical diversification of floodplain forest specialist species in the Amazon: a case study with two species of the avian genus *Xiphorhynchus* (Aves: Dendrocolaptidae). *Biol. J. Linn. Soc. Lond.*, 89, 383–395.
- Anthony, N.M., Johnson-Bawe, M., Jeffery, K., Clifford, S.L., Abernethy, K.A., Tutin, C.E. *et al.* (2007). The role of Pleistocene refugia and rivers in shaping gorilla genetic diversity in central Africa. *Proc. Natl Acad. Sci. USA*, 104, 20432–20436.
- Bernatchez, L. & Wilson, C.C. (1998). Comparative phylogeography of Nearctic and Palearctic fishes. *Mol. Ecol.*, 7, 431–452.
- Berrío, J.C. (2002). *Late glacial and Holocene vegetation and climate change in lowland Colombia*, PhD Dissertation, University of Amsterdam, Amsterdam.
- Brown, J.H. (1984). On the relationship between abundance and distribution of species. *Am. Nat.*, 124, 255–279.
- Brown, J.H., Mehlman, D.W. & Stevens, G.C. (1995). Spatial variation in abundance. *Ecology*, 76, 2028–2043.
- Brumfield, R.T. (2005). Mitochondrial variation in Bolivian populations of the Variable Antshrike (*Thamnophilus caerulescens*). *Auk*, 122, 414–432.

- Brumfield, R.T. & Capparella, A.P. (1996). Historical diversification of birds in northwestern South America: a molecular perspective on the role of vicariant events. *Evolution*, 50, 1607–1624.
- Brussard, P.F. (1984). Geographic patterns and environmental gradients: the central-marginal model in *Drosophila* revisited. *Annu. Rev. Ecol. Syst.*, 15, 25–64.
- Cleary, D.F.R., Fauvelot, C., Genner, M.J., Menken, S.B.J. & Mooers, A.O. (2006). Parallel responses of species and genetic diversity to El Niño Southern Oscillation-induced environmental destruction. *Ecol. Lett.*, 9, 304–310.
- Colinvaux, P.A. (1996). Quaternary environmental history and forest diversity in the Neotropics. In: *Evolution and Environment in Tropical America* (eds Jackson, J.B.C., Budd, A.F. & Coates, A.G.). University of Chicago Press, Chicago, pp. 359–406.
- Colwell, R.K. & Hurtt, G.C. (1994). Non-biological gradients in species richness and a spurious Rapoport effect. *Am. Nat.*, 144, 570–595.
- Colwell, R.K. & Lees, D.C. (2000). The mid-domain effect: geometric constraints on the geography of species richness. *Trends Ecol. Evol.*, 15, 70–76.
- Colwell, R.K., Rahbek, C. & Gotelli, N.J. (2004). The mid-domain effect and species richness patterns: what have we learned so far? *Am. Nat.*, 163, E1–E23.
- da Cunha, A.B., Burla, H. & Dobzhansky, T. (1950). Adaptive chromosomal polymorphism in *Drosophila willistoni*. *Evolution*, 4, 212–235.
- Eckert, C.G., Samis, K.E. & Lougheed, S.C. (2008). Genetic variation across species' geographical ranges: the central-marginal hypothesis and beyond. *Mol. Ecol.*, 17, 1170–1188.
- Hewitt, G.M. (1996). Some genetic consequences of ice ages, and their role in divergence and speciation. *Biol. J. Linn. Soc. Lond.*, 58, 247–276.
- Hillesheim, M.B., Hodell, D.A., Leyden, B.W., Brenner, M., Curtis, J.H., Anselmetti, F.S. et al. (2005). Climate change in lowland Central America during the late deglacial and early Holocene. *J. Quat. Sci.*, 20, 363–376.
- Hughes, A.L. & Hughes, M.A.K. (2007). Coding sequence polymorphism in avian mitochondrial genomes reflects population histories. *Mol. Ecol.*, 16, 1369–1376.
- Hughes, A.R., Inouye, B.D., Johnson, M.T.J., Underwood, N. & Vellend, M. (2008). Ecological consequences of genetic diversity. *Ecol. Lett.*, 11, 609–623.
- Jaarola, M. & Tegelström, H. (1995). Colonization history of north European field voles (*Microtus agrestis*) revealed by mitochondrial DNA. *Mol. Ecol.*, 4, 299–310.
- Jetz, W. & Rahbek, C. (2001). Geometric constraints explain much of the species richness pattern in African birds. *Proc. Natl Acad. Sci. USA*, 98, 5661–5666.
- Johansson, M., Primmer, C.R. & Merilä, J. (2006). History vs. current demography: explaining the genetic population structure of the common frog (*Rana temporaria*). *Mol. Ecol.*, 15, 975–983.
- Karr, J.R. & Freemark, K.E. (1983). Habitat selection and environmental gradients: dynamics in the "stable" tropics. *Ecology*, 64, 1481–1494.
- Lees, D.C., Kremen, C. & Andriamampianina, L. (1999). A null model for species richness gradients: bounded range overlap of butterflies and other rainforest endemics in Madagascar. *Biol. J. Linn. Soc.*, 67, 529–584.
- Lessa, E.P., Cook, J.A. & Patton, J.L. (2003). Genetic footprints of demographic expansion in North America, but not Amazonia, during the Late Quaternary. *Proc. Natl Acad. Sci. USA*, 100, 10331–10334.
- Leyden, B.W. (1984). Guatemalan forest synthesis after Pleistocene aridity. *Proc. Natl Acad. Sci. USA*, 81, 4856–4859.
- MacArthur, R.H. (1972). *Geographical Ecology: Patterns in the Distribution of Species*. Princeton University Press, Princeton, NJ.
- Mallet, J., Isaac, N.J.B. & Mace, G.M. (2005). Response to Harris and Froufe, and Knapp et al.: taxonomic inflation. *Trends Ecol. Evol.*, 20, 8–9.
- Marchant, R., Boom, A., Behling, H., Hooghiemstra, H., Melief, B., Van Geel, B. et al. (2004). Colombian vegetation at the Last Glacial Maximum: a comparison of model- and pollen-based biome reconstructions. *J. Quat. Sci.*, 19, 721–732.
- Martin, P.R. & McKay, J.K. (2004). Latitudinal variation in genetic divergence of populations and the potential for future speciation. *Evolution*, 58, 938–945.
- Merilä, J., Björklund, M. & Baker, A.J. (1997). Historical demography and present day population structure of the Greenfinch, *Carduelis chloris* – an analysis of mtDNA control-region sequences. *Evolution*, 51, 946–956.
- Milá, B., Girman, D.J., Kimura, M. & Smith, T.B. (2000). Genetic evidence for the effect of a postglacial population expansion on the phylogeography of a North American songbird. *Proc. R. Soc. Lond. B Biol. Sci.*, 267, 1033–1040.
- Miller, M.J., Birmingham, E., Klicka, J., Escalante, P., Raposo do Amaral, F.S., Weir, J.T. et al. (2008). Out of Amazonia again and again: episodic crossing of the Andes promotes diversification in a lowland forest flycatcher. *Proc. R. Soc. Lond. B Biol. Sci.*, 275, 1133–1142.
- Nei, M. (1987). *Molecular Evolutionary Genetics*. Columbia University Press, New York.
- Orians, G.H. (1969). The number of bird species in some tropical forests. *Ecology*, 50, 783–801.
- Orme, C., Davies, R., Burgess, M., Eigenbrod, F., Pickup, N., Olson, V. et al. (2005). Global hotspots of species richness are not congruent with endemism or threat. *Nature*, 436, 1016–1019.
- Phillips, O.L., Hall, P., Gentry, A.H., Sawyer, S.A. & Vasquez, R. (1994). Dynamics and species richness of tropical rain forests. *Proc. Natl Acad. Sci. USA*, 91, 2805–2809.
- Ridgway, T., Riginos, C., Davis, J. & Hoegh-Guldberg, O. (2008). Genetic connectivity patterns of *Pocillopora verrucosa* in southern African Marine Protected Areas. *Mar. Ecol. Prog. Ser.*, 354, 161–168.
- Rosenzweig, M.L. (1995). *Species Diversity in Space and Time*. Cambridge University Press, Cambridge.
- Rozas, J., Sánchez-Delbarrio, J.C., Messeguer, X. & Rozas, R. (2003). DnaSP, DNA polymorphism analyses by the coalescent and other methods. *Bioinformatics*, 19, 2496–2497.
- Sagarin, R. & Gaines, S. (2002). The 'abundant centre' distribution: to what extent is it a biogeographic rule?. *Ecol. Lett.*, 5, 137–147.
- Schneider, C. & Moritz, C. (1999). Rainforest refugia and evolution in Australia's Wet Tropics. *Proc. R. Soc. Lond. B Biol. Sci.*, 266, 191–196.
- Terborgh, J. (1973). On the notion of favorability in plant ecology. *Am. Nat.*, 197, 481–501.
- Vellend, M. (2003). Island Biogeography of genes and species. *Am. Nat.*, 162, 358–365.

- Vellend, M. & Geber, M.A. (2005). Connections between species diversity and genetic diversity. *Ecol. Lett.*, 8, 767–781.
- Vucetich, J.A. & Waite, T.A. (2003). Spatial patterns of demography and genetic processes across the species' range: Null hypotheses for landscape conservation genetics. *Conserv. Genet.*, 4, 639–645.
- Wehenkel, C., Bergmann, F. & Gregorius, H.-R. (2006). Is there a trade-off between species diversity and genetic diversity in forest tree communities? *Plant Ecol.*, 185, 151–161.
- Willig, M.R., Kaufman, D.M. & Stevens, R.D. (2003). Latitudinal gradients of biodiversity: pattern, process, scale and synthesis. *Annu. Rev. Ecol. Syst.*, 34, 273–309.

SUPPORTING INFORMATION

Additional Supporting Information may be found in the online version of this article:

Table S1 Effect of removing small sample-size populations on the test of an inverse relationship between latitude and nucleotide diversity.

Table S2 Effect of removing small sample-size populations on the test of whether the maximum π value occurs in edge populations less frequently than expected by chance.

Appendix S1 Specimens and tissue samples used in this study, with corresponding GenBank accession numbers.

Appendix S2 Number of breeding landbirds at four biological stations along a latitudinal gradient in the Neotropical lowlands north and west of the Andes.

Appendix S3 Relative abundances of populations of nine focal species of Neotropical landbirds near their range limits and in the centres of their ranges.

Appendix S4 Sample size analysis and permutations.

As a service to our authors and readers, this journal provides supporting information supplied by the authors. Such materials are peer-reviewed and may be re-organized for online delivery, but are not copy-edited or typeset. Technical support issues arising from supporting information (other than missing files) should be addressed to the authors.

Editor, Marcel Holyoak

Manuscript received 11 June 2009

First decision made 17 July 2009

Second decision made 30 December 2009

Manuscript accepted 18 January 2010

Comparative Genomics Reveals Evolution of a Beak Morphology Locus in a High-Altitude Songbird

Yalin Cheng ,¹ Matthew J. Miller,² Dezhi Zhang,¹ Gang Song,¹ Chenxi Jia,¹ Yanhua Qu,¹ and Fumin Lei*,^{1,3,4}

¹Key Laboratory of Zoological Systematics and Evolution, Institute of Zoology, Chinese Academy of Sciences, Beijing, China

²Sam Noble Oklahoma Museum of Natural History and Department of Biology, University of Oklahoma, Norman, OK

³University of Chinese Academy of Sciences, Beijing, China

⁴Center for Excellence in Animal Evolution and Genetics, Chinese Academy of Sciences, Kunming, China

*Corresponding author: E-mail: leifm@ioz.ac.cn.

Associate editor: Guang Yang

Raw reads are available in the NCBI Sequence Read Archive (PRJNA553273). Individual sequence accession numbers are provided in [supplementary table S2, Supplementary Material](#) online.

Abstract

The Ground Tit (*Pseudopodoces humilis*) has lived on the Qinghai-Tibet Plateau for ~5.7 My and has the highest altitudinal distribution among all parids. This species has evolved an elongated beak in response to long-term selection imposed by ground-foraging and cavity-nesting habits, yet the genetic basis for beak elongation remains unknown. Here, we perform genome-wide analyses across 14 parid species and identify 25 highly divergent genomic regions that are significantly associated with beak length, finding seven candidate genes involved in bone morphogenesis and remolding. Neutrality tests indicate that a model allowing for a selective sweep in the highly conserved *COL27A1* gene best explains variation in beak length. We also identify two nonsynonymous fixed mutations in the collagen domain that are predicted to be functionally deleterious yet may have facilitated beak elongation. Our study provides evidence of adaptive alleles in *COL27A1* with major effects on beak elongation of *Ps. humilis*.

Key words: genomics, beak, adaptation, major effect, fixation.

The avian beak has a multitude of forms, which is the consequence of the variety of functions that beaks serve (e.g., foraging, preening, nest-building, cavity excavation) and the diversity of habitats where birds live. As a result, the beak is a highly evolvable structure that permits birds to rapidly respond to environmental changes (Grant and Grant 2011). However, the high plasticity and diversity of beak morphology, along with the fact that beak shape, like most quantitative phenotypes (Yang et al. 2011), is a polygenic trait (Bosse et al. 2017), presents challenges to our understanding of the genetic mechanisms underlying beak evolution. Under the polygenic model, natural selection often acts on many loci simultaneously (Pritchard et al. 2010), resulting in the combination of a few loci with major effects and many loci with small effects controlling adaptive changes in phenotypes (Orr 1998; Rockman 2012). Due to the characteristics of being more likely to be fixed by strong selective coefficients (Olson-Manning et al. 2012) and less susceptible to loss by genetic drift (Kimura 1962), major loci with high allele frequency may be more relevant to phenotypes and easier to be detected from the genome. As a result, previous studies have identified species-specific major genes affecting distinct beak morphology in chickens (Wu et al. 2004), Darwin's finches

(Abzhanov et al. 2004; Mallarino et al. 2011; Lamichhaney et al. 2016), and great tits (Bosse et al. 2017).

Around 5.7 Ma, the Ground Tit (*Pseudopodoces humilis*; Aves: Paridae) split from a common ancestor with genus *Machlolophus* and colonized the Qinghai-Tibet Plateau (QTP) (Qu et al. 2013; Cheng YL, unpublished data). As a result of millions of years of isolation in this sparsely vegetated and high-altitude environment (fig. 1a), *Ps. humilis* has evolved pale plumage, large body size, long tarsi, and a long-decurved beak (Qu et al. 2013; Shao et al. 2016; Gosler et al. 2019). Because of phenotypic similarities with ground jays, for over a century *Ps. humilis* was believed to be a member of the family Corvidae (Monroe and Sibley 1993; Hume 2008). After molecular systematics recognized it as the largest of parids (James et al. 2003), many studies have attempted to understand which processes underlie this unique phenotype and how genetic changes control its development. Morphological analyses found significant correlations of tarsus length and beak morphology with altitude, suggesting that long tarsi and a long-decurved beak are the result of ground-living in open plateau habitats (Shao et al. 2016). Comparative transcriptomic analyses identified differential expression of genes involved in skeletal development that

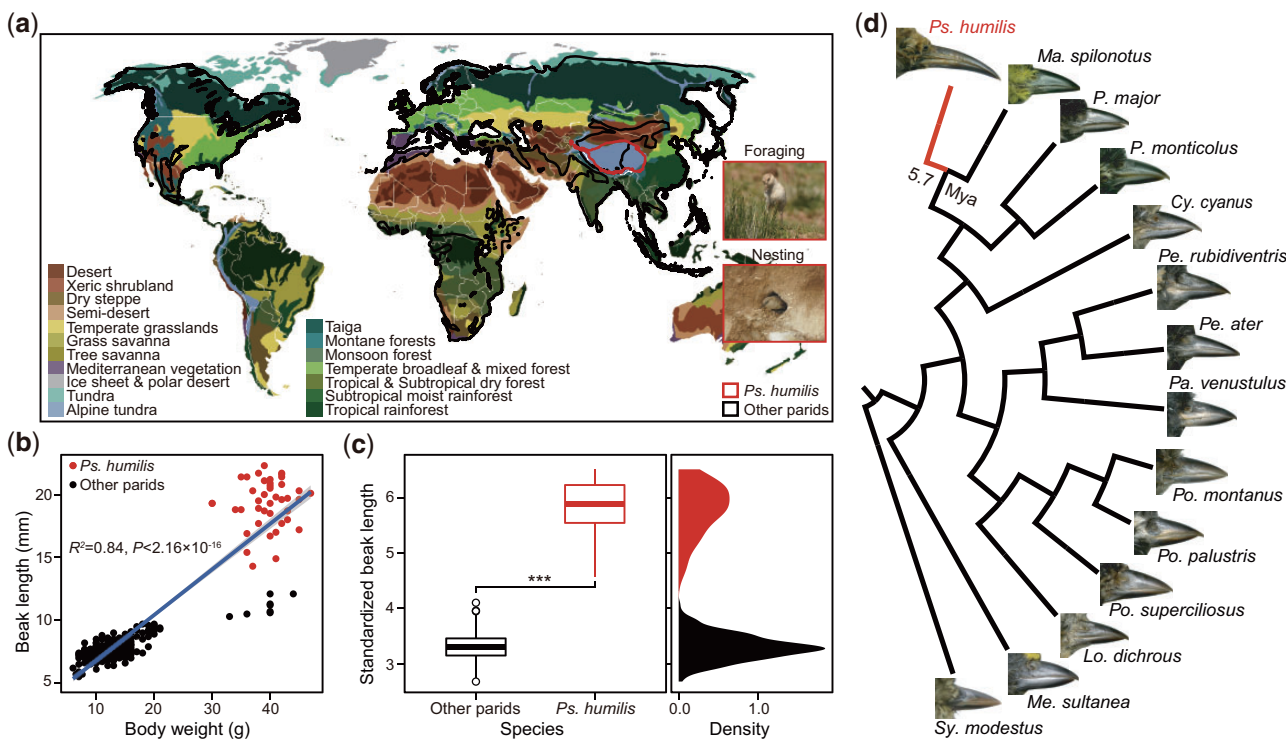


Fig. 1. Long beaks in response to ground-living habits. (a) Vegetation types in the distribution ranges of tits and chickadees (Paridae). Only *Pseudopodoces humilis* lives in open steppe habitats of the QTP. (b) Significant correlation between beak length and body weight. (c) Standardized beak length of *Ps. humilis* is significantly longer than that of other parids. (d) Beak images of 14 parid species. These images are from Cheng et al. (2017), which shows the distinct beak morphology between *Ps. humilis* and other 13 parids. Mya indicates million years ago. The vegetation map was downloaded from Wikipedia (<https://en.wikipedia.org/wiki/Vegetation#/media/File:Vegetation-no-legend.PNG>, last accessed March 9, 2020). Distribution maps of parids downloaded from BirdLife International (<http://datazone.birdlife.org/>, last accessed April 16, 2020) were projected onto the vegetation map in ArcGIS v10.0 (ESRI, Redlands, CA).

probably affect beak morphogenesis (Cheng et al. 2017). However, to date, adaptive alleles at major loci responsible for the morphological transformation of the beak in *Ps. humilis* remain unknown. Here, we use whole-genome sequences of 14 parid species (supplementary table S1, Supplementary Material online), to compare the long-beaked *Ps. humilis* with short-beaked parids via the integration of multiple genome-wide scanning analyses. Furthermore, we assess the selection signals and predicted the function for mutations in candidate genes.

Results and Discussion

Morphological traits are commonly correlated with body size, which may veil adaptive variation. In 14 parids, we found that body length, wing length, tail length, tarsus length, and beak length were strongly correlated with body weight ($r = 0.46\text{--}0.92$; fig. 1b; supplementary fig. S1a, Supplementary Material online). Among these measurements, both tarsus length and beak length are strikingly larger in *Ps. humilis* in relative to all other 13 parids (fig. 1b; supplementary fig. S1a, Supplementary Material online), even after standardizing for body weight differences (fig. 1c; supplementary fig. S1b, Supplementary Material online). In fact, after standardizing for body weight, the difference in beak length between *Ps. humilis* and the other parids was the most extreme of all of our measurements (Wilcoxon-rank sum = 0,

$P < 2.16 \times 10^{-16}$; fig. 1c; supplementary fig. S1b, Supplementary Material online), suggesting that the elongated beak may be the most adaptive morphological change in *Ps. humilis*, allowing for ground-foraging and burrow-nesting in the open steppe QTP habitat (fig. 1a and d).

Candidate Genes Correlated with Beak Length

To identify genes controlling beak elongation, we calculated Z-transformed F_{ST} (ZF_{ST}) values between the long-beaked *Ps. humilis* and the short-beaked group (the other 13 species) to identify highly divergent regions (supplementary table S2, Supplementary Material online). Mantel tests (Mantel 1967) identify outliers between two distance matrices and can identify nonneutral phenotypic evolution (Ho et al. 2017); here, we performed partial Mantel tests (PMT) to look for outliers between the F_{ST} matrix and the difference matrix of body weight-standardized beak lengths across these 14 species (supplementary fig. S2, Supplementary Material online).

The F_{ST} analysis identified 202 highly diverged windows ($ZF_{ST} > 2.69$ for autosomes, $ZF_{ST} > 2.63$ for chromosome Z), whereas the PMT identified 258 significantly correlated windows ($-\log_{10}P > 1.30$) (fig. 2a), with 25 windows shared between the two sets (supplementary fig. S3, Supplementary Material online). We assume these 25 regions are most likely to be under divergent selection. We used SnpEff v4.3 (Cingolani et al. 2012) to annotate genes and predict gene

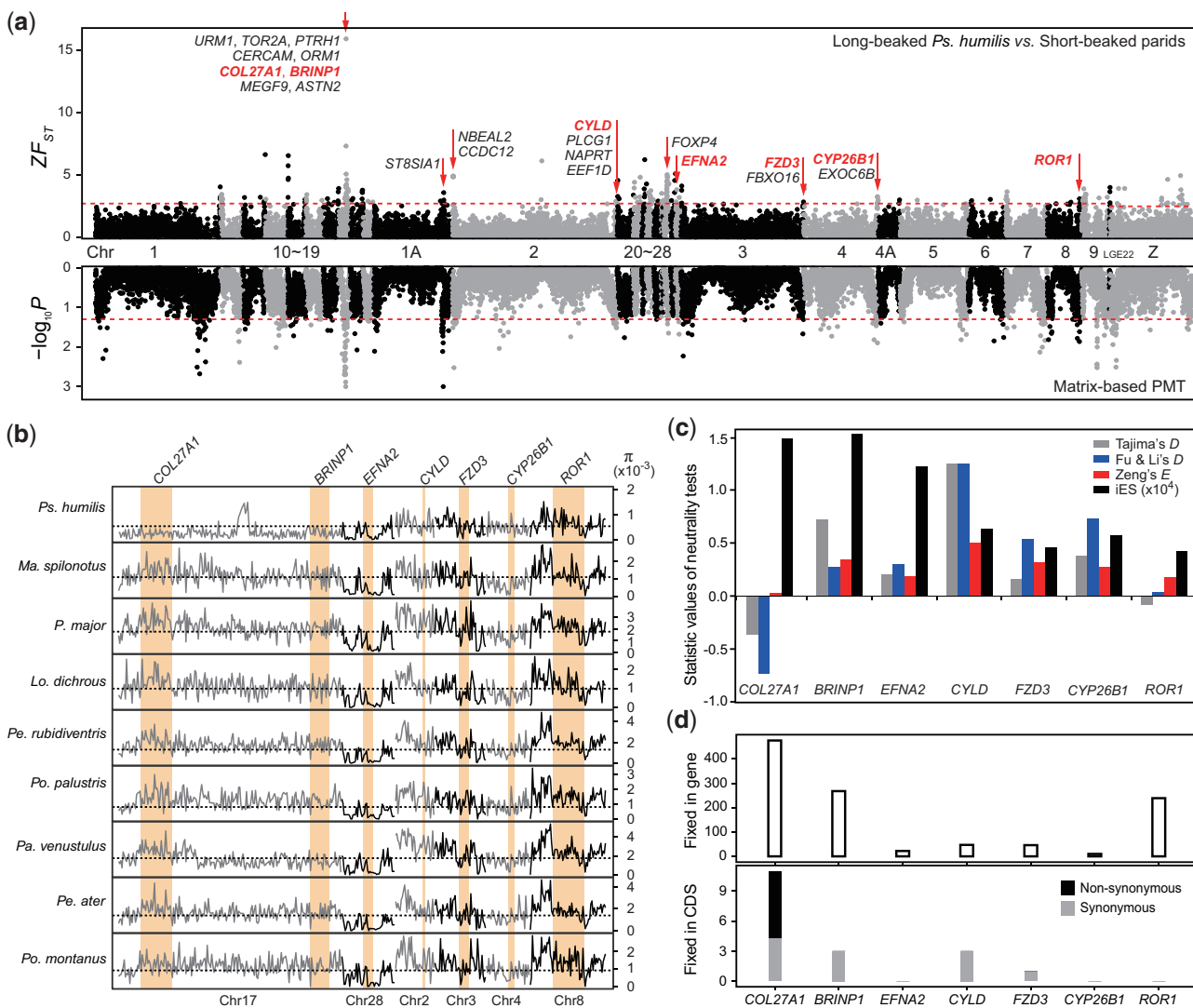


Fig. 2. Screening for candidate genes associated with beak length. (a) Genome-wide F_{ST} analysis between long-beaked *Pseudopodoces humilis* and short-beaked parids (upper panel), and partial Mantel tests (PMT) between pairwise F_{ST} matrix and a pairwise difference matrix of beak lengths (lower panel). Red dash lines represent cutoff values in both analyses. Red arrows indicate regions identified as outliers in both F_{ST} and PMT analyses. Candidate genes are in bold and red. (b) Nucleotide diversity of the seven candidate genes in species with sample sizes >5 , orange shading covers the regions of these genes, and dashed lines show the mean nucleotide diversity of each species. (c) Neutrality tests for the seven candidate genes within *Ps. humilis*; negative Tajima's D and Fu & Li's D , nearly zero for Zeng's E , and high iES are signals of positive selection. (d) Count of fixed sites in the seven genes. *COL27A1* had the most fixed sites between the two groups across the entire gene (introns and exons) and only the coding regions (CDS).

function in each of these. We found 23 genes in our windows, seven of which were functionally annotated as candidate genes involved in bone morphogenesis and remodeling (supplementary fig. S4, Supplementary Material online), including frizzled-3 (FZD3), receptor tyrosine kinase-like orphan receptor 1 (ROR1), BMP/retinoic acid-inducible neural-specific protein 1 (BRINP1), cytochrome P450 26B1 (CYP26B1), collagen alpha-1(XXVII) chain (COL27A1), ubiquitin carboxyl-terminal hydrolase CYLD, and ephrin-A2 (EFNA2) (fig. 2a; supplementary table S3, Supplementary Material online). Although these genes have not been found to be related to beak morphology in other birds (Lamichhaney et al. 2015, 2016; Bosse et al. 2017), their functional pathways play roles in beak development (Mallarino et al. 2011; Medio et al. 2012;

Elba et al. 2015). Our previous analysis also indicated that transcriptional changes in genes related to bone morphogenesis and remodeling affect beak development in embryos of *Ps. humilis* (Cheng et al. 2017).

FZD3 and ROR1 were associated with the most significant ontology term “Wnt-protein binding” (GO: 0017147) ($P = 7.5 \times 10^{-4}$; supplementary fig. S4, Supplementary Material online) involved in the Wnt signaling pathway, which is known to promote osteoblast differentiation (Hartmann 2006) and which plays role in beak morphogenesis (Medio et al. 2012). Multiple studies have reported other Wnt-protein binding genes, such as FZD1 (Brugmann et al. 2010), DKK3 (Mallarino et al. 2011), FRZB1, and WIF1 (Cheng et al. 2017), as responsible for craniofacial or beak

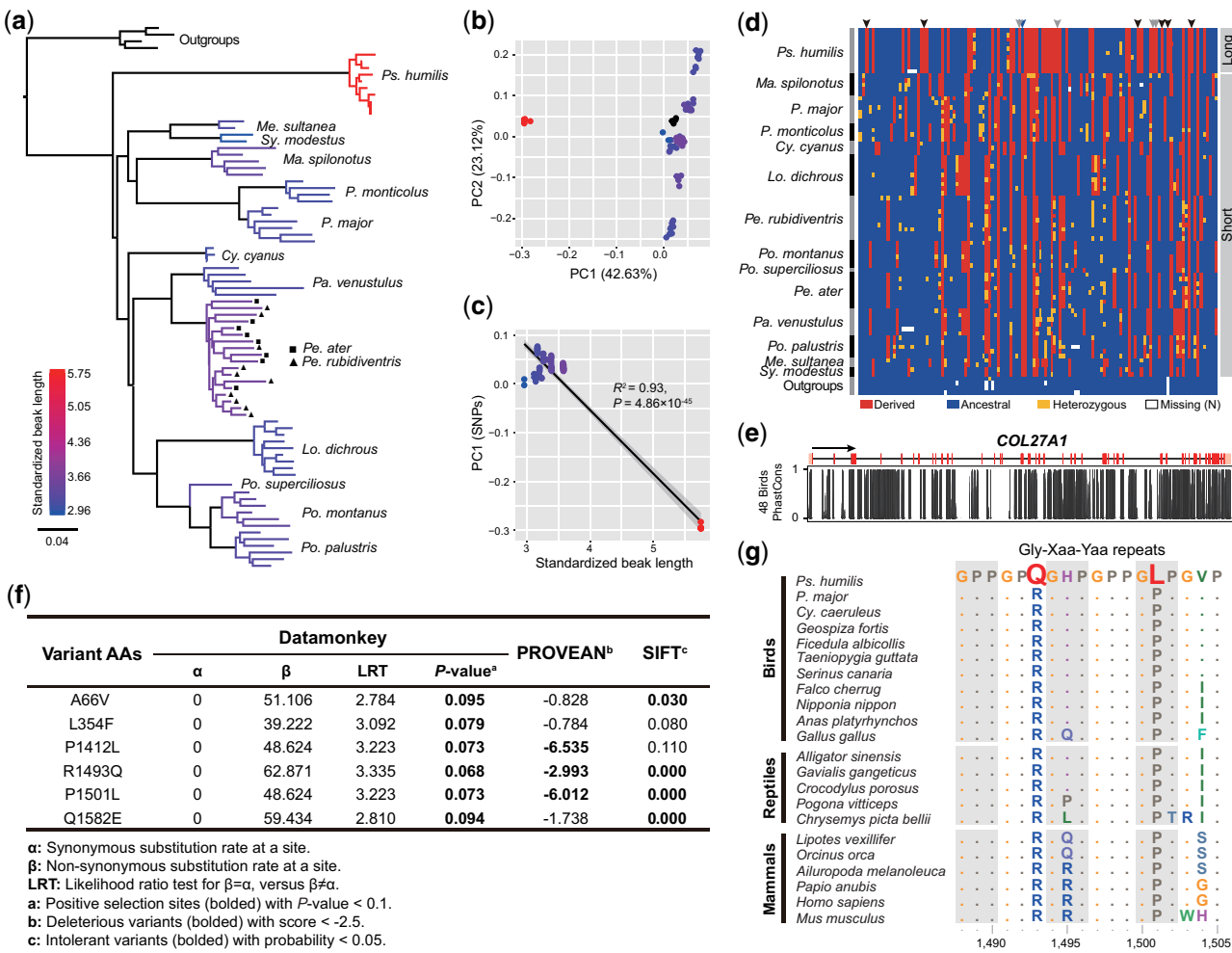


Fig. 3. *COL27A1* genotypes and adaptive SNPs affect beak length. (a) A phylogenetic tree based on *COL27A1* coding region SNPs. Branches are colored by beak length. (b) PCA analysis of all *COL27A1* coding SNPs; *Pseudopodoces humilis* is separated from other parids. (c) Significant correlation between beak length and PC1. (d) Genotypes at all coding SNPs, showing striking difference between *Ps. humilis* and other parids. Fixed SNPs are indicated with arrows; black and gray arrows indicate nonsynonymous and synonymous derived sites, respectively, blue arrows indicate ancestral sites. Outgroup genotypes determined allele states of parids. (e) Conservation of nucleotide bases in *COL27A1* among 48 avian species based on PhastCons scores from Zhang et al. (2014). (f) Selection detection and function predictions for the six completely fixed nonsynonymous substitutions in *COL27A1*. All nonsynonymous mutations are under positive selection, and only two mutations are intolerant. (g) Conservation of the two deleterious amino acid sites among birds, reptiles, and mammals. These two mutations occur only in *Ps. humilis*.

development at the expression level. *BRINP1* and *CYP26B1* respond to retinoic acid, which is required for facial morphogenesis in chickens (Lee et al. 2001; Schneider et al. 2001). Mutations in *CYP26B1* result in craniofacial disorders in mice and zebra fish (Yashiro et al. 2004; Laue et al. 2011). *COL27A1*, located in one of the three most significant outlying regions (fig. 2a; supplementary table S2, Supplementary Material online), is a type XXVII collagen gene, and plays a role in the transition of cartilage to bone during bone morphogenesis (Hjorten et al. 2007). A homologous gene of *COL27A1*, *COL4A5* is associated with the elongated beak of *Parus major* as a response to supplementary feeding at bird feeders (Bosse et al. 2017). *CYLD* and *EFNA2* were also identified to be under likely divergent selection but they did not have the highest Z_{ST} values; however, they are associated with osteoclast differentiation participating bone resorption that negatively affects beak length (Ealba et al. 2015). Interestingly, *FGF13* and *ITGB3*—two genes associated with beak development that

we previously found to be differently expressed between *Ps. humilis* and *P. major* (Cheng et al. 2017)—were not identified as candidate genes in this analysis.

Strong Selection on One Locus

To detect the strength of selection on the seven candidate genes, we calculated multiple statistics to test their evolutionary neutrality. Among the seven genes, only *COL27A1* had reduced nucleotide diversity in *Ps. humilis* and elevated diversity in other parids (fig. 2b). Furthermore, *COL27A1* had a long haplotype block (IES = 1.49×10^4), whereas neutrality test values for Tajima's D (-0.36) (Tajima 1989), Fu & Li's D (-0.73) (Fu and Li 1993), and Zeng's E (0.02) (Zeng et al. 2006) were consistent with strong positive selection (fig. 2c). Furthermore, *COL27A1* had the highest frequency of completely fixed sites in introns and exons (476) and in just exons (11) (fig. 2d). Phylogenetic analysis of *COL27A1* exonic SNPs shows reciprocal monophly and deep divergence between *Ps. humilis* and other parids

(fig. 3a) but not in a data set of SNPs from both exons and introns (supplementary fig S5, Supplementary Material online). Collectively, these results suggest that COL27A1 underwent strong divergent selection in *Ps. humilis*, with most molecular evolution occurring in coding regions.

Principal component analysis (PCA) for COL27A1 coding region SNPs separated long-beaked *Ps. humilis* from the short-beaked parids (fig. 3b), and PC1 was significantly correlated with beak length ($r = -0.96$, $P = 4.86 \times 10^{-45}$; fig. 3c). Short branch lengths in the gene tree and low variation in PC values within *Ps. humilis* were associated with low genetic variation in COL27A1 (fig. 3a and b). We observed the highest level of derived homozygous genotypes in *Ps. humilis*, with only five heterozygous sites (fig. 3d), which is consistent with a selective sweep (Nielsen 2005). A selective sweep is also supported by the high ratio of fixed SNPs to all coding SNPs (11/120). All but one of the fixed SNPs were derived, as determined by comparison with outgroup sequences (fig. 3d). Among the ten derived fixed SNPs, six were nonsynonymous, and the remaining four were synonymous (fig. 3d; supplementary table S4, Supplementary Material online). Given the highly conserved nature of COL27A1 across 48 birds (Zhang et al. 2014) (fig. 3e), the high ratio of nonsynonymous to synonymous substitutions observed here (6/4) is likely to result in protein function change.

Potential Adaptive Substitutions in COL27A1

To assess selection signals and predict function for the six nonsynonymous substitutions, we reconstructed COL27A1 coding sequences (CDS) for each species using our high-coverage SNP data (supplementary fig. S6, Supplementary Material online). We compared our constructed sequences with the *Ps. humilis* published sequence (XM_014256225.1) and found high identity between them, especially at fixed sites, suggesting that our constructed CDS are accurate. We performed a selection analysis in Datammonkey (Weaver et al. 2018) on the COL27A1 alignment across all 14 parid species. All six nonsynonymous substitutions were identified as under positive selection (fig. 3f). Likewise, functional prediction from PROVEAN (Protein Variation Effect Analyzer) (Choi and Chan 2015) and SIFT (Sorting Intolerant From Tolerant) (Kumar et al. 2009), respectively, classed three and four substitutions as intolerant, including two substitutions (R1493Q and P1501L) identified as intolerant in both predictions (fig. 3f). These two mutations occur in a Gly-Xaa-Yaa repeat region of the collagen domain (supplementary fig. S7, Supplementary Material online), which determines the structure and property of type XXVII collagen (Pace et al. 2003). Mutations in this region would likely change the biological function of COL27A1 protein, leading to skeletal abnormalities, such as a long and oval-shaped face (Gonzaga-Jauregui et al. 2015), chondrodysplasia (Plumb et al. 2011), and scoliosis (Christiansen et al. 2009). These two amino acid sites show high conservation among birds, reptiles, and mammals, which supports the hypothesis that these two missense mutations in *Ps. humilis* may have caused a fundamental change in beak form (fig. 3g), ultimately allowing for adaptive elongation of the beak.

Conclusion

The prominent beak of *Ps. humilis* is likely the result of adaptation for foraging and cavity nest excavation in open habitats of the QTP. F_{ST} and PMT analyses across 14 parid species identify 25 genomic regions under divergent selection that correlate to beak length and contain seven candidate genes known to be involved in bone morphogenesis and remodeling. Among these genes, only COL27A1 appears to have experienced a selective sweep in *Ps. humilis*. Additionally, COL27A1 has high fixation probability and high homozygosity, especially in the coding region. All non-synonymous fixed substitutions show evidence of positive selection, but being part of a single linkage group, we cannot determine whether all five were targets of selection. However, the two substitutions in the collagen domain are predicted to be deleterious; and likely lead to large changes in COL27A1 protein function. These findings suggest that COL27A1 has major effects on the extreme beak evolution in *Ps. humilis*.

Materials and Methods

A complete description of our methods is provided in the Supplementary Material online.

Supplementary Material

Supplementary data are available at Molecular Biology and Evolution online.

Acknowledgments

This work was supported by the National Natural Science Foundation of China (Grant Nos. 31630069 and 31900320). The field work of sample collection was supported by the Second Tibetan Plateau Scientific Expedition and Research (STEP) program (Grant Nos. 2019QZKK0304 and 2019QZKK0501). The authors wish to thank A. Townsend Peterson for helpful discussion. They also thank the editor and two anonymous reviewers for their valuable comments and suggestions.

Author Contributions

F.L. and Y.C. designed this research. Y.C., M.J.M., and D.Z. analyzed the data. All authors wrote and approved the article.

References

- Abzhanov A, Protas M, Grant BR, Grant PR, Tabin CJ. 2004. Bmp4 and morphological variation of beaks in Darwin's finches. *Science* 305(5689):1462–1465.
- Bosse M, Spurgin LG, Laine VN, Cole EF, Firth JA, Gienapp P, Gosler AG, McMahon K, Poissant J, Verhagen I, et al. 2017. Recent natural selection causes adaptive evolution of an avian polygenic trait. *Science* 358(6361):365–368.
- Brugmann SA, Powder KE, Young NM, Goodnough LH, Hahn SM, James AW, Helms JA, Lovett M. 2010. Comparative gene expression analysis of avian embryonic facial structures reveals new candidates for human craniofacial disorders. *Hum Mol Genet*. 19(5):920–930.
- Cheng Y, Gao B, Wang H, Han N, Shao S, Wu S, Song G, Zhang YE, Zhu X, Lu X, et al. 2017. Evolution of beak morphology in the Ground Tit revealed by comparative transcriptomics. *Front Zool*. 14(1):58.

- Choi Y, Chan AP. 2015. PROVEAN web server: a tool to predict the functional effect of amino acid substitutions and indels. *Bioinformatics* 31(16):2745–2747.
- Christiansen HE, Lang MR, Pace JM, Parichy DM. 2009. Critical early roles for col27a1a and col27a1b in zebrafish notochord morphogenesis, vertebral mineralization and post-embryonic axial growth. *PLoS One* 4(12):e8481.
- Cingolani P, Platts A, Wang LL, Coon M, Nguyen T, Wang L, Land SJ, Lu XY, Ruden DM. 2012. A program for annotating and predicting the effects of single nucleotide polymorphisms, SnpEff: SNPs in the genome of *Drosophila melanogaster* strain w(1118); iso-2; iso-3. *Fly* 6(2):80–92.
- Ealba EL, Jheon AH, Hall J, Curantz C, Butcher KD, Schneider RA. 2015. Neural crest-mediated bone resorption is a determinant of species-specific jaw length. *Dev Biol.* 408(1):151–163.
- Fu YX, Li WH. 1993. Statistical tests of neutrality of mutations. *Genetics* 133(3):693–709.
- Gonzaga-Jauregui C, Gamble CN, Yuan B, Penney S, Jhangiani S, Muzny DM, Gibbs RA, Lupski JR, Hecht JT. 2015. Mutations in COL27A1 cause Steel syndrome and suggest a founder mutation effect in the Puerto Rican population. *Eur J Hum Genet.* 23(3):342–346.
- Gosler AG, Clement P, Bonan A. 2019. Tits and Chickadees (Paridae). In: Del Hoyo J, Elliott A, Sargatal J, Christie DA, de Juana E, editors. *Handbook of the birds of the world*. Barcelona: Lynx Edicions.
- Grant PR, Grant BR. 2011. How and why species multiply: the radiation of Darwin's finches. Princeton: Princeton University Press.
- Hartmann C. 2006. A Wnt canon orchestrating osteoblastogenesis. *Trends Cell Biol.* 16(3):151–158.
- Hjorten R, Hansen U, Underwood RA, Telfer HE, Fernandes RJ, Krakow D, Sebald E, Wachsmann-Hogiu S, Bruckner P, Jacquet R, et al. 2007. Type XXVII collagen at the transition of cartilage to bone during skeletogenesis. *Bone* 41(4):535–542.
- Ho W-C, Ohya Y, Zhang J. 2017. Testing the hypothesis of neutral evolution. *Proc Natl Acad Sci U S A.* 114(46):12219–12224.
- Hume A. 2008. Stray notes on ornithology in India. *Ibis* 13(1):23–38.
- James HF, Ericson PCG, Slikas B, Lei FM, Gill FB, Olson SL. 2003. *Pseudopodoces humilis*, a misclassified terrestrial tit (Paridae) of the Tibetan Plateau: evolutionary consequences of shifting adaptive zones. *Ibis* 145(2):185–202.
- Kimura M. 1962. On the probability of fixation of mutant genes in a population. *Genetics* 47:713–719.
- Kumar P, Henikoff S, Ng PC. 2009. Predicting the effects of coding non-synonymous variants on protein function using the SIFT algorithm. *Nat Protoc.* 4(7):1073–1082.
- Lamichhaney S, Berglund J, Almen MS, Maqbool K, Grabherr M, Martinez-Barrio A, Promerova M, Rubin CJ, Wang C, Zamani N, et al. 2015. Evolution of Darwin's finches and their beaks revealed by genome sequencing. *Nature* 518(7539):371–375.
- Lamichhaney S, Han F, Berglund J, Wang C, Almen MS, Webster MT, Grant BR, Grant PR, Andersson L. 2016. A beak size locus in Darwin's finches facilitated character displacement during a drought. *Science* 352(6284):470–474.
- Laue K, Pogoda HM, Daniel PB, van Haeringen A, Alanay Y, von Ameln S, Rachwalski M, Morgan T, Gray MJ, Breuning MH, et al. 2011. Craniostenosis and multiple skeletal anomalies in humans and zebrafish result from a defect in the localized degradation of retinoic acid. *Am J Hum Genet.* 89(5):595–606.
- Lee SH, Fu KK, Hui JN, Richman JM. 2001. Noggin and retinoic acid transform the identity of avian facial prominences. *Nature* 414(6866):909–912.
- Mallarino R, Grant PR, Grant BR, Herrel A, Kuo WP, Abzhanov A. 2011. Two developmental modules establish 3D beak-shape variation in Darwin's finches. *Proc Natl Acad Sci U S A.* 108(10):4057–4062.
- Mantel N. 1967. The detection of disease clustering and a generalized regression approach. *Cancer Res.* 27(2):209–220.
- Medio M, Yeh E, Popelut A, Babajko S, Berdal A, Helms JA. 2012. Wnt/beta-catenin signaling and Msx1 promote outgrowth of the maxillary prominences. *Front Physiol.* 3:375.
- Monroe BLJ, Sibley CG. 1993. A world checklist of birds. New Haven: Yale University Press.
- Nielsen R. 2005. Molecular signatures of natural selection. *Annu Rev Genet.* 39(1):197–218.
- Olson-Manning CF, Wagner MR, Mitchell-Olds T. 2012. Adaptive evolution: evaluating empirical support for theoretical predictions. *Nat Rev Genet.* 13(12):867–877.
- Orr HA. 1998. The population genetics of adaptation: the distribution of factors fixed during adaptive evolution. *Evolution* 52(4):935–949.
- Pace JM, Corrado M, Missero C, Byers PH. 2003. Identification, characterization and expression analysis of a new fibrillar collagen gene, COL27A1. *Matrix Biol.* 22(1):3–14.
- Plumb DA, Ferrara L, Torbica T, Knowles L, Mironov A Jr, Kadler KE, Briggs MD, Boot-Hanford RP. 2011. Collagen XXVII organizes the pericellular matrix in the growth plate. *PLoS One* 6(12):e29422.
- Pritchard JK, Pickrell JK, Coop G. 2010. The genetics of human adaptation: hard sweeps, soft sweeps, and polygenic adaptation. *Curr Biol.* 20(4):208–215.
- Qu YH, Zhao HF, Han NJ, Zhou G, Song G, Gao B, Tian SL, Zhang J, Zhang R, Meng X, et al. 2013. Ground tit genome reveals avian adaptation to living at high altitudes in the Tibetan plateau. *Nat Commun.* 4(1):2071.
- Rockman MV. 2012. The QTN program and the alleles that matter for evolution: all that's gold does not glitter. *Evolution* 66(1):1–17.
- Schneider RA, Hu D, Rubenstein JLR, Maden M, Helms JA. 2001. Local retinoid signaling coordinates forebrain and facial morphogenesis by maintaining FGF8 and SHH. *Development* 128(14):2755–2767.
- Shao S, Quan Q, Cai T, Song G, Qu Y, Lei F. 2016. Evolution of body morphology and beak shape revealed by a morphometric analysis of 14 Paridae species. *Front Zool.* 13(1):30.
- Tajima F. 1989. Statistical-method for testing the neutral mutation hypothesis by DNA polymorphism. *Genetics* 123(3):585–595.
- Weaver S, Shank SD, Spielman SJ, Li M, Muse SV, Pond S. 2018. Datamonitor 2.0: a modern web application for characterizing selective and other evolutionary processes. *Mol Biol Evol.* 35(3):773–777.
- Wu P, Jiang TX, Suksaweang S, Widelitz RB, Chuong CM. 2004. Molecular shaping of the beak. *Science* 305(5689):1465–1466.
- Yang J, Manolio TA, Pasquale LR, Boerwinkle E, Caporaso N, Cunningham JM, de Andrade M, Feenstra B, Feingold E, Hayes MG, et al. 2011. Genome partitioning of genetic variation for complex traits using common SNPs. *Nat Genet.* 43(6):519–544.
- Yashiro K, Zhao XL, Uehara M, Yamashita K, Nishijima M, Nishino J, Sajioh Y, Sakai Y, Hamada H. 2004. Regulation of retinoic acid distribution is required for proximodistal patterning and outgrowth of the developing mouse limb. *Dev Cell.* 6(3):411–422.
- Zeng K, Fu YX, Shi SH, Wu CI. 2006. Statistical tests for detecting positive selection by utilizing high-frequency variants. *Genetics* 174(3):1431–1439.
- Zhang GJ, Li C, Li QY, Li B, Larkin DM, Lee C, Storz JF, Antunes A, Greenwald MJ, Meredith RW, et al. 2014. Comparative genomics reveals insights into avian genome evolution and adaptation. *Science* 346(6215):1311–1320.

1 **Title**

2 Parallel genomic responses to historical climate change and high elevation in East Asian
3 songbirds

4 **Short title:** Parallel genomic evolution in East Asian tits

5 **Authors**

6 Yalin Cheng^{1,2,†}, Matthew J. Miller^{3,4,†}, Dezhi Zhang¹, Ying Xiong^{1,2}, Yan Hao^{1,2}, Chenxi Jia¹,
7 Tianlong Cai^{1,2}, Shou-Hsien Li⁵, Ulf S. Johansson⁶, Yang Liu⁷, Yongbin Chang^{1,2}, Gang Song¹,
8 Yanhua Qu¹ and Fumin Lei^{1,2,8,*}

9 **Affiliations**

10 ¹Key Laboratory of Zoological Systematics and Evolution, Institute of Zoology, Chinese
11 Academy of Sciences, Beijing 100101, China

12 ²University of Chinese Academy of Sciences, Beijing 100049, China

13 ³Department of Anthropology, Pennsylvania State University, Pennsylvania, USA

14 ⁴University of Alaska Museum, University of Alaska Fairbanks, Alaska, USA

15 ⁵Department of Life Sciences, National Taiwan Normal University, Taipei, 116, Taiwan, China

16 ⁶Department of Zoology, Swedish Museum of Natural History, Box 50007, SE-104 05 Stockholm,
17 Sweden

18 ⁷State Key Laboratory of Biocontrol, Department of Ecology/School of Life Sciences, Sun Yat-
19 sen University, Guangzhou, 510275, Guangdong, China

20 ⁸Center for Excellence in Animal Evolution and Genetics, Chinese Academy of Sciences,
21 Kunming, 650223, China

22 [†]These authors contributed equally to this work.

23 ***Corresponding author:** Fumin Lei, E-mail: leifm@ioz.ac.cn

24 **Abstract**

25 Parallel genomic evolution may be expected in organisms that co-occur in landscapes in which
26 environments shift over space and time. Among 19 East Asian parid species (“tits and
27 chickadees”), we found that species from the Pleistocene unglaciated eastern lowlands showed
28 consistent high genomic diversity and signatures of late Pleistocene stability or expansion, while
29 all parids from the glaciated western highlands showed low genomic diversity and late
30 Pleistocene demographic contraction. Comparisons between closely related high- and low-
31 elevation parids reveal no evidence for convergent adaptation in any single mutation or gene, nor
32 evidence for a common toolkit of high-elevation genes. Instead, each has distinct highly
33 differentiated outlier genomic regions each over-represented by hypoxia-related genes and *a*
34 *priori* hypothesized functional pathways enriched more often than expected by chance. These
35 results suggest that historical demographic change leaves predictable genome-wide signatures
36 while contemporary adaptation is characterized by parallel evolution at functional, rather than
37 genic levels.

38

39 **Introduction**

40 For many plants and animals, Pleistocene climate change substantially altered their
41 geographic range and population size (1) and often left an imprint on genetic diversity (2). At the
42 same time, the pervasive hypoxia encountered in the Earth’s montane regions has been shown to
43 exert strong selective pressure (3-5), especially in endotherms that are unable to reduce metabolic
44 output as a response to the reduced partial pressure of atmospheric oxygen (6). However, it remains
45 unclear the extent to which animal genomes respond predictably to demographic and selective
46 pressures caused by complex patterns of historical and contemporary environmental variation.

47 East Asia is a region of extreme environmental variation. Most of the east is at or near sea
48 level, but western East Asia is dominated by the Qinghai–Tibet Plateau (QTP), with an average

49 elevation above 4,500 meters (Fig. 1A). During the Pleistocene, the region's western highlands
50 (WH) were covered by glaciers, whereas the eastern lowlands (EL) were largely ice free (7-9).
51 Presently, in contrast to the near sea level EL, the WH, especially the QTP, is characterized by
52 several extreme environmental conditions including low availability of oxygen and colder annual
53 temperatures that provide strong selective pressures driving local adaptation (10-12).

54 The tits and chickadees (Passeriformes: Paridae) are an avian lineage with low dispersal
55 ability that originated in the Sino-Himalayas (13) and are distributed in both EL (down to sea
56 level) and WH (up to 5,500 m). Phylogeographic studies (based on mitochondrial DNA) of bird
57 species with ranges that span the WH and the EL show a consistent pattern of lack of gene flow
58 and population differentiation that dates to the Early-Mid Pleistocene or earlier, likely driven by
59 ecological differences between WH and EL, as well as physical barriers to gene flow (14-17).
60 These studies also indicate that EL birds show demographic signals of population expansion
61 during the late Pleistocene, whereas WH birds show evidence of reduced genetic diversity, which
62 may be the result of population contraction, but could also be the consequence of adaptation to
63 life at high elevation. East Asian parids show evidence for various genomic adaptations to life at
64 the extreme high elevations found in much of the WH. Populations of the Great Tit (*Parus major*)
65 have elevationally divergent alpha-hemoglobin genes (18), while a comparative transcriptomic
66 analysis between two WH native parids (*Lophophanes dichrous* and *Periparus rubidiventris*)
67 detected similarity in genes associated with high-altitude adaptations at the gene-expression level
68 (19). However, the QTP-native *Pseudopodoces humilis* and the widespread *P. major* evolved
69 distinct adaptive responses for increased energy metabolism in order to cope with high elevation:
70 *Ps. humilis* shows enrichment of fatty acid metabolism (12), whereas high elevation populations
71 of *P. major* show positive selection in genes associated with carbohydrate metabolism (20). Here,
72 we analyze genome data from all 19 extant East Asian tit species to identify patterns of shared
73 genetic variation and selection. Contemporary and historical variation in environments across

74 East Asia provides a rare opportunity to investigate the degree of parallelism in closely related
75 species' responses to shared extreme environmental variation across space and time.

76

77 **Results**

78 **Sequence analysis and time trees**

79 We sequenced whole genomes from 19 parid species ($n = 87$) and two species from the closely
80 related Remizidae ($n = 4$; Fig 1A) to a mean genome-wide depth of coverage of $18.7\times$ (10.2–
81 47.8×) per individual. On average 95% (71%–98%) of the reads aligned to the chromosome-
82 assembled *P. major* reference genome (21) (fig. S1) and resulted in a dataset of 43,458,033 single
83 nucleotide polymorphisms (SNPs; table S1).

84 Phylogenies constructed from this SNP dataset consistently recovered a single identical
85 topology with fully supported nodes for all 19 parid species, irrespective of tree-building method
86 or whether we used only autosomal SNPs or only Z-linked SNPs (fig. S2). We converted this
87 phylogeny to a timetree using the coding genes from the *de novo* assemblies as follows: for each
88 species (or population, for widespread species that span both WH and EL) we generated a “rough”
89 *de novo* genome assembly from which we recovered orthologous protein-coding genes. After
90 translating nucleotide sequences to amino acid sequences, we identified a set of 1,885 one-to-one
91 orthologs among the 24 assemblies (table S2). Of these orthologs, we found that 246 had evolved
92 in a clock-like manner. We then concatenated these 246 genes, constrained the above topology,
93 and enforced a rate calibrated molecular clock. The resulting timetree shows that Paridae diverged
94 from Remizidae around 26 million years ago (Mya), with subsequent splits between extant EL
95 and WH taxa spanning a range from ~13–1.3 Mya (Fig. 1B). WH and EL taxa do not form
96 independent clades, instead they are distributed across the tree. Likewise, our principal
97 components analysis (PCA) and multidimensional scaling analysis (MDS) reject the hypothesis
98 that WH and EL genomes form distinct clusters (fig. S3). Nodes connecting EL and WH species

99 date to earlier than 3 Mya divergence (prior to the Pleistocene), except for intraspecific nodes
100 within three widespread species (*P. major*, *Poecile montanus* and *Periparus ater*) that occur in
101 both the EL and WH regions and exhibit shallower divergence times, as expected for within-
102 species comparisons. Here, estimated intraspecific divergence times between EL and WH
103 populations range from 1.8–1.3 Mya (Fig. 1B). These results more or less agree with previous
104 phylogenetic dating efforts for Paridae (13, 22, 23), and confirm that the most recent intraspecific
105 splits between WH and EL populations date to the early to mid-Pleistocene.

106

107 **Spatial patterns of genetic diversity**

108 Most East Asian parids had relatively low levels of genome-wide nucleotide diversity (π)
109 (average: 0.74×10^{-3} ; table S1). The widespread *P. major* had the highest nucleotide diversity
110 (1.77×10^{-3}), whereas the Taiwan island endemic *Machlolophus holsti* had the lowest nucleotide
111 diversity (0.07×10^{-3}), consistent with insularization. We found an extremely high correlation
112 between π and heterozygosity (H) ($R^2 = 0.97$, $P = 6.76 \times 10^{-16}$; fig. S5A), so we used the latter to
113 analyze landscape-level patterns of genomic diversity, as H is less likely to be influenced by
114 sample size and uneven geographic sampling. Kriging-smoothed estimates of phylogroup-wide H
115 were significantly lower in the WH compared to the EL (Wilcoxon-rank-sum = 634, $P = 0.008$;
116 Fig. 1C), indicating congruent and species-independent patterns of genomic diversity across all
117 East Asian parids. In the three widespread species, all WH populations had significantly lower H
118 (and π) compared to their conspecific EL populations (fig. S5, B and C).

119

120 **Spatial distribution of demographic history**

121 Pairwise sequentially Markovian coalescent (PSMC) estimates of effective population size (Ne)
122 through time showed markedly different patterns in the demographic history of WH and EL
123 species during the Pleistocene. All nine taxa that occur only in WH show significant decline in Ne

124 during this period. For six of these, the decline began at or near the beginning of the Last Glacial
125 Period (LGP, 0.011 Mya); for the other three, demographic contraction began at the Last Glacial
126 Maximum (LGM, 0.023-0.018 Mya) (Fig. 2A and table S3). In contrast, five of six EL taxa show
127 significant demographic expansion during Pleistocene. Here, three show expansion starting at or
128 near the LGM, while for the remaining two, expansion started earlier during the LGP (Fig. 2B). In
129 all three widespread taxa, the EL populations show significant population expansion during the
130 LGP, while two of the three WH populations show significant expansion during the LGP, rather
131 than the contraction seen in other WH taxa (Fig. 2C). This finding, along with the lower π
132 observed in the WH relative to the EL population of each widespread species (see above; fig.
133 S5B), suggests that all three species underwent population expansion from lowland areas into the
134 WH region during the Pleistocene, and not the reverse, which would also agree with the split
135 dates obtained in our time tree (Fig. 1B). Therefore, we expect that these three widespread taxa (*P.*
136 *major*, *Po. montanus* and *Pe. ater*) have had less time to adapt to living at high elevation than the
137 nine deeply diverged species found exclusively in WH. Finally, the Taiwan endemic species (*Ma.*
138 *holsti*) shows significant and constant population expansion throughout LGP, which is consistent
139 with population recovery after a founder event (Fig. 2D).

140

141 **Genome-wide patterns of elevation-associated differentiation**

142 At our sampling locations ranging from sea level to 4,550 meters, available oxygen (partial
143 pressure of oxygen: PO_2) declines sharply with increased elevation from 21% to 12% ($R^2 =$
144 0.9987, $P < 2.2 \times 10^{-16}$; Fig. 3A), representing an almost 50% reduction in inspired O_2 . Annual
145 mean temperature also declines with elevation ($R^2 = 0.4536$, $P = 9.85 \times 10^{-13}$; Fig. 3A), but the
146 relationship is more variable, such that several low elevation sites are as cold as high elevation
147 sites, demonstrating the ubiquity of hypoxia as a principal selective force on birds living in the
148 East Asian highlands (24). For small-bodied endotherms such as tits, altitude and cold tolerance

149 are inexorably linked, because such animals cannot reduce metabolic activity to mitigate against
150 reduced oxygen availability given their thermogenic requirements (4, 11).

151 To better understand the effect of altitude on the molecular evolution of East Asian parids,
152 we classified 37 birds sampled at or above 3,000 m as high altitude (HA) parids and classified 43
153 bird sampled at or below 1,000 m as low altitude (LA) parids (Fig. 3A and data file S1). Some
154 WH birds are not HA parids (but all EL are LA parids), and the three widespread species (*P.*
155 *major*, *Pe. ater*, and *Po. montanus*) have both HA and LA populations. Comparing all HA to all
156 LA individuals, allele frequency distributions show that none of the more than 43M SNPs that we
157 recovered in our dataset (see above) are differentially fixed between HA and LA parids (Fig. 3B).
158 This is also reflected in overall low levels of fixation index (F_{ST}) found between HA and LA
159 parids: only 5589 (0.013%) SNPs had F_{ST} values above 0.6 (Fig. 3C). Furthermore, outlier F_{ST}
160 windows were not coincident along the genome among our seven species pairs (Fig. 4A). Given
161 the high genomic synteny found across all songbirds (25), including parids (26), this result
162 suggests that high-altitude adaptation has largely independent macrogenomic consequences
163 among co-occurring montane East Asian parids.

164

165 **Genes in highly differentiated windows are disproportionately related to hypoxia response**

166 We pre-identified 17 parent-level Gene Ontogeny (GO) terms associated with the oxygen
167 transport cascade and/or hypoxia (see Methods for details) to identify genes potentially important
168 for hypoxia adaptation (Fig. 4B). Including dependent (i.e. “children”) terms in this analysis,
169 resulted in a list of 973 hypoxia-related GO terms that we used for GO analysis (data file
170 S2). After annotating all protein-coding genes with at least one variable site, we find that total
171 number of variable protein-coding genes did not vary between outlier windows and random
172 windows (two-sample t -test, $t(6) = 0.72$, $P = 0.50$; Fig. 5A). However, F_{ST} outlier windows did
173 have significantly more genes attributable to our set of hypoxia-related GO terms (i.e. genes

174 potentially associated with hypoxia) than did random windows (two-sample *t*-test, $t(6) = 5.24$, $P =$
175 0.0002; Fig. 5B). Furthermore, hypoxia-related GO terms were significantly more likely to be
176 enriched in F_{ST} outlier windows compared to random windows (two-sample *t*-test, $t(6) = 3.67$, $P =$
177 0.003; Fig. 5C).

178

179 **Little overlap of hypoxia-related genes among HA–LA comparisons**

180 Per species, the number of hypoxia-related genes varied from a high of 95 in the WH endemic *Ps.*
181 *humilus* to a low of 40 in the widespread *Pe. ater*. There was no difference in the number of
182 hypoxia-related genes between WH endemic and widespread taxa (two-sample *t*-test, $t(5) = 0.54$,
183 $P = 0.62$). On average, any two HA–LA parids pairs shared only 8.5 such genes (range: 0–24; fig.
184 S7A). Only one hypoxia-related gene (*PLBI*) was found in six of the seven F_{ST} outlier windows
185 (fig. S7B); no such genes occurred in all seven sets of F_{ST} outlier windows (fig. S7C). *PLBI*, in
186 particular, is associated with lipid metabolic processes (27, 28), a GO term enriched in all seven
187 HA–LA comparisons (see below). As a whole, these results suggest a lack of parallelism among
188 particular genes likely to be involved in adaptation to hypoxia and/or associated with high
189 elevation among East Asian parids.

190

191 **Substantial overlap of hypoxia-related GO terms among HA–LA comparisons**

192 While individual genes showed little overlap among our comparisons, the proportion of hypoxia-
193 related enriched GO terms co-occurring between any two HA–LA comparisons was significantly
194 higher than expected by chance (Wilcoxon-rank-sum = 886,932, $P < 2.2 \times 10^{-16}$; Fig. 5D), and the
195 set of enriched hypoxia-related GO terms co-occurring between any two HA–LA comparisons
196 also had significantly greater semantic similarity than expected by chance (Wilcoxon-rank-sum =
197 707,173, $P < 2.2 \times 10^{-16}$; Fig. 5E). In contrast, enriched GO terms unrelated to hypoxia were
198 significantly less likely to co-occur in outlier windows than expected by chance (Wilcoxon-rank-

199 sum = 130,094, $P = 1.9 \times 10^{-15}$; fig. S7D) and sets of co-occurring non-hypoxia related GO terms
200 between pairs of HA–LA comparisons had significantly less semantic similarity in outlier
201 windows than did sets from random windows (Wilcoxon-rank-sum = 325,874, $P = 0.002$; fig.
202 S7E).

203

204 **Biological functions and processes associated with genomic outlier windows**

205 The 17 GO terms (and their dependents) varied in the frequency in which they were enriched
206 among our seven HA–LA comparisons (Fig. 4B and table S4). Terms associated with respiration,
207 circulation, and oxygen diffusion in tissues were less often enriched (on average, between 1.5 and
208 2.8 out of 7 comparisons), although we note that within the circulation terms, two terms more
209 directly associated with circulatory system development (i.e. vascularization) were enriched in six
210 of seven comparisons. The three terms associated with utilization of oxygen in tissues and cells
211 (GO:0046034, GO:0006629, and GO:0005975) were most frequently enriched (on average 5.7
212 out of 7 comparisons), as was the hypoxia specific term (GO:0036293, six of seven comparisons).
213 Importantly, both lipid metabolic processes (GO:0006629) and carbohydrate metabolic processes
214 (GO:0005975) were enriched in all seven HA–LA comparisons, processes which serve dual
215 functions related to oxygen transport and thermogenesis.

216

217 **Evidence for selection in hypoxia-related genes**

218 We found evidence for positive selection on amino acid changes in just one HA–LA comparison,
219 and only in two genes, out of 273 hypoxia-related genes (data file S3). The two genes, *MAN1B1*
220 and *EDEM3*, are involved in the carbohydrate metabolic process (29, 30), a process that has been
221 shown previously to be important for high elevation adaptation in several vertebrates (6, 31, 32).
222 We note that the codon-based selection tests used here (33) have less power and cannot identify
223 adaptive evolution in regulatory and other non-coding regions unlike selective sweep tests, which

224 require population level sampling beyond the scope of this project. Nonetheless, our observation
225 of over-representation of genes with hypoxia-related function in outlier windows, but limited
226 evidence for positively-selected amino acid substitutions in those genes is consistent with
227 hypotheses that emphasize selection on gene expression and regulatory processes, rather than on
228 novel amino acids, in explaining vertebrate adaptation to high elevation (6, 19, 34-38).

229

230 **Discussion**

231 The genomes of East Asian parids have been shaped by both history and environment. The
232 demographic legacy of Pleistocene climate change had a predictable effect on genome-wide
233 patterns of diversity. All nine WH endemic species showed a significant reduction in effective
234 population size during the LGP, consistent with demographic contraction in western East Asia
235 (Fig. 1C). Glaciations of the western highlands would have made most of the region uninhabitable
236 – WH parids likely persisted during much of the Quaternary in tiny refugia relative to their
237 current distributions (39). While some previous studies indicate that mitochondrial diversity (and
238 thus effective population size) increased since the LGM in a few WH endemic birds (14), our data
239 demonstrate that genome-wide autosomal variation remains low compared to the variation
240 estimated at the beginning of the LGP. In contrast, EL parids do not show a reduction in genome-
241 wide diversity. The EL were unglaciated during the LGP (Fig. 1C) resulting in relatively stable
242 environments through the Quaternary (7, 9), and our results demonstrate stable avian population
243 sizes in this region during this period, in agreement with previous studies (15, 16, 40, 41). In fact,
244 we recovered evidence of population growth since the LGM for some EL parids, which is
245 different from previous hypothesized post-LGM expansion scenario based solely on mtDNA
246 sequences (16, 39), and would be consistent with poleward expansion of suitable habitat.
247 Importantly, previous studies (20, 42) have hypothesized that reduced genetic diversity in high-
248 elevation animal populations may be a direct consequence of adaptation to life at high altitude

249 and/or the founder events that permitted these populations to become established in the first place.
250 The extremely low levels of fixed SNPs across HA–LA comparisons reject these alternative
251 hypotheses for East Asian parids. Instead, landscape-wide differences in genomic diversity are
252 more likely the result of different demographic histories between highland and lowland tits,
253 almost certainly driven by Pleistocene glacial patterns.

254 For small bodied, active endotherms, such as East Asian tits, hypoxia presents the greatest
255 challenge to survival at extreme altitudes such as found on much of the Qinghai-Tibet Plateau and
256 across the Himalayas. Across seven HA–LA comparisons of East Asian parids, we find that the
257 most divergent genomic regions are significantly over-represented by protein-coding genes with
258 biological processes and functions related to hypoxia (Fig. 5B). Because the chromosomal
259 locations of these outlier regions show little overlap among high-low comparisons (Fig. 4A) and
260 given the high level of chromosomal synteny known generally in birds (25) and more specifically
261 in tits (26), this indicates little overlap in the particular genes involved in hypoxia adaptation.
262 Indeed, we identified a total of 273 genes across all East Asian tits that may be involved in
263 hypoxia adaptation, on average only 8.5 of these were shared across any two high elevation tit
264 taxa, and just one was found in only six of our seven comparisons. This result mirrors hemoglobin
265 adaptation in high-elevation birds: while occasional cases of parallel evolution at particular
266 hemoglobin amino acid substitutions have been observed (5), more generally, hemoglobin
267 proteins in high-elevation birds have convergent function that is the result of distinct molecular
268 evolutionary solutions (11, 38, 43). Recent studies of genome-wide avian adaptation to life at high
269 altitude provide additional support for convergence in function but not necessarily identity (44–
270 46). Furthermore, evidence for amino acid substitutions consistent with positive selection was not
271 found in most taxa. This may indicate that hypoxia adaptation in birds relies as much – or more –
272 on gene regulation as on protein evolution, as has previously been suggested (6, 35). Future
273 studies of convergent evolution for high-elevation birds should consider non-coding regions (19),

274 recognizing that genomic adaptation to high elevation is likely polygenic, with many loci of
275 relatively minor effect (46, 47). In the case of East Asian parids, certain biological processes and
276 functions are more consistently enriched in outlier genomic regions than others. Circulatory and
277 metabolic pathways were enriched in nearly all comparisons, whereas respiratory and tissue
278 diffusion pathways were seldom enriched. Importantly, we found that both carbohydrate and lipid
279 metabolic processes were enriched in all seven HA–LA comparisons; these processes are
280 consistently shown to be important for avian adaptation to high elevation (12, 20, 44–46). It has
281 recently been argued that evolution of carbohydrate metabolism precedes adaptation for increased
282 lipid metabolism (20, 44, 48). We found evidence for enrichment for carbohydrate and lipid
283 metabolic processes in both WH endemics, which presumably have inhabited the QTP for
284 millions of years, and also in western populations of widespread parids, which separated from EL
285 populations during the early to mid-Pleistocene (Fig. 1B). This suggests either that evolution of
286 lipid and carbohydrate metabolism is coincident rather than serial in East Asian parids, or that the
287 pace of high elevation metabolic adaptation is relatively rapid, as has been shown recently for
288 another East Asian songbird (46) and Andean waterfowl (44). Our finding of no significant
289 difference in the number of potentially hypoxia-related genes between highland endemics and
290 widespread taxa would be consistent with a hypothesis of rapid high elevation adaptation.

291 In sum, East Asian tits show predictable genomic responses to environmental variation in
292 both time and space in both neutral and adaptive evolutionary processes. However, the particular
293 genomic pathways for adaption to extreme environments appear unique to each species. Thus,
294 researchers should consider at what scale (SNP, gene, chromosome, or function) adaptation is
295 likely to occur when addressing the question of convergence and parallelism in evolutionary
296 processes.

297

298 **Materials and Methods**

299 **Sampling and sequencing**

300 We sampled 91 individuals of parids and penduline-tits. Field sampling conformed to the
301 National Wildlife Conservation Law with the permission from the local forestry administration.
302 We extracted total genomic DNA from muscle and blood samples using the Tissue/Cell Genomic
303 DNA Extraction Kit (Aidlab Biotechnologies, Beijing, China). We prepared genomic libraries
304 with a mean insert size of 350 bp according to manufacturer's protocols, which were sequenced
305 on an Illumina HiSeq X Ten machine to obtain 150 bp paired end reads at Berry Genomics
306 (Beijing, China). Prior to downstream analyses, we cleaned the reads by removing adapter
307 sequences, as well as reads with $\geq 3\%$ unidentified nucleotides and reads with over 50% of bases
308 having Phred quality scores < 3 . Detailed information including sample identification number,
309 collecting location, sequencing depth of coverage, NCBI Sequence Read Archive accession
310 numbers, and more are available in data file S1.

311

312 **Read aligning and variant calling**

313 We aligned reads to the *P. major* reference genome (Assembly: GCA_001522545.2) (21) using
314 BWA v0.7.15 (49) with default parameters. Alignments were reordered, sorted, and marked for
315 PCR duplicates using PICARD v2.8.3 (<http://broadinstitute.github.io/picard>). We additionally
316 performed local realignment for insertion-deletion (indel) polymorphisms using the Genome
317 Analysis Toolkit (GATK) v3.7 (50). Variants were first called across all samples independently
318 using both *HaplotypeCaller* in GATK and *mpileup* in Samtools v1.3.1 (51). Sites identified as
319 variant in either tool were subjected to a second round of variant calling in *HaplotypeCaller* to
320 confirm genotypes.

321 To further improve variant quality, we conducted a hard filtration for raw variant calls. We
322 only retained variant sites for downstream analyses when they met the following criteria: quality $>$
323 1000, 900 $<$ overall depth (DP) $<$ 2700, quality by depth (QD) $>$ 10, mapping quality (MQ) $>$ 55,

324 Fisher strand bias (FS) < 10, mapping quality rank sum (MQRankSum) > -5, read position rank
325 sum (ReadPosRankSum) > -10, and Symmetric Odds Ratio (SOR) < 2. Cut-offs for these
326 parameters were chosen based on their density distributions. We also removed short indels, and
327 only retained SNPs that had < 10 individuals with missing data.

328

329 **Phylogenetic construction and dating**

330 We reconstructed maximum-likelihood (ML) phylogenetic trees separately for autosomal and Z-
331 chromosome SNPs (52), and we also generated one coalescent-based species tree based on 50
332 subsamples from the genome-wide SNP set (~50,000 SNPs per replicate). For both the autosomes
333 and Z-chromosome dataset we concatenated all SNPs and constructed maximum-likelihood
334 phylogenies using RAxML v8.2.10 (53) with 100 bootstrap replicates under the
335 ASC_GTRGAMMA model. We also constructed a species tree using a coalescent-based method
336 in ASTRAL-II (54), based on 50 random subsets of ~50,000 SNPs. All tree-building approached
337 generated a single topology (see Results), and so we dated nodes on this tree as follows.

338 Following Jarvis et al. (55) (see Supplementary Methods for details) we generated a dataset of
339 clock-like evolving protein coding genes (see Results) and enforced the above topology, which
340 was loaded into the *MCMCTree* program in PAML v4.9 (56) and generated both uncorrelated and
341 autocorrelated relaxed clocks. We estimated posterior distributions of divergence time by Markov
342 chain Monte Carlo sampling, with samples drawn every 2,000 steps over a total of 10^8 steps after
343 a discarded burnin of 2×10^7 steps.

344

345 **Genetic diversity calculation**

346 We calculated nucleotide diversity (π) and heterozygosity (H) for each species or population in
347 VCFtools v0.1.13 (57). We used individual heterozygosity across all species and populations to

348 simulate the spatial distribution of the lineage-wide genetic diversity using kriging routines (58)
349 in ArcGIS v10.0 (ESRI, Redlands, CA, USA) based on the heterozygosity at each locality.

350

351 **Demographic history inference**

352 For each species and geographic population, we selected the individual with the highest
353 sequencing depth to infer population size over time using PSMC (59). We generated consensus
354 sequences that were filtered by removing sites with mapping quality below 25, low inferred
355 consensus quality (below 20), and low read depth (less than 6 \times , one-third of the mean coverage).

356 According to suggestions by Nadachowska-Brzyska et al. (60), PSMC parameters (-p and -t
357 options) were set as ‘-N25 -t5 -r5 -p 4+30*2+4+6+10’ with 100 bootstrap replicates. PSMC
358 results were scaled using species-specific mutation rates and generation times (table S5). The
359 synonymous substitution rate per synonymous site was calculated using the *codeml* program of
360 PAML (61) based on the time tree (see above) and was used to calculate the species-specific
361 mutation rate (μ) for each species. We used the age of sexual maturity (62) multiplied by two as a
362 proxy for the generation time (g) (63).

363 We scaled relative population size to effective size (N_e) using approximated mutation rate
364 (μ) based on the equation: $N_k = (\theta_0 \times \lambda_k) / 4\mu s$; provided by H. Li and R. Durbin
365 (<https://github.com/lh3/psmc>). We used generation time to convert coalescent time to calendar
366 time using the following equation [$T_k = (\theta_0 \times t_k \times g) / 2\mu s$]. θ_0 , t_k and λ_k are estimated by the
367 PSMC model and s is the bin size, which we set at the default value = 100. We used this equation
368 to generate N_e estimates at three times in the past: 0.012 Mya (end of the LGP), 0.023 Mya
369 (beginning of the LGM) and 0.11 Mya (beginning of the LGP). We used Wilcoxon rank sum tests
370 to test for significant differences between N_e estimates at the beginning of the LGP or LGM and
371 at the end of the LGP (table S3).

372

373 **Linkage disequilibrium analysis**

374 To select a suitable window size for genome-wide scanning, we estimated levels of linkage

375 disequilibrium (LD) within species for all species with sample size of at least five. We phased

376 haplotypes for each species using BEAGLE v4.1 (64). Levels of LD (r^2) were then calculated

377 using VCFtools between pairs of loci in every 50 kb window of the genome. Haplotype r^2 values

378 were used to measure the LD decay by averaging the r^2 values in each bin of 500 bp over 20 kb.

379 LD decreased rapidly within 5 kb and then slowly declined until 15 kb, suggesting that a window

380 size of greater than 15 kb would avoid autocorrelation between adjacent windows (fig. S6).

381

382 **Genome-wide scanning and annotation of SNPs**

383 We scanned the whole genome to identify adaptive genetic variation at different levels using

384 several F_{ST} analyses, including both SNP-based and region-based F_{ST} calculations. For each of the

385 seven HA–LA pairs, we extracted each SNP's allele frequency (AF) using *VariantsToTable* in

386 GATK, and we calculated F_{ST} for each SNP in VCFtools. Additionally, we calculated F_{ST} in 50 kb

387 sliding windows, a window size more $>3 \times$ greater than indicated by the maximum observed LD

388 (see above). We Z-transformed autosomal and Z-chromosome windows separately. We defined

389 outlier windows as those with ZF_{ST} values exceeding the 99th percentile of the distribution.

390 Therefore, each pair had 186 autosomal outlier windows and 16 Z-chromosome outlier windows.

391 For comparison purposes, we generated 20 replicates of randomly selected sets of 186 autosomal

392 and 16 Z-chromosome windows for each pair. For both the outlier and random replicate window

393 sets, we annotated all SNPs using SnpEff v4.3 (65) based on the location of SNPs in the *P. major*

394 genome. SnpEff determines whether SNPs are found in coding or non-coding regions, and for

395 coding-region SNPs determines whether the substitution is synonymous or non-synonymous.

396

397 **Functional enrichment and similarity analyses**

398 Because they are metabolically active and homeotherms, most birds living at high altitude cannot
399 compensate for hypoxia by behavioral change and must adapt physiologically to reduced oxygen
400 availability (4, 11). Physiological adaptations are most likely to occur at the four stages of the
401 oxygen transport cascade (breathing/pulmonary oxygen diffusion, circulation oxygen delivery,
402 tissue oxygen diffusion, and tissue oxygen utilization) where oxygen is transferred via either
403 diffusion or convection between atmospheric air and oxidative phosphorylation (4). Prior to all
404 analyses, we identified Gene Ontology (GO) molecular functions and biological processes
405 associated with these four stages (35, 66-68). This resulted in a list of 16 parental GO terms as
406 well as an additional term directly associated with hypoxia (Fig. 4B). We also used the QuickGO
407 database (<https://www.ebi.ac.uk/QuickGO/>) (69) to identify direct descendants of these parental GO
408 terms (child terms) associated with these 17 parental GO terms, and filtered out only the GO
409 terms found in the union of human, mouse, and chicken gene ontologies, which resulted in a set
410 of 973 GO terms (data file S2). We used topGO v2.32.0 (70) to annotate the SnpEff-identified
411 variable coding genes by GO term. From this, we separated genes into two groups: those
412 assignable to one of 973 hypoxia-related GO terms, which we defined as hypoxia-related genes,
413 e.g. “potentially associated with hypoxia”, and those not assignable to the 973 GO terms, which
414 we defined as “hypoxia-unrelated”. Finally, we used topGO to calculate whether certain GO
415 terms were associated with genes found in our windows more often than expected by chance (e.g.
416 enriched). We used a cut-off *P*-value of 0.05 corrected for the false discovery rate using the
417 Benjamini and Hochberg method (71).

418 For the set of seven HA-LA paired taxa, we compared *i*) the number of coding genes; *ii*)
419 the number of coding genes associated with the 973 hypoxia-related GO terms; and *iii*) the
420 number of enriched hypoxia-related GO terms found in outlier windows to the average found in
421 the 20 random replicates using two-sample *t*-tests. To test whether the same hypoxia-related
422 enriched GO terms occurred in each of the seven outlier comparisons more often than expected by

423 chance, we conducted pairwise hypergeometric tests using the *dhyper* function in R; these results
424 were compared with the outcome of pairwise hypergeometric tests between the 20 random
425 window replicates. Additionally, we measured the semantic similarity between hypoxia-related
426 enriched GO term sets using GOSemSim v3.11 package (72). Finally, to compare these results to
427 null expectations, we repeated the hypergeometric and semantic similarity analyses, but with
428 “hypoxia-unrelated” enriched GO terms.

429

430 **McDonald-Kreitman test**

431 We constructed consensus sequences for each hypoxia-related gene from HA–LA comparisons
432 using *vcf-consensus* (57) based on our SNP data, and aligned each hypoxia-related gene using
433 MUSCLE (73). Based on these alignments of hypoxia-related genes, we conducted the
434 McDonald-Kreitman test (33) in PopGenome (74) to detect signals of positive selection by
435 comparing the ratio of fixed non-synonymous sites (D_n) and fixed synonymous sites (D_s) with the
436 ratio of polymorphic non-synonymous sites (P_n) and polymorphic synonymous sites (P_s) using a
437 Fisher’s exact test. Under positive selection, the ratio of D_n to D_s is significantly larger than the
438 ratio of P_n to P_s .

439

440 **Ecological analyses**

441 Atmospheric partial pressure of oxygen (PO_2) was calculated by a simple formula based on
442 altitude: $\text{PO}_2 = 21\% \times 101.325 \times (1 - \text{Elevation} / 44300)^{5.256}$, assuming a constant pressure
443 (101.325 kPa) and temperature (15°C) at sea level. To estimate range size of parid species, we
444 calculated the geometric area of distribution maps downloaded from BirdLife International
445 (<http://datazone.birdlife.org/>) in ArcGIS. We estimated the annual temperature for each sampling
446 locality based on 19 bioclimatic variables with 30-second resolution from WorldClim (75) using
447 the “Zonal” tool in ArcGIS.

449 **Supplementary Materials**

450 Supplementary Methods

451 Fig. S1. Statistics for whole genome re-sequencing data.

452 Fig. S2. Phylogenetic analyses.

453 Fig. S3. Dimensionality reduction analyses of all individuals based on all SNPs.

454 Fig. S4. Time trees for East Asian parids based on autocorrelated relaxed clock.

455 Fig. S5. Relationships between nucleotide diversity and heterozygosity.

456 Fig. S6. Linkage disequilibrium (LD) decay measure by haplotype r^2 values.457 Fig. S7. Lack of similarity in hypoxia-related genes among the seven high-altitude vs. low-
458 altitude (HA–LA) comparisons, and similarity comparison of enriched hypoxia-unrelated
459 Gene Ontogeny (GO) terms between outlier windows and randomly selected windows.

460 Table S1. Summary for samples of parid and outgroup species used in this study.

461 Table S2. Statistics for the assemblies and protein-coding genes from 24 species or populations.

462 Table S3. Comparisons between effective population sizes (N_e) at the end and the beginning of
463 the glaciations.464 Table S4. Enrichment statistics for 17 Gene Ontogeny (GO) terms associated with the oxygen
465 transport cascade and hypoxia response in all HA–LA comparisons.

466 Table S5. Mutation rates for each species calculated by PAML.

467 Data file S1. Detail information for sequenced samples, including sources and tissue types of
468 samples, ecological data, quality and coverage of sequencing, NCBI accessions of
469 sequencing data, as well as heterozygosity of each individual.470 Data file S2. List of 973 Gene Ontogeny (GO) terms (i.e. 17 parental-level GO terms and their
471 child terms) associated with the oxygen transport cascade and hypoxia response.

472 Data file S3. List of hypoxia-related genes found in FST outlier windows for each high altitude
473 (HA) and low altitude (LA) parids comparison, and the corresponding statistics for
474 McDonald-Kreitman test, including number of Dn, Ds, Pn, Ps sites and the significance
475 value of Fisher's exact test.

476 **References and Notes**

- 477 1. G. Hewitt, The genetic legacy of the Quaternary ice ages. *Nature* **405**, 907-913 (2000).
- 478 2. G. M. Hewitt, Genetic consequences of climatic oscillations in the Quaternary. *Philos. Trans. R. Soc. Lond. B Biol. Sci.* **359**, 183-195 (2004).
- 479 3. C. M. Beall, Andean, Tibetan, and Ethiopian patterns of adaptation to high-altitude hypoxia. *Integr. Comp. Biol.* **46**, 18-24 (2006).
- 480 4. J. F. Storz, G. R. Scott, Z. A. Cheviron, Phenotypic plasticity and genetic adaptation to high-altitude hypoxia
481 in vertebrates. *J. Exp. Biol.* **213**, 4125-4136 (2010).
- 482 5. J. Projecto-Garcia, C. Natarajan, H. Moriyama, R. E. Weber, A. Fago, Z. A. Cheviron, R. Dudley, J. A.
483 McGuire, C. C. Witt, J. F. Storz, Repeated elevational transitions in hemoglobin function during the
484 evolution of Andean hummingbirds. *Proc. Natl. Acad. Sci. U. S. A.* **110**, 20669-20674 (2013).
- 485 6. Z. A. Cheviron, G. C. Bachman, A. D. Connaty, G. B. McClelland, J. F. Storz, Regulatory changes
486 contribute to the adaptive enhancement of thermogenic capacity in high-altitude deer mice. *Proc. Natl. Acad.*
487 *Sci. U. S. A.* **109**, 8635-8640 (2012).
- 488 7. Z. J. Cui, Y. Q. Wu, G. N. Liu, D. K. Ge, Q. Q. Pang, Q. H. Xu, On Kunlun Yellow River tectonic movement.
489 *Sci. China Ser. D* **41**, 592-600 (1998).
- 490 8. Y. Q. Wu, Z. J. Cui, G. N. Liu, D. K. Ge, J. R. Yin, Q. H. Xu, Q. Q. Pang, Quaternary geomorphological
491 evolution of the Kunlun Pass area and uplift of the Qinghai-Xizang (Tibet) Plateau. *Geomorphology* **36**, 203-
492 216 (2001).
- 493 9. S. Z. Zhou, X. L. Wang, J. Wang, L. B. Xu, A preliminary study on timing of the oldest Pleistocene
494 glaciation in Qinghai-Tibetan Plateau. *Quatern. Int.* **154**, 44-51 (2006).
- 495 10. F. R. Lorenzo, C. Huff, M. Myllymaki, B. Olenchock, S. Swierczek, T. Tashi, V. Gordeuk, T. Wuren, G. Ri-
496 Li, D. A. McClain, T. M. Khan, P. A. Koul, P. Guchhait, M. E. Salama, J. Xing, G. L. Semenza, E. Liberzon,
497 A. Wilson, T. S. Simonson, L. B. Jorde, W. G. Kaelin, Jr., P. Koivunen, J. T. Prchal, A genetic mechanism for
498 Tibetan high-altitude adaptation. *Nat. Genet.* **46**, 951-956 (2014).

- 501 11. X. J. Zhu, Y. Y. Guan, A. V. Signore, C. Natarajan, S. G. Dubay, Y. L. Cheng, N. J. Han, G. Song, Y. H. Qu,
502 H. Moriyama, F. G. Hoffmann, A. Fago, F. M. Lei, J. F. Storz, Divergent and parallel routes of biochemical
503 adaptation in high-altitude passerine birds from the Qinghai-Tibet Plateau. *Proc. Natl. Acad. Sci. U. S. A.*
504 **115**, 1865-1870 (2018).
- 505 12. Y. H. Qu, H. F. Zhao, N. J. Han, G. Zhou, G. Song, B. Gao, S. L. Tian, J. Zhang, R. Zhang, X. Meng, Y.
506 Zhang, Y. Zhang, X. J. Zhu, W. Wang, D. Lambert, P. G. Ericson, S. Subramanian, C. Yeung, H. Zhu, Z.
507 Jiang, R. Q. Li, F. M. Lei, Ground tit genome reveals avian adaptation to living at high altitudes in the
508 Tibetan plateau. *Nat. Commun.* **4**, 2071 (2013).
- 509 13. U. S. Johansson, S. Nylander, J. I. Ohlson, D. T. Tietze, Reconstruction of the late Miocene biogeographical
510 history of tits and chickadees (Aves: Passeriformes: Paridae): A comparison between discrete area analyses
511 and probabilistic diffusion approach. *J. Biogeogr.* **45**, 14-25 (2018).
- 512 14. Y. H. Qu, P. G. P. Ericson, Q. Quan, G. Song, R. Y. Zhang, B. Gao, F. M. Lei, Long-term isolation and
513 stability explain high genetic diversity in the Eastern Himalaya. *Mol. Ecol.* **23**, 705-720 (2014).
- 514 15. W. J. Wang, B. D. McKay, C. Y. Dai, N. Zhao, R. Y. Zhang, Y. H. Qu, G. Song, S. H. Li, W. Liang, X. J.
515 Yang, E. Pasquet, F. M. Lei, Glacial expansion and diversification of an East Asian montane bird, the green-
516 backed tit (*Parus monticolus*). *J. Biogeogr.* **40**, 1156-1169 (2013).
- 517 16. N. Zhao, C. Y. Dai, W. J. Wang, R. Y. Zhang, Y. H. Qu, G. Song, K. Chen, X. J. Yang, F. S. Zou, F. M. Lei,
518 Pleistocene climate changes shaped the divergence and demography of Asian populations of the great tit
519 *Parus major*: evidence from phylogeographic analysis and ecological niche models. *J. Avian Biol.* **43**, 297-
520 310 (2012).
- 521 17. G. Song, R. Zhang, F. Machado-Stredel, P. Alström, U. S. Johansson, M. Irestedt, H. L. Mays Jr, B. D.
522 McKay, I. Nishiumi, Y. Cheng, Y. Qu, P. G. P. Ericson, J. Fjeldså, A. T. Peterson, F. Lei, Great journey of
523 Great Tits (*Parus major* group): Origin, diversification and historical demographics of a broadly distributed
524 bird lineage. *J. Biogeogr.* **47**, 1585–1598 (2020).
- 525 18. X. J. Zhu, Y. Y. Guan, Y. H. Qu, G. David, G. Song, F. M. Lei, Elevational divergence in the great tit
526 complex revealed by major hemoglobin genes. *Curr. Zool.* **64**, 455-464 (2018).
- 527 19. Y. Hao, Y. Xiong, Y. L. Cheng, G. Song, C. X. Jia, Y. H. Qu, F. M. Lei, Comparative transcriptomics of 3
528 high-altitude passerine birds and their low-altitude relatives. *Proc. Natl. Acad. Sci. U. S. A.* **116**, 11851-
529 11856 (2019).
- 530 20. Y. H. Qu, S. L. Tian, N. J. Han, H. W. Zhao, B. Gao, J. Fu, Y. L. Cheng, G. Song, P. G. P. Ericson, Y. E.
531 Zhang, D. W. Wang, Q. Quan, Z. Jiang, R. Q. Li, F. M. Lei, Genetic responses to seasonal variation in

- 532 altitudinal stress: whole-genome resequencing of great tit in eastern Himalayas. *Sci. Rep.* **5**, 14256 (2015).
- 533 21. V. N. Laine, T. I. Gossmann, K. M. Schachtschneider, C. J. Garraway, O. Madsen, K. J. F. Verhoeven, V. de
534 Jager, H. J. Megens, W. C. Warren, P. Minx, R. P. M. A. Crooijmans, P. Corcoran, B. C. Sheldon, J. Slate, K.
535 Zeng, K. van Oers, M. E. Visser, M. A. M. Groenen, G. T. H. Consortium, Evolutionary signals of selection
536 on cognition from the great tit genome and methylome. *Nat. Commun.* **7**, 10474 (2016).
- 537 22. J. C. Illera, K. Koivula, J. Broggi, M. Packert, J. Martens, L. Kvist, A multi-gene approach reveals a
538 complex evolutionary history in the *Cyanistes* species group. *Mol. Ecol.* **20**, 4123-4139 (2011).
- 539 23. T. D. Price, D. M. Hooper, C. D. Buchanan, U. S. Johansson, D. T. Tietze, P. Alstrom, U. Olsson, M. Ghosh-
540 Harihar, F. Ishtiaq, S. K. Gupta, J. Martens, B. Harr, P. Singh, D. Mohan, Niche filling slows the
541 diversification of Himalayan songbirds. *Nature* **509**, 222-225 (2014).
- 542 24. Z. A. Cheviron, R. T. Brumfield, Genomic insights into adaptation to high-altitude environments. *Heredity*
543 (*Edinb.*) **108**, 354-361 (2012).
- 544 25. G. J. Zhang, C. Li, Q. Y. Li, B. Li, D. M. Larkin, C. Lee, J. F. Storz, A. Antunes, M. J. Greenwold, R. W.
545 Meredith, A. Odeen, J. Cui, Q. Zhou, L. H. Xu, H. L. Pan, Z. J. Wang, L. J. Jin, P. Zhang, H. F. Hu, W. Yang,
546 J. Hu, J. Xiao, Z. K. Yang, Y. Liu, Q. L. Xie, H. Yu, J. M. Lian, P. Wen, F. Zhang, H. Li, Y. L. Zeng, Z. J.
547 Xiong, S. P. Liu, L. Zhou, Z. Y. Huang, N. An, J. Wang, Q. M. Zheng, Y. Q. Xiong, G. B. Wang, B. Wang, J.
548 J. Wang, Y. Fan, R. R. da Fonseca, A. Alfaro-Nunez, M. Schubert, L. Orlando, T. Mourier, J. T. Howard, G.
549 Ganapathy, A. Pfenning, O. Whitney, M. V. Rivas, E. Hara, J. Smith, M. Farre, J. Narayan, G. Slavov, M. N.
550 Romanov, R. Borges, J. P. Machado, I. Khan, M. S. Springer, J. Gatesy, F. G. Hoffmann, J. C. Opazo, O.
551 Hastad, R. H. Sawyer, H. Kim, K. W. Kim, H. J. Kim, S. Cho, N. Li, Y. H. Huang, M. W. Bruford, X. J.
552 Zhan, A. Dixon, M. F. Bertelsen, E. Derryberry, W. Warren, R. K. Wilson, S. B. Li, D. A. Ray, R. E. Green, S.
553 J. O'Brien, D. Griffin, W. E. Johnson, D. Haussler, O. A. Ryder, E. Willerslev, G. R. Graves, P. Alstrom, J.
554 Fjeldsa, D. P. Mindell, S. V. Edwards, E. L. Braun, C. Rahbek, D. W. Burt, P. Houde, Y. Zhang, H. M. Yang,
555 J. Wang, E. D. Jarvis, M. T. P. Gilbert, J. Wang, A. G. Consortium, Comparative genomics reveals insights
556 into avian genome evolution and adaptation. *Science* **346**, 1311-1320 (2014).
- 557 26. Q. Cai, X. Qian, Y. Lang, Y. Luo, J. Xu, S. Pan, Y. Hui, C. Gou, Y. Cai, M. Hao, J. Zhao, S. Wang, Z. Wang,
558 X. Zhang, R. He, J. Liu, L. Luo, Y. Li, J. Wang, Genome sequence of ground tit *Pseudopodoces humilis* and
559 its adaptation to high altitude. *Genome Biol.* **14**, R29 (2013).
- 560 27. A. Gassamadiagne, P. Rogalle, J. Fauvel, M. Willson, A. Klaebe, H. Chap, Substrate-specificity of
561 phospholipase-B from guinea-pig intestine - a glycerol ester lipase with broad specificity. *J. Biol. Chem.* **267**,
562 13418-13424 (1992).

- 563 28. H. Takemori, F. N. Zolotaryov, L. Ting, T. Urbain, T. Komatsubara, O. Hatano, M. Okamoto, H. Tojo,
564 Identification of functional domains of rat intestinal phospholipase B/lipase - Its cDNA cloning, expression,
565 and tissue distribution. *J. Biol. Chem.* **273**, 2222-2231 (1998).
- 566 29. D. S. Gonzalez, K. Karaveg, A. S. Vandersall-Nairn, A. Lal, K. W. Moremen, Identification, expression, and
567 characterization of a cDNA encoding human endoplasmic reticulum mannosidase I, the enzyme that
568 catalyzes the first mannose trimming step in mammalian Asn-linked oligosaccharide biosynthesis. *J. Biol.*
569 *Chem.* **274**, 21375-21386 (1999).
- 570 30. S. Olivari, C. Galli, H. Alanen, L. Ruddock, M. Molinari, A novel stress-induced EDEM variant regulating
571 endoplasmic reticulum-associated glycoprotein degradation. *J. Biol. Chem.* **280**, 2424-2428 (2005).
- 572 31. K. C. Welch, D. L. Altshuler, R. K. Suarez, Oxygen consumption rates in hovering hummingbirds reflect
573 substrate-dependent differences in P/O ratios: carbohydrate as a 'premium fuel'. *J. Exp. Biol.* **210**, 2146-2153
574 (2007).
- 575 32. D. S. Lau, A. D. Connaty, S. Mahalingam, N. Wall, Z. A. Cheviron, J. F. Storz, G. R. Scott, G. B.
576 McClelland, Acclimation to hypoxia increases carbohydrate use during exercise in high-altitude deer mice.
577 *Am. J. Physiol. Regul. Integr. Comp. Physiol.* **312**, R400-R411 (2017).
- 578 33. J. H. McDonald, M. Kreitman, Adaptive protein evolution at the Adh locus in *Drosophila*. *Nature* **351**, 652-
579 654 (1991).
- 580 34. M. A. Lui, S. Mahalingam, P. Patel, A. D. Connaty, C. M. Ivy, Z. A. Cheviron, J. F. Storz, G. B. McClelland,
581 G. R. Scott, High-altitude ancestry and hypoxia acclimation have distinct effects on exercise capacity and
582 muscle phenotype in deer mice. *Am. J. Physiol. Regul. Integr. Comp. Physiol.* **308**, R779-791 (2015).
- 583 35. G. R. Scott, T. S. Elogio, M. A. Lui, J. F. Storz, Z. A. Cheviron, Adaptive modifications of muscle phenotype
584 in high-altitude deer mice are associated with evolved changes in gene regulation. *Mol. Biol. Evol.* **32**, 1962-
585 1976 (2015).
- 586 36. J. C. Opazo, F. G. Hoffmann, C. Natarajan, C. C. Witt, M. Berenbrink, J. F. Storz, Gene turnover in the avian
587 globin gene families and evolutionary changes in hemoglobin isoform expression. *Mol. Biol. Evol.* **32**, 871-
588 887 (2015).
- 589 37. J. F. Storz, Z. A. Cheviron, in *Hypoxia*. R. Roach, P. Hackett, P. Wagner, Eds. (Springer, Boston, MA.,
590 Advances in Experimental Medicine and Biology, 2016), vol. 903, pp. 113.
- 591 38. C. Natarajan, J. Projecto-Garcia, H. Moriyama, R. E. Weber, V. Munoz-Fuentes, A. J. Green, C. Kopuchian,
592 P. L. Tubaro, L. Alza, M. Bulgarella, M. M. Smith, R. E. Wilson, A. Fago, K. G. McCracken, J. F. Storz,
593 Convergent evolution of hemoglobin function in high-altitude Andean waterfowl involves limited

- 594 parallelism at the molecular sequence level. *PLoS Genet.* **11**, (2015).
- 595 39. F. M. Lei, Y. H. Qu, G. Song, Species diversification and phylogeographical patterns of birds in response to
596 the uplift of the Qinghai-Tibet Plateau and Quaternary glaciations. *Curr. Zool.* **60**, 149-161 (2014).
- 597 40. F. Dong, C. M. Hung, X. L. Li, J. Y. Gao, Q. Zhang, F. Wu, F. M. Lei, S. H. Li, X. J. Yang, Ice age unfrozen:
598 severe effect of the last interglacial, not glacial, climate change on East Asian avifauna. *BMC Evol. Biol.* **17**,
599 244 (2017).
- 600 41. Y. H. Qu, X. Luo, R. Y. Zhang, G. Song, F. S. Zou, F. M. Lei, Lineage diversification and historical
601 demography of a montane bird *Garrulax elliotii* - implications for the Pleistocene evolutionary history of the
602 eastern Himalayas. *BMC Evol. Biol.* **11**, 174 (2011).
- 603 42. W. Amos, J. Harwood, Factors affecting levels of genetic diversity in natural populations. *Philos. Trans. R.
604 Soc. Lond. B Biol. Sci.* **353**, 177-186 (1998).
- 605 43. C. Natarajan, F. G. Hoffmann, R. E. Weber, A. Fago, C. C. Witt, J. F. Storz, Predictable convergence in
606 hemoglobin function has unpredictable molecular underpinnings. *Science* **354**, 336-339 (2016).
- 607 44. N. J. Dawson, L. Alza, G. Nandal, G. R. Scott, K. G. McCracken, Convergent changes in muscle metabolism
608 depend on duration of high-altitude ancestry across Andean waterfowl. *eLife* **9**, (2020).
- 609 45. M. C. W. Lim, C. C. Witt, C. H. Graham, L. M. Dávalos, Parallel molecular evolution in pathways, genes,
610 and sites in high-elevation hummingbirds revealed by comparative transcriptomics. *Genome Biol. Evol.* **11**,
611 1552-1572 (2019).
- 612 46. Y. H. Qu, C. H. Chen, Y. Xiong, H. S. She, Y. E. Zhang, Y. L. Cheng, S. DuBay, D. M. Li, P. G. P. Ericson, Y.
613 Hao, H. Y. Wang, H. F. Zhao, G. Song, H. L. Zhang, T. Yang, C. Zhang, L. P. Liang, T. Y. Wu, J. Y. Zhao, Q.
614 Gao, W. W. Zhai, F. M. Lei, Rapid phenotypic evolution with shallow genomic differentiation during the
615 early stage of high elevation adaptation in Eurasian Tree Sparrows. *Natl. Sci. Rev.* **7**, 113-127 (2020).
- 616 47. Y. Cheng, M. J. Miller, D. Zhang, G. Song, C. Jia, Y. Qu, F. Lei, Comparative genomics reveals evolution of
617 a beak morphology locus in a high-altitude songbird. *Mol. Biol. Evol.* (2020).
- 618 48. M. P. Schippers, O. Ramirez, M. Arana, P. Pinedo-Bernal, G. B. McClelland, Increase in carbohydrate
619 utilization in high-altitude Andean mice. *Curr. Biol.* **22**, 2350-2354 (2012).
- 620 49. H. Li, R. Durbin, Fast and accurate long-read alignment with Burrows-Wheeler transform. *Bioinformatics*
621 **26**, 589-595 (2010).
- 622 50. A. McKenna, M. Hanna, E. Banks, A. Sivachenko, K. Cibulskis, A. Kernytsky, K. Garimella, D. Altshuler, S.
623 Gabriel, M. Daly, M. A. DePristo, The Genome Analysis Toolkit: A MapReduce framework for analyzing
624 next-generation DNA sequencing data. *Genome Res.* **20**, 1297-1303 (2010).

- 625 51. H. Li, A statistical framework for SNP calling, mutation discovery, association mapping and population
626 genetical parameter estimation from sequencing data. *Bioinformatics* **27**, 2987-2993 (2011).
- 627 52. H. Ellegren, L. Smeds, R. Burri, P. I. Olason, N. Backstrom, T. Kawakami, A. Kunstner, H. Makinen, K.
628 Nadachowska-Brzyska, A. Qvarnstrom, S. Uebbing, J. B. W. Wolf, The genomic landscape of species
629 divergence in Ficedula flycatchers. *Nature* **491**, 756-760 (2012).
- 630 53. A. Stamatakis, RAxML version 8: a tool for phylogenetic analysis and post-analysis of large phylogenies.
631 *Bioinformatics* **30**, 1312-1313 (2014).
- 632 54. S. Mirarab, T. Warnow, ASTRAL-II: coalescent-based species tree estimation with many hundreds of taxa
633 and thousands of genes. *Bioinformatics* **31**, 44-52 (2015).
- 634 55. E. D. Jarvis, S. Mirarab, A. J. Aberer, B. Li, P. Houde, C. Li, S. Y. W. Ho, B. C. Faircloth, B. Nabholz, J. T.
635 Howard, A. Suh, C. C. Weber, R. R. da Fonseca, J. W. Li, F. Zhang, H. Li, L. Zhou, N. Narula, L. Liu, G.
636 Ganapathy, B. Boussau, M. S. Bayzid, V. Zavidovych, S. Subramanian, T. Gabaldon, S. Capella-Gutierrez, J.
637 Huerta-Cepas, B. Rekepalli, K. Munch, M. Schierup, B. Lindow, W. C. Warren, D. Ray, R. E. Green, M. W.
638 Bruford, X. J. Zhan, A. Dixon, S. B. Li, N. Li, Y. H. Huang, E. P. Derryberry, M. F. Bertelsen, F. H. Sheldon,
639 R. T. Brumfield, C. V. Mello, P. V. Lovell, M. Wirthlin, M. P. C. Schneider, F. Prosdocimi, J. A. Samaniego,
640 A. M. V. Velazquez, A. Alfaro-Nunez, P. F. Campos, B. Petersen, T. Sicheritz-Ponten, A. Pas, T. Bailey, P.
641 Scofield, M. Bunce, D. M. Lambert, Q. Zhou, P. Perelman, A. C. Driskell, B. Shapiro, Z. J. Xiong, Y. L.
642 Zeng, S. P. Liu, Z. Y. Li, B. H. Liu, K. Wu, J. Xiao, X. Yinqi, Q. M. Zheng, Y. Zhang, H. M. Yang, J. Wang,
643 L. Smeds, F. E. Rheindt, M. Braun, J. Fjeldsa, L. Orlando, F. K. Barker, K. A. Jonsson, W. Johnson, K. P.
644 Koepfli, S. O'Brien, D. Haussler, O. A. Ryder, C. Rahbek, E. Willerslev, G. R. Graves, T. C. Glenn, J.
645 McCormack, D. Burt, H. Ellegren, P. Alstrom, S. V. Edwards, A. Stamatakis, D. P. Mindell, J. Cracraft, E. L.
646 Braun, T. Warnow, W. Jun, M. T. P. Gilbert, G. J. Zhang, Whole-genome analyses resolve early branches in
647 the tree of life of modern birds. *Science* **346**, 1320-1331 (2014).
- 648 56. M. dos Reis, Z. H. Yang, Approximate likelihood calculation on a phylogeny for Bayesian estimation of
649 divergence times. *Mol. Biol. Evol.* **28**, 2161-2172 (2011).
- 650 57. P. Danecek, A. Auton, G. Abecasis, C. A. Albers, E. Banks, M. A. DePristo, R. E. Handsaker, G. Lunter, G. T.
651 Marth, S. T. Sherry, G. McVean, R. Durbin, G. P. A. Grp, The variant call format and VCFtools.
652 *Bioinformatics* **27**, 2156-2158 (2011).
- 653 58. M. A. Oliver, R. Webster, Kriging: a method of interpolation for geographical information systems. *Int. J.*
654 *Geogr. Inf. Sci.* **4**, 313-332 (1990).
- 655 59. H. Li, R. Durbin, Inference of human population history from individual whole-genome sequences. *Nature*

- 656 475, 493-496 (2011).
- 657 60. K. Nadachowska-Brzyska, C. Li, L. Smeds, G. J. Zhang, H. Ellegren, Temporal dynamics of avian
658 populations during Pleistocene revealed by whole-genome sequences. *Curr. Biol.* **25**, 1375-1380 (2015).
- 659 61. Z. Yang, PAML 4: phylogenetic analysis by maximum likelihood. *Mol. Biol. Evol.* **24**, 1586-1591 (2007).
- 660 62. A. G. Gosler, P. Clement, A. Bonan, in *Handbook of the birds of the world*, J. Del Hoyo, A. Elliott, J.
661 Sargatal, D. A. Christie, E. de Juana, Eds. (Lynx Edicions, Barcelona, 2019), pp. 662-744.
- 662 63. J. E. Brommer, L. Gustafsson, H. Pietiainen, J. Merila, Single-generation estimates of individual fitness as
663 proxies for long-term genetic contribution. *Am. Nat.* **163**, 505-517 (2004).
- 664 64. S. R. Browning, B. L. Browning, Rapid and accurate haplotype phasing and missing-data inference for
665 whole-genome association studies by use of localized haplotype clustering. *Am. J. Hum. Genet.* **81**, 1084-
666 1097 (2007).
- 667 65. P. Cingolani, A. Platts, L. L. Wang, M. Coon, T. Nguyen, L. Wang, S. J. Land, X. Y. Lu, D. M. Ruden, A
668 program for annotating and predicting the effects of single nucleotide polymorphisms, SnpEff: SNPs in the
669 genome of Drosophila melanogaster strain w(1118); iso-2; iso-3. *Fly* **6**, 80-92 (2012).
- 670 66. G. R. Scott, Elevated performance: the unique physiology of birds that fly at high altitudes. *J. Exp. Biol.* **214**,
671 2455-2462 (2011).
- 672 67. G. R. Scott, S. Egginton, J. G. Richards, W. K. Milsom, Evolution of muscle phenotype for extreme high
673 altitude flight in the bar-headed goose. *Proc. R. Soc. B Biol. Sci.* **276**, 3645-3653 (2009).
- 674 68. E. R. Weibel, in *The Pathway for Oxygen*, M. P. Hlastala, Ed. (Harvard University Press, Cambridge, MA,
675 1984), pp. 49-79.
- 676 69. R. P. Huntley, D. Binns, E. Dimmer, D. Barrell, C. O'Donovan, R. Apweiler, QuickGO: a user tutorial for the
677 web-based Gene Ontology browser. *Database (Oxford)* **2009**, bap010 (2009).
- 678 70. A. Alexa, J. Rahnenfuhrer, topGO: enrichment analysis for gene ontology. *R package version 2.32.0*, (2010).
- 679 71. Y. Benjamini, Y. Hochberg, Controlling the False Discovery Rate - a Practical and Powerful Approach to
680 Multiple Testing. *J. Roy. Stat. Soc. B Met.* **57**, 289-300 (1995).
- 681 72. G. Yu, F. Li, Y. Qin, X. Bo, Y. Wu, S. Wang, GOSemSim: an R package for measuring semantic similarity
682 among GO terms and gene products. *Bioinformatics* **26**, 976-978 (2010).
- 683 73. R. C. Edgar, MUSCLE: multiple sequence alignment with high accuracy and high throughput. *Nucleic Acids
684 Res.* **32**, 1792-1797 (2004).
- 685 74. B. Pfeifer, U. Wittelsburger, S. E. Ramos-Onsins, M. J. Lercher, PopGenome: an efficient Swiss army knife
686 for population genomic analyses in R. *Mol. Biol. Evol.* **31**, 1929-1936 (2014).

- 687 75. R. J. Hijmans, S. E. Cameron, J. L. Parra, P. G. Jones, A. Jarvis, Very high resolution interpolated climate
688 surfaces for global land areas. *Int. J. Climatol.* **25**, 1965-1978 (2005).
- 689 76. J. C. Zachos, G. R. Dickens, R. E. Zeebe, An early Cenozoic perspective on greenhouse warming and
690 carbon-cycle dynamics. *Nature* **451**, 279-283 (2008).
- 691 77. J. Hansen, M. Sato, G. Russell, P. Kharecha, Climate sensitivity, sea level and atmospheric carbon dioxide.
692 *Phil. Trans. R. Soc. A* **371**, 20120294 (2013).
- 693 78. S. Purcell, B. Neale, K. Todd-Brown, L. Thomas, M. A. R. Ferreira, D. Bender, J. Maller, P. Sklar, P. I. W. de
694 Bakker, M. J. Daly, P. C. Sham, PLINK: A tool set for whole-genome association and population-based
695 linkage analyses. *Am. J. Hum. Genet.* **81**, 559-575 (2007).
- 696 79. R. B. Luo, B. H. Liu, Y. L. Xie, Z. Y. Li, W. H. Huang, J. Y. Yuan, G. Z. He, Y. X. Chen, Q. Pan, Y. J. Liu, J.
697 B. Tang, G. X. Wu, H. Zhang, Y. J. Shi, Y. Liu, C. Yu, B. Wang, Y. Lu, C. L. Han, D. W. Cheung, S. M. Yiu,
698 S. L. Peng, X. Q. Zhu, G. M. Liu, X. K. Liao, Y. R. Li, H. M. Yang, J. Wang, T. W. Lam, J. Wang,
699 SOAPdenovo2: an empirically improved memory-efficient short-read de novo assembler. *Gigascience* **1**, 18
700 (2012).
- 701 80. R. Q. Li, W. Fan, G. Tian, H. M. Zhu, L. He, J. Cai, Q. F. Huang, Q. L. Cai, B. Li, Y. Q. Bai, Z. H. Zhang, Y.
702 P. Zhang, W. Wang, J. Li, F. W. Wei, H. Li, M. Jian, J. W. Li, Z. L. Zhang, R. Nielsen, D. W. Li, W. J. Gu, Z.
703 T. Yang, Z. L. Xuan, O. A. Ryder, F. C. C. Leung, Y. Zhou, J. J. Cao, X. Sun, Y. G. Fu, X. D. Fang, X. S.
704 Guo, B. Wang, R. Hou, F. J. Shen, B. Mu, P. X. Ni, R. M. Lin, W. B. Qian, G. D. Wang, C. Yu, W. H. Nie, J.
705 H. Wang, Z. G. Wu, H. Q. Liang, J. M. Min, Q. Wu, S. F. Cheng, J. Ruan, M. W. Wang, Z. B. Shi, M. Wen,
706 B. H. Liu, X. L. Ren, H. S. Zheng, D. Dong, K. Cook, G. Shan, H. Zhang, C. Kosiol, X. Y. Xie, Z. H. Lu, H.
707 C. Zheng, Y. R. Li, C. C. Steiner, T. T. Y. Lam, S. Y. Lin, Q. H. Zhang, G. Q. Li, J. Tian, T. M. Gong, H. D.
708 Liu, D. J. Zhang, L. Fang, C. Ye, J. B. Zhang, W. B. Hu, A. L. Xu, Y. Y. Ren, G. J. Zhang, M. W. Bruford, Q.
709 B. Li, L. J. Ma, Y. R. Guo, N. An, Y. J. Hu, Y. Zheng, Y. Y. Shi, Z. Q. Li, Q. Liu, Y. L. Chen, J. Zhao, N. Qu,
710 S. C. Zhao, F. Tian, X. L. Wang, H. Y. Wang, L. Z. Xu, X. Liu, T. Vinar, Y. J. Wang, T. W. Lam, S. M. Yiu, S.
711 P. Liu, H. M. Zhang, D. S. Li, Y. Huang, X. Wang, G. H. Yang, Z. Jiang, J. Y. Wang, N. Qin, L. Li, J. X. Li,
712 L. Bolund, K. Kristiansen, G. K. S. Wong, M. Olson, X. Q. Zhang, S. G. Li, H. M. Yang, J. Wang, J. Wang,
713 The sequence and de novo assembly of the giant panda genome. *Nature* **463**, 311-317 (2010).
- 714 81. S. F. Altschul, T. L. Madden, A. A. Schaffer, J. H. Zhang, Z. Zhang, W. Miller, D. J. Lipman, Gapped
715 BLAST and PSI-BLAST: a new generation of protein database search programs. *Nucleic Acids Res.* **25**,
716 3389-3402 (1997).
- 717 82. R. She, J. S. C. Chu, K. Wang, J. Pei, N. S. Chen, genBlastA: Enabling BLAST to identify homologous gene

- 718 sequences. *Genome Res.* **19**, 143-149 (2009).
- 719 83. G. S. Slater, E. Birney, Automated generation of heuristics for biological sequence comparison. *BMC*
720 *Bioinformatics* **6**, 31 (2005).
- 721 84. R. C. Edgar, Search and clustering orders of magnitude faster than BLAST. *Bioinformatics* **26**, 2460-2461
722 (2010).
- 723 85. G. Talavera, J. Castresana, Improvement of phylogenies after removing divergent and ambiguously aligned
724 blocks from protein sequence alignments. *Syst. Biol.* **56**, 564-577 (2007).
- 725 86. R. Bouckaert, J. Heled, D. Kuhnert, T. Vaughan, C. H. Wu, D. Xie, M. A. Suchard, A. Rambaut, A. J.
726 Drummond, BEAST 2: a software platform for Bayesian evolutionary analysis. *PLoS Comput. Biol.* **10**,
727 e1003537 (2014).
- 728 87. A. J. Drummond, S. Y. W. Ho, M. J. Phillips, A. Rambaut, Relaxed phylogenetics and dating with
729 confidence. *PLoS Biol.* **4**, 699-710 (2006).
- 730 88. A. Manegold, Earliest fossil record of the Certhioidea (treecreepers and allies) from the early Miocene of
731 Germany. *J. Ornithol.* **149**, 223-228 (2008).

734 **Acknowledgements**

735 **General:** We thank Scott Edwards for suggestions on data analysis, and Huateng Huang, Kevin
736 McCracken, and A. Townsend Peterson for discussion and valuable comments on an early version
737 of the manuscript.

738

739 **Funding:** This work was supported by the National Natural Science Foundation of China (Nos.
740 31630069, 31572249). The field work of sample collection was supported by the Second Tibetan
741 Plateau Scientific Expedition and Research (STEP) program (Nos. 2019QZKK0501,
742 2019QZKK0304).

743

744 **Author contributions:** F.M.L. and Y.L.C. devised this research. C.X.J., G.S., Y.L.C., T.L.C. and
745 Y.B.C. did fieldwork for sample collections, S.H.L. and Y.L. provided samples. Y.X. prepared
746 DNA samples. Y.L.C. and M.J.M. analyzed the genomic data. D.Z.Z. and Y.H. assisted in
747 analyzing data. T.L.C. performed the ecological analyses. Y.B.C. constructed the genetic diversity
748 map. U.S.J. provided mtDNA-based phylogeny of parids. Y.L.C., M.J.M., G.S., Y.H.Q. and
749 F.M.L. drafted the manuscript, and all authors commented and approved.

750

751 **Competing interests:** The authors declare that they have no competing interests.

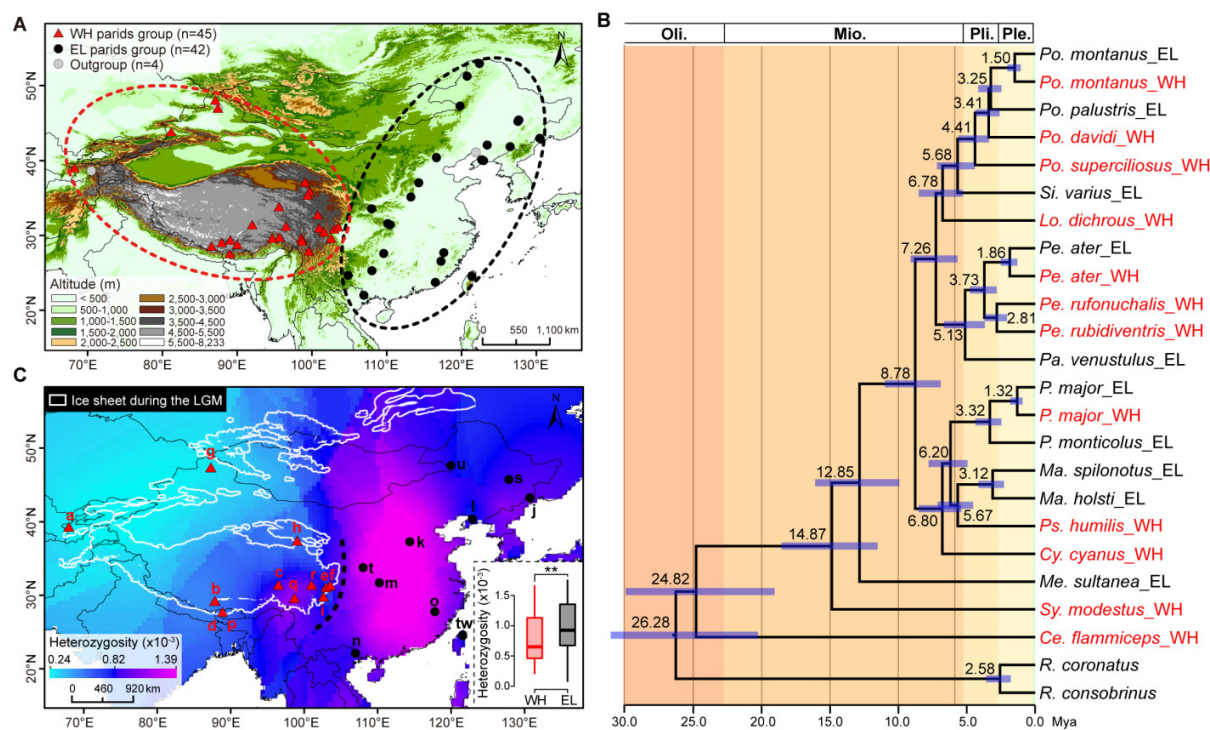
752

753 **Data and materials availability:** Raw sequencing reads have been deposited into the NCBI
754 Sequence Read Archive (BioProject: PRJNA553273). Sample accessions are listed in data file S1.
755 All other data needed to evaluate the conclusions in the paper are present in the paper and/or the
756 Supplementary Materials. Additional data related to this paper may be requested from the authors.

757

758

Figures



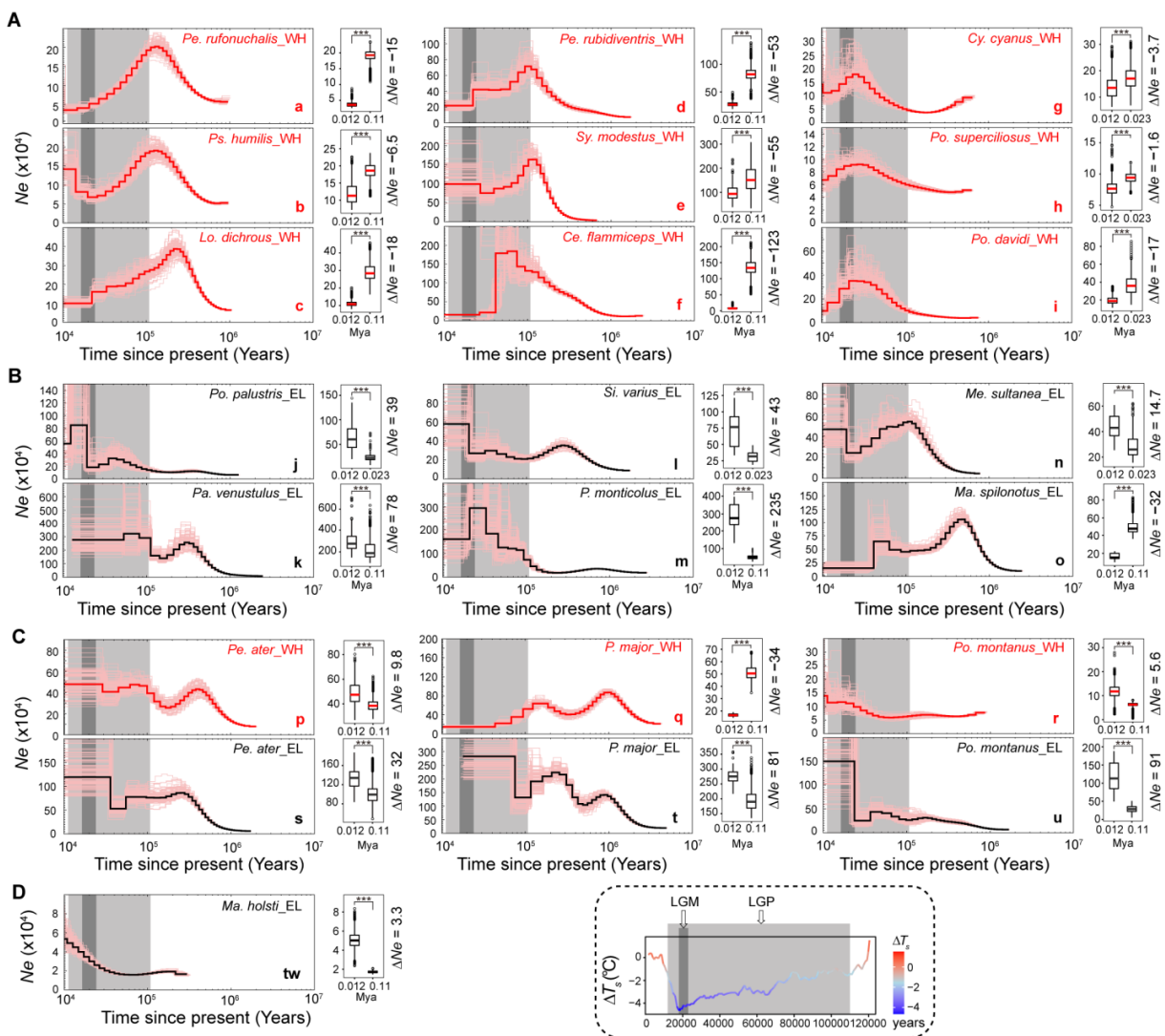
759

760 **Fig. 1. Sampling localities, time tree, and lineage-wide pattern of landscape genomic**
 761 **diversity of true tits (Paridae) in East Asia. (A)** Sampling localities for 91 birds (19 parid
 762 species and two outgroup species) across East Asia. Western Highland (WH) parids (red triangles)
 763 represent individuals from the Qinghai-Tibet Plateau and adjacent regions (e.g. the Pamirs Plateau,
 764 the Tianshan Mountains and the Altai Mountains). Eastern Lowland (EL) parids (black circles)
 765 were sampled throughout eastern mainland China and Taiwan Island below 1,000 m. The
 766 elevational base map was downloaded from <https://lta.cr.usgs.gov/GTOPO30>. **(B)** Time tree for
 767 East Asian parids based on uncorrelated relaxed clock. Best-estimate divergence times are
 768 displayed above the nodes and are largely similar with results from autocorrelated relaxed clocks
 769 (fig. S4). Blue bars on the nodes indicate the highest posterior density of the divergence time. Oli.,
 770 Oligocene; Mio., Miocene; Pli., Pliocene; Ple., Pleistocene. **(C)** Spatial distribution of lineage-
 771 wide genomic diversity based on the heterozygosity (H) of each individual. WH parids had
 772 significantly lower H than EL parids (** indicates $P < 0.01$). The white contour lines indicate the
 773 extent of glaciers during the Last Glacial Maximum (LGM, 0.023-0.018 Mya). The map of

774 glaciers is from <https://www.deviantart.com/atlas-v7x>. Capital letters correspond to panels in Fig.

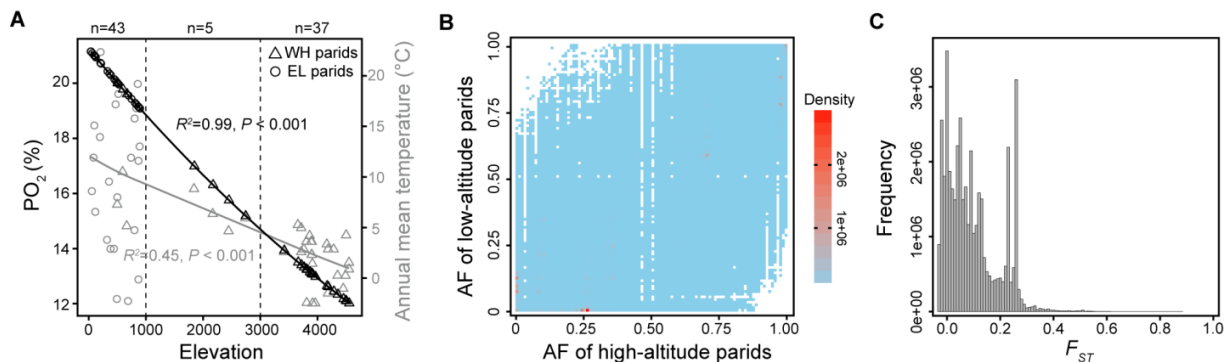
775 2.

776

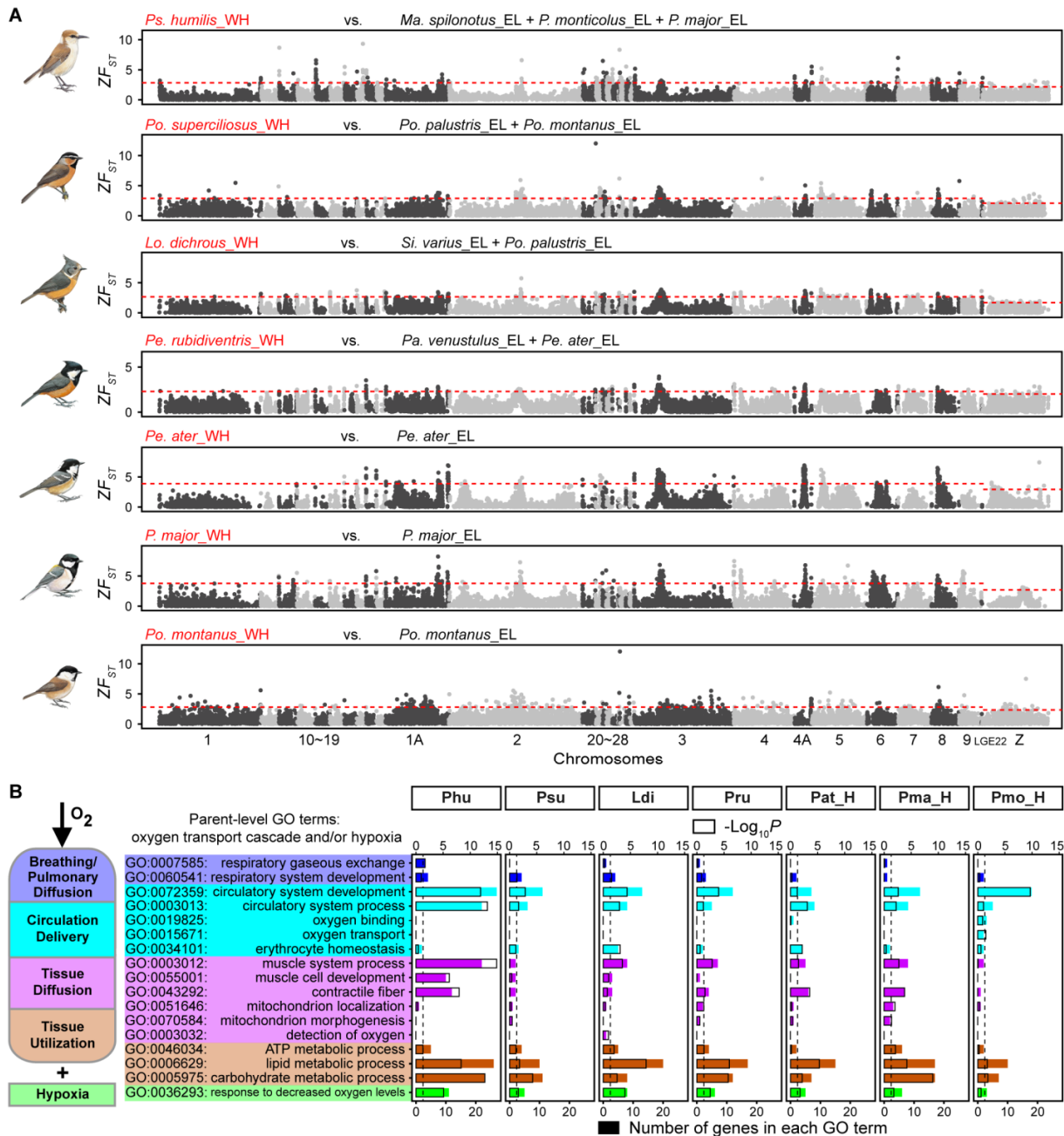


778 **Fig. 2. Demographic responses to Pleistocene varied consistently between Western Highland**
779 **(WH) and Eastern Lowland (EL) parids. (A)** Historical demography of WH parids inferred by
780 pairwise sequentially Markovian coalescent (PSMC): all nine species experienced a contraction of
781 effective population size (i.e. N_e contraction) during the Last Glacial Period (LGP; 0.11–0.012
782 Mya). Six taxa (a–f) declined from a high point at or near the beginning of the LPG, while in
783 three (g–i) the decline started at or near the Last Glacial Maximum (LGM; 0.023 Mya). **(B)**
784 Historical demography of EL parids: five of six species (j–n) experienced significant increase in

785 N_e during the LGP, the sixth (o) experienced a decline. (C) Historical demography of three
 786 widespread East Asian parid species. Here, the EL population of each species experienced
 787 significant demographic expansion during the LGP, yet two WH populations (*Pe. ater* and *Po.*
 788 *montanus*) also experienced significant expansion (in contrast, WH *P. major* experienced a
 789 significant contraction). (D) Significant increase in N_e during the LGP for the Taiwan Island
 790 endemic *Ma. holsti*. For all PSMC reconstructions, the box plot to the right side compares N_e at
 791 the end of the LGP versus the beginning of the LGP or LGM. “***” above the boxes indicates P
 792 < 0.001 . Capital letters corresponding to the locations in Fig. 1C. The legend shows changes in
 793 temperature during the past 120,000 years and indicates the intervals of the LGP and LGM glacial
 794 periods. ΔT_s is the global mean surface temperature anomaly from Zachos et al. (76) and Hansen
 795 et al. (77) plotted by years.
 796



797
 798 **Fig. 3. SNP-based differentiation between high-altitude (HA) and low-altitude (LA) parids.**
 799 (A) Atmospheric partial pressure of oxygen (PO₂) declines more rapidly than mean annual
 800 temperature across our East Asian sampling locations. We defined birds sampled at elevations
 801 above 3,000 m as HA parids, whereas those sampled below 1,000 m were defined as LA parids.
 802 (B) Allele frequency (AF) distribution for 43,458,033 single nucleotide polymorphisms (SNPs):
 803 zero SNPs are fixed between HA and LA parids. (C) Frequency distribution of site based F_{ST}
 804 between HA and LA parids: only 5589 (0.013%) SNPs had F_{ST} greater than 0.6.
 805



806

807

808

809

810

811

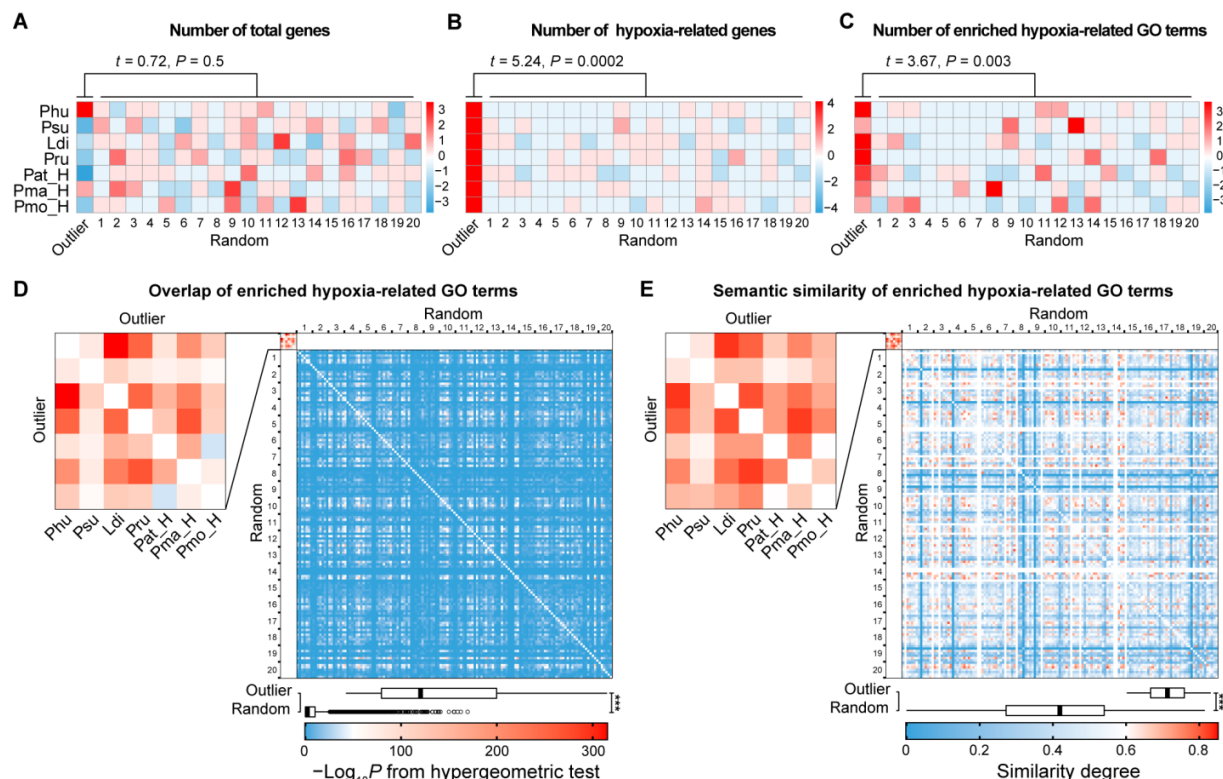
812

813

Fig. 4. F_{ST} outlier windows are enriched with hypoxia-related genes. (A) Window-based comparisons of each high-altitude (HA) taxon with its low-altitude (LA) relatives. Red dash lines indicate cutoff values of the ZF_{ST} distribution in autosomes and Z chromosome. 202 highly divergent windows were identified for each high-altitude species. Illustrations of parids are from ref. (62). (B) Number of potentially hypoxia-related genes found in F_{ST} outlier windows by Gene Ontogeny (GO) term. The 17 hypoxia-related GO terms are grouped by the four physiological stages of the O_2 transport cascade plus a sixth hypoxia category. The unfilled bar represents the

814 log-transformed P -value for the enrichment of GO term, and the color-filled bar represents the
 815 observed number of genes associated with that GO term found in outlier F_{ST} windows.
 816 Enrichment is a measure of the over-representation of particular genes by GO term. Phu = *Ps.*
 817 *humilis*; Psu = *Po. supercilirosus*; Ldi = *Lo. dichrous*; Pru = *Pe. rubidiventris*; Pat_H = *Pe. ater*
 818 (HA); Pma_H = *P. major* (HA); Pmo_H = *Po. montanus* (HA).

819



820
 821 **Fig. 5. East Asian tits show parallel adaptive responses to high elevation at the level of**
 822 **biological function.** (A) High F_{ST} outlier windows have a similar number of total genes compared
 823 to random windows. (B) However, outlier windows have significantly more hypoxia-related genes
 824 than random windows. (C) Also, outlier windows have significantly more enriched hypoxia-
 825 related Gene Ontogeny (GO) terms than random windows. Cell color in A-C indicates the scaled
 826 z -score (by standard deviation) within each high-altitude (HA) and low-altitude (LA) comparison.
 827 (D) High F_{ST} outlier windows have significantly higher overlap of enriched hypoxia-related GO
 828 terms than random windows. Cell color indicates the log-transformed P -value generated by the

829 hypergeometric test. (**E**) Likewise, enriched hypoxia-related GO terms have significantly
830 semantic similarity in high F_{ST} outlier windows than in random windows. Cell color indicates the
831 similarity degree. In the box plots for **D** and **E**, “***” indicates $P < 0.001$.

1

2 Supplementary Materials for

3

4 **Parallel genomic responses to historical climate change and high elevation in East Asian**
5 **songbirds**

6

7 Yalin Cheng[†], Matthew J. Miller[†], Dezhi Zhang, Ying Xiong, Yan Hao, Chenxi Jia, Tianlong Cai,
8 Shou-Hsien Li, Ulf S. Johansson, Yang Liu, Yongbin Chang, Gang Song, Yanhua Qu and Fumin
9 Lei^{*}

10

11 [†]These authors contributed equally to this work

12 ^{*}**Correspondence to:** Fumin Lei, E-mail: leifm@ioz.ac.cn

13

14

15 **This file includes:**

16 Supplementary Methods

17 Figs. S1 to S7

18 Tables S1 to S5

19 Legends for data files S1 to S3

22 **Supplementary Methods**

23 **Cluster analyses**

24 We performed two cluster analyses, e.g., principal components analysis (PCA) and
25 multidimensional scaling (MDS), on the filtered SNP dataset using PLINK v1.9 (78).

26

27 **Rough assembly**

28 One individual with deep coverage from each species or population was passed to SOAPdenovo
29 v2.04 (79) for *de novo* simple step by step assembly. We tried different k-mers (from 20-mer to
30 50-mer) to construct contigs and chose the k-mer with the largest N50 contig length. All usable
31 reads were mapped back to contig sequences to construct scaffolds. Gap filling of the assembly
32 was done using the intrinsic function of SOAPdenovo as well as Gapcloser v1.10 (80). All rough
33 assemblies had similar genome sizes, ranging from 0.95 Gb to 1.25 Gb, with an 14.24 kb average
34 N50 scaffold length (1.26 kb to 48.73 kb) and an 1.61 kb average N50 contig length (0.37–6.04
35 kb; table S2).

36

37 **Protein-coding sequence prediction**

38 We obtained 14,150 putative orthologs from 15,781 single-copy proteins for *Pseudopodoces*
39 *humilis* and 15,203 for *Parus major*. This orthologous set was used as a reference to predict
40 protein-coding sequences for all assemblies. We roughly aligned reference protein sequences to
41 each assembled genome by TBLASTN (81) with an E-value cut-off of 1e-5, and linked the
42 fragmental blast hits into putative candidate gene loci using genBlastA v1.0.4 (82) with a
43 coverage cut-off of 50%. The corresponding genomic sequences of candidate gene loci were
44 extracted to perform further alignment with Exonerate v2.2.0 (83). We then extracted predicted
45 coding sequences from the outcomes of Exonerate and clustered them into a non-redundant gene
46 set using Usearch v10.0 (84)). After filtering out sequences with lengths of <100 bp, we finally
47 obtained around 11,000 protein-coding sequences for each assembly with an average length of
48 1000 bp (table S2).

49

50 **Orthology and clocklike-testing**

51 We translated coding sequences into amino acid sequences, and identified 1,885 one-to-one
52 orthologs among 24 species or populations (including outgroups). Orthologous protein sequences

were aligned by MUSCLE v3.8.31 (73), and gaps and poorly aligned regions were removed using Gblocks v0.91 (85). To estimate the timescale for the evolution of parids, we tested the clocklike evolution of each ortholog. We first translated proteins back into coding sequences and removed the third codon position (C3) for each code because of its high degeneracy. The clocklike test was performed on the retained first and second codon positions (C12) of each alignment using BEAST v2.4.5 (86) under the uncorrelated lognormal relaxed-clock model (87). This model produces a coefficient of variation (CoV) of rates that measures the degree of the variation in rates among lineages. A CoV close to zero reflects no variation in rates, indicating the ortholog is clocklike. Here, we selected 246 orthologs (124,080 nucleotides) for the dating analysis when their CoV was less than 0.5 and the lower and upper limits of the 95% credibility interval of the CoV were less than 0.1 and 1.0, respectively (55).

64

65 **Time estimation**

66 Bayesian dating analysis was conducted using a concatenated alignment of orthologs based on
67 the above species tree (fig. S2c). Divergence times were estimated using the uncorrelated and
68 autocorrelated relaxed clocks in the *MCMCTree* program of PAML v4.9 (56). We used the
69 HKY85+GAMMA substitution model, with four rate categories for gamma-distributed rates
70 across sites. Given the large size of the dataset, we used the approximate-likelihood method with
71 substitution rate and branch lengths estimated in the *baseml* and *MCMCTree* programs. We also
72 used the estimated substitution rate to set the gamma for the overall rates for genes
73 (rgene_gamma). Posterior distributions of divergence times were estimated using Markov chain
74 Monte Carlo sampling, with samples drawn every 2,000 steps over a total of 10^8 steps after a
75 discarded burn-in of 2×10^7 steps. We repeatedly ran each step to ensure the results began to
76 converge.

77

78 **Calibration**

79 Our dating analysis was calibrated using soft-bound age constraints because no relevant parid
80 was known. In Johansson's comprehensive phylogenetic analysis, a fossil of *Certhiops rummeli*
81 was used as a calibration (88), and they found a separation of Paridae from Remizidae at
82 16.0–22.4 Mya (13). We used the upper limits of the 95% confidence interval (22.4 Mya) to
83 calculate the substitution rate using the *baseml* program. Then we estimated branch lengths based

84 on an approximate root age (30 Mya) that was the divergence time between oscines and
85 suboscines (55). Finally, a genome-based age between *Ps. humilis* and *Machlolophus spilonotus*
86 (11.9–4.8 Mya) (12) was used as a soft-bound calibration point to estimate the divergence times
87 between parids.

88

89

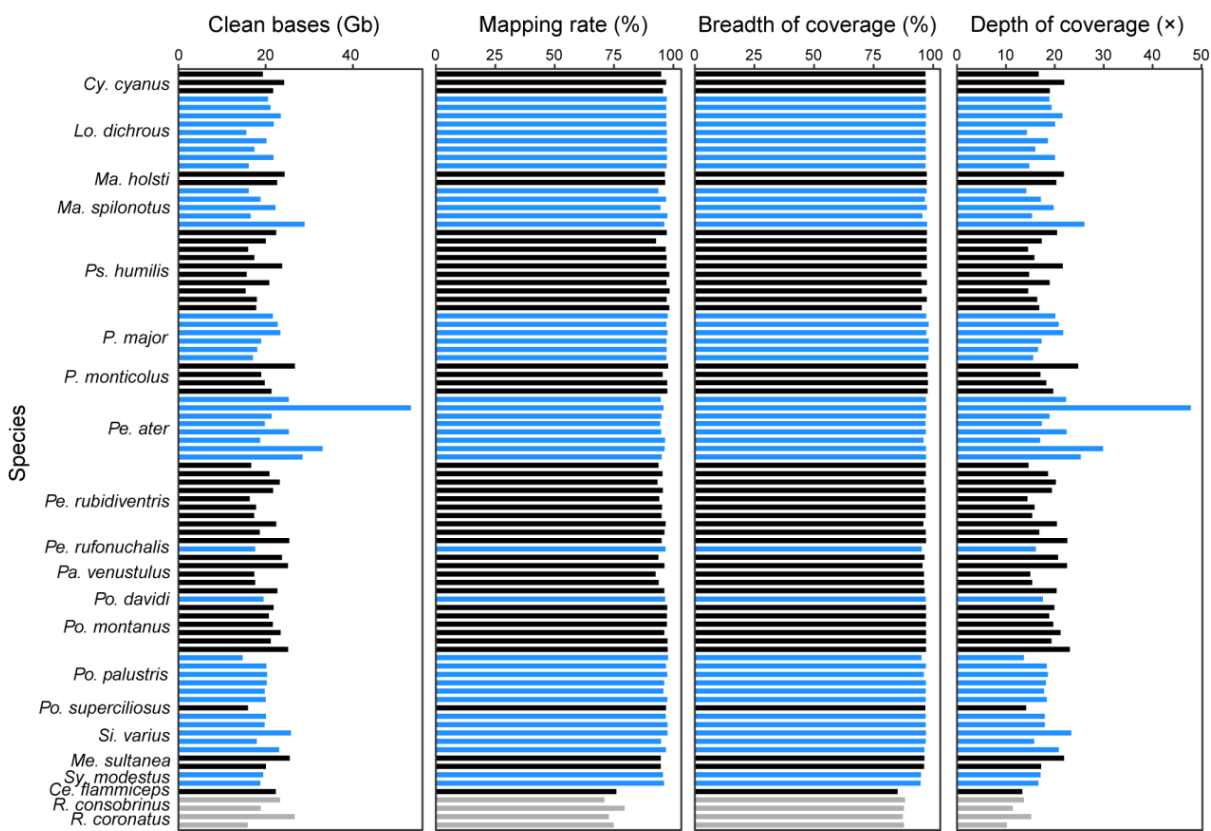


Fig. S1. Statistics for whole genome re-sequencing data. A total of 1,921 Gb whole-genome sequences were generated with an average of 18.66 \times (10.18–47.80 \times) coverage per individual. Reads were aligned to the *Parus major* reference, resulting in an average mapping rate of 95% (71%–98%).

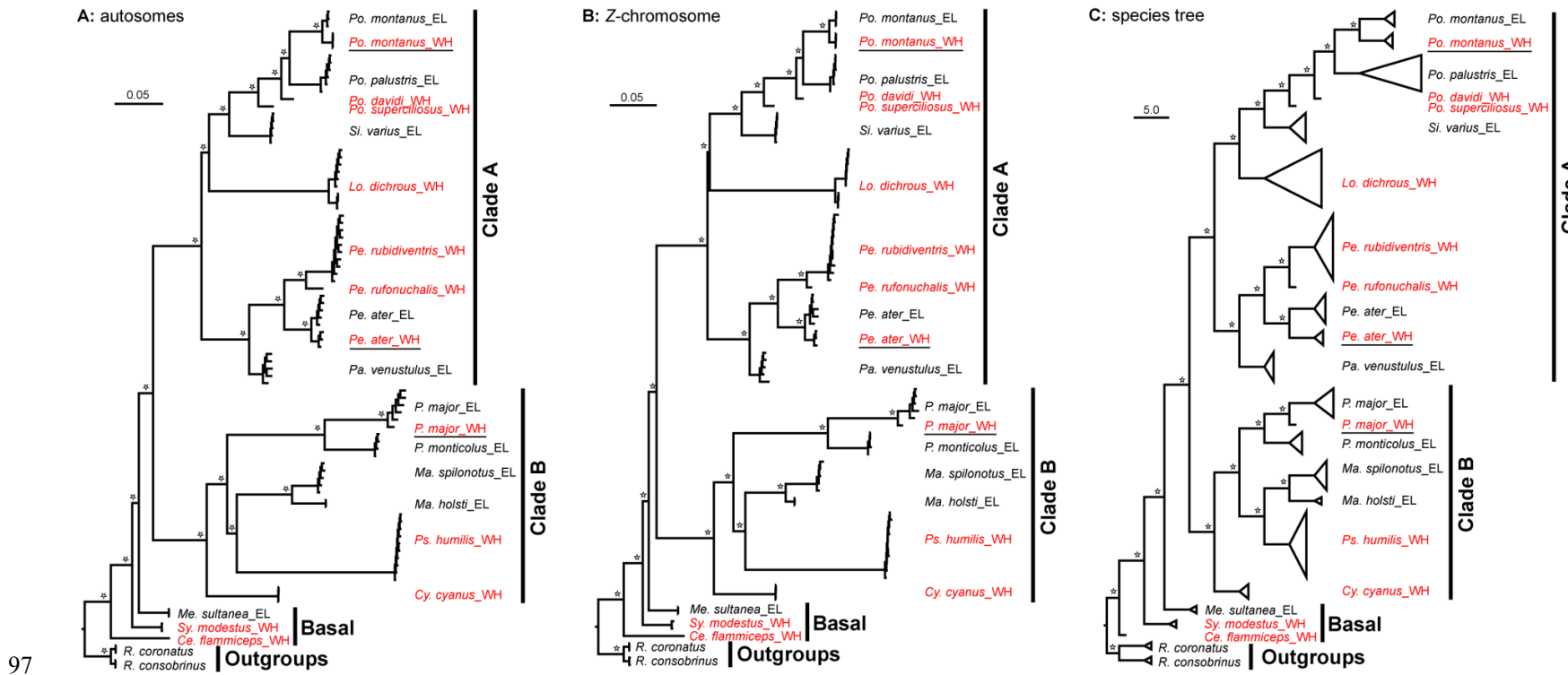
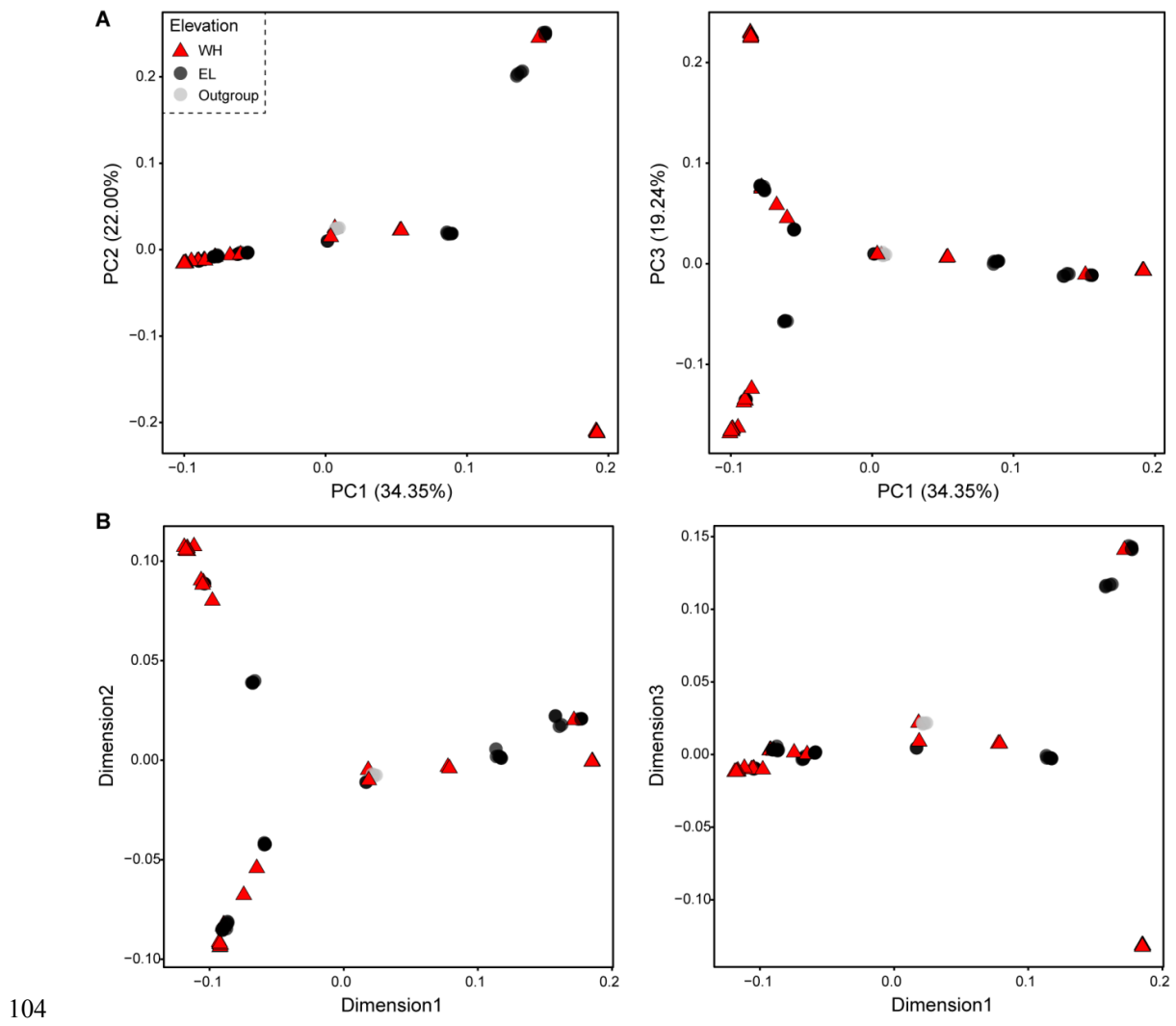


Fig. S2. Phylogenetic analyses. (A) ML phylogenetic tree based on autosomal SNPs. (B) ML phylogenetic tree based on Z-chromosomal SNPs. (C) Coalescent-based species tree constructed by ASTRAL using 50 random subsets of ~50,000 SNPs. Three basal species successively branch off, and the remaining parids consist of two large clades (clade A and clade B). All nodes marked by stars have high bootstrap values (100%). Western Highland (WH) populations are highlighted by red; WH populations of widespread species are underlined.



105 **Fig. S3. Dimensionality reduction analyses of all individuals based on all SNPs. (A)**
106 Principal components analysis (PCA) analysis. **(B)** Multidimensional scaling (MDS)
107 analysis. Western Highland (WH) and Eastern Lowland (EL) individuals do not form
108 unique clusters.

109

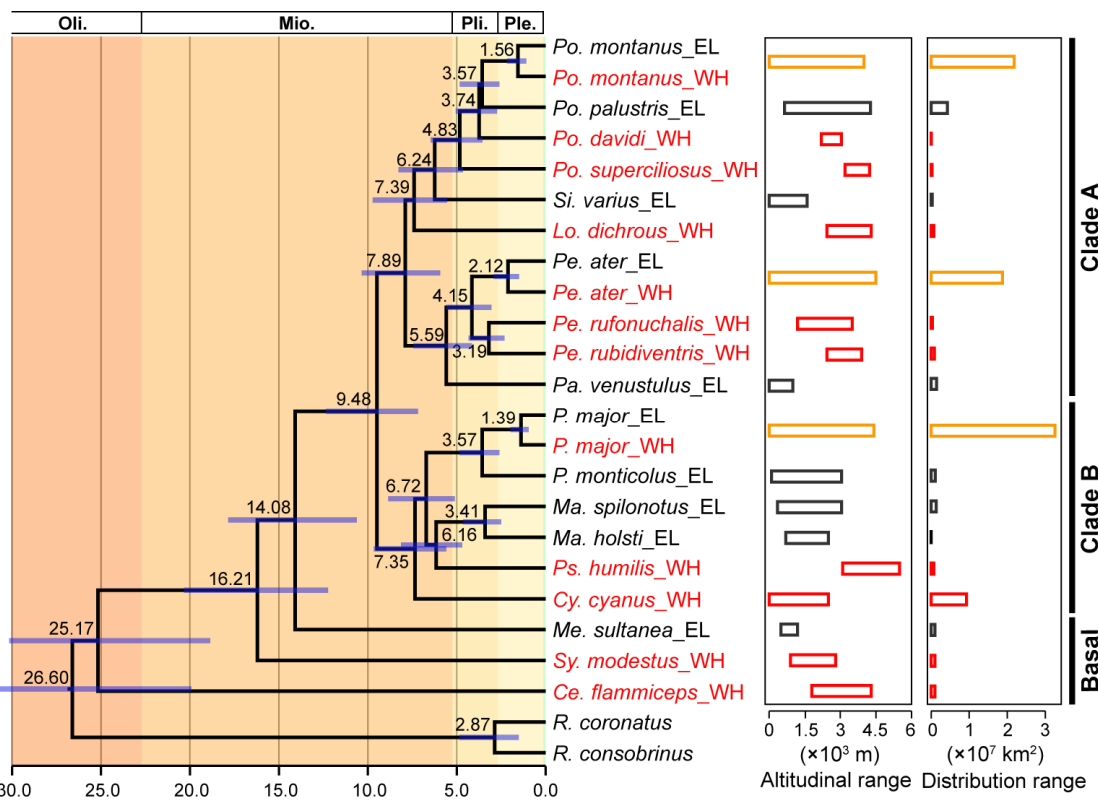
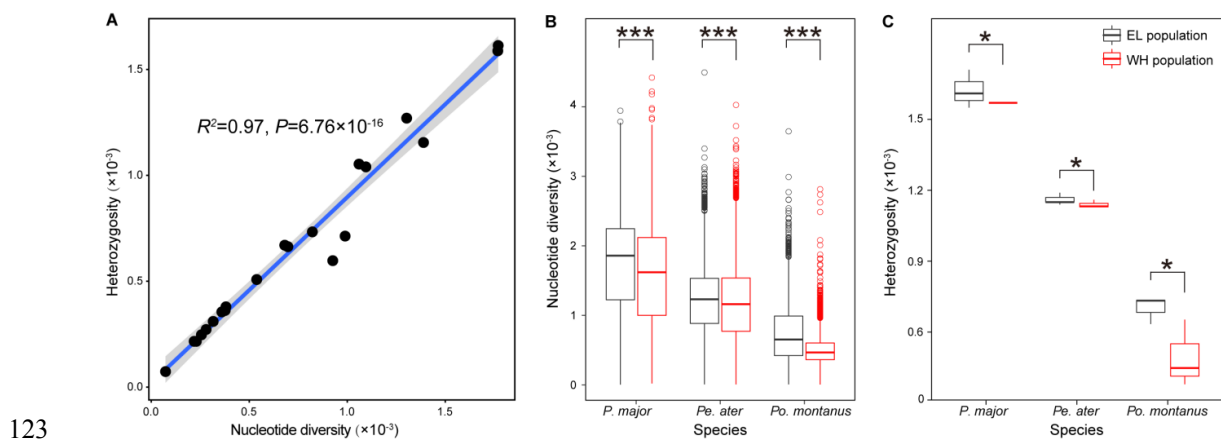


Fig. S4. Time trees for East Asian parids based on autocorrelated relaxed clock.

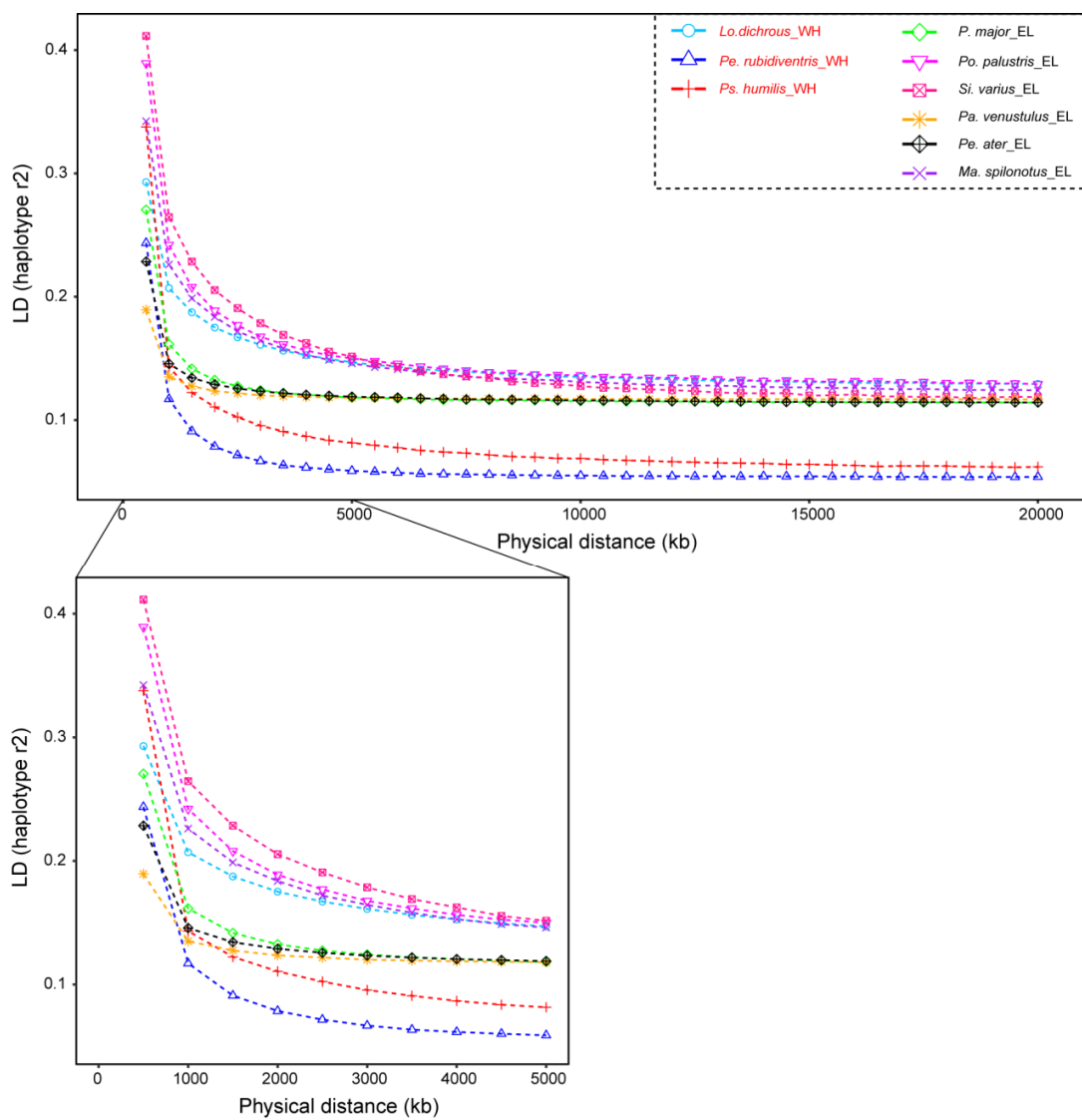
Time estimates are displayed above the branches and similar with estimates generated by uncorrelated relaxed clock (Fig. 1b). Blue bars on the nodes indicate the highest posterior density of the divergence time. Western Highland (WH) parids are highlighted in red; Eastern Lowland (EL) parids are in black. Oli., Oligocene; Mio., Miocene; Pli., Pliocene; Ple., Pleistocene. Epoch ages were determined according to the International Stratigraphic Chart (2016) from the International Commission on Stratigraphy. Altitudinal ranges are from Gosler et al. (62), and distribution range sizes were calculated in ArcGIS based on distribution maps from BirdLife International (<http://datazone.birdlife.org/>). Red bars indicate WH native parids; black bars indicate EL native parids; orange bars indicate widespread species.



124 **Fig. S5. Relationships between nucleotide diversity and heterozygosity. (A)**

125 Heterozygosity is significantly correlated to nucleotide diversity, suggesting that we can
 126 use the heterozygosity as the genetic diversity. (B) Western Highland (WH) populations
 127 of three widespread species have significantly lower nucleotide diversity than Eastern
 128 Lowland (EL) population. “***” above the boxes indicates $P < 0.001$. *P. major*: W =
 129 184198789, $P < 2.2 \times 10^{-16}$; *Pe. ater*: W = 199023579, $P < 2.2 \times 10^{-16}$; *Po. montanus*: W
 130 = 138119300, $P < 2.2 \times 10^{-16}$. (C) WH populations of three widespread species have
 131 significantly lower heterozygosity than EL population. “*” above the boxes indicates $P <$
 132 0.05. *P. major*: t = 2.4495, df = 3, $P = 0.046$, *Pe. ater*: t = 2.2361, df = 4, $P = 0.044$; *Po.*
 133 *montanus*: t = 6.1969, df = 2, $P = 0.013$.

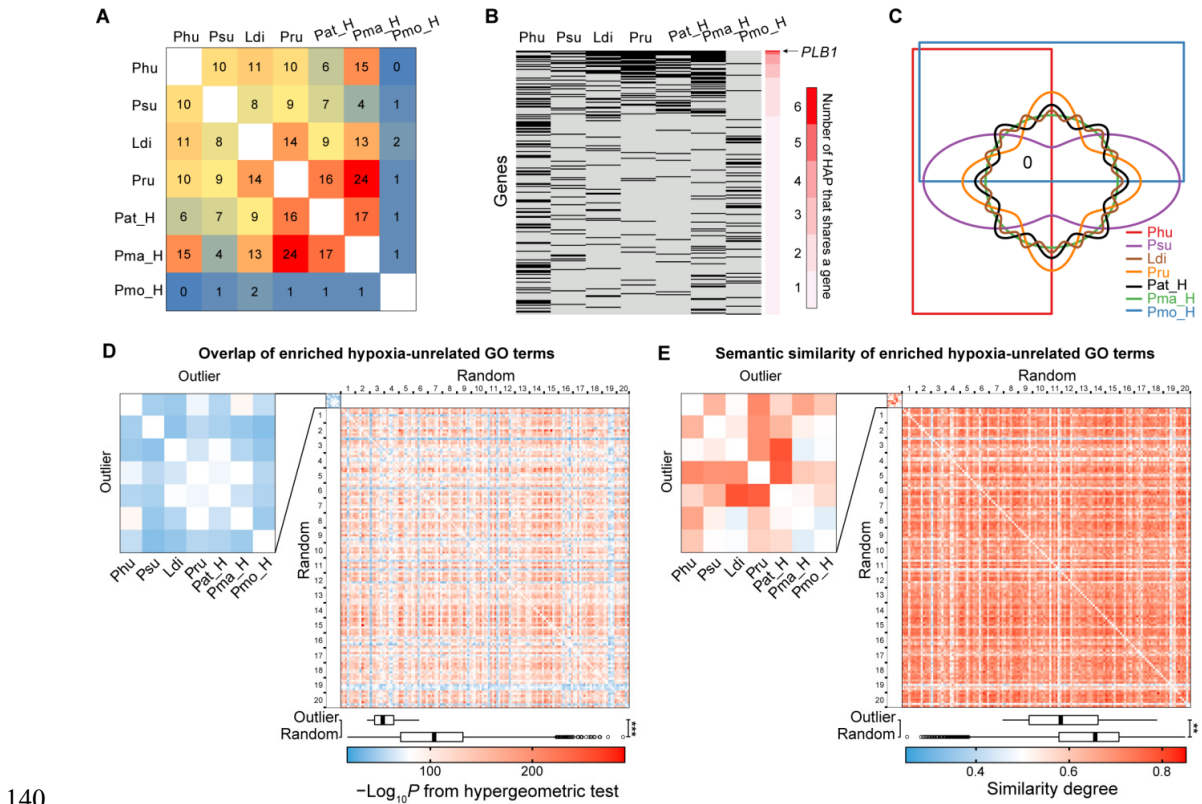
134



135

136 **Fig. S6. Linkage disequilibrium (LD) decay measure by haplotype r^2 values.** Average
 137 haplotype r^2 values in 500 bp windows over 20 kb (upper). Subtracted LD over the first
 138 5kb is showed in the lower panel.

139



140
141 **Fig. S7. Lack of similarity in hypoxia-related genes among the seven high-altitude vs.
142 low-altitude (HA – LA) comparisons, and similarity comparison of enriched
143 hypoxia-unrelated Gene Ontology (GO) terms between outlier windows and
144 randomly selected windows.** (A) Gene number shared by each pair of HA–LA
145 comparison. *Po. montanus* had few genes in common with any other species. (B) Genes
146 shared by the seven HA–LA comparisons. Comparisons except the pair that includes high
147 elevation population of *Po. montanus* have a convergent gene, the *PLB1*. (C) Venn
148 diagram showing no shared genes across the seven HA–LA comparisons. (D)
149 Hypergeometric test for overlap of GO terms enriched by genes unrelated to hypoxia,
150 showing significant lower overlap among outlier windows than among random windows.
151 Cell color indicates the log-transformed *P*-value generated by the hypergeometric test. (E)
152 Significantly lower semantic similarity in GO terms enriched by genes unrelated to
153 hypoxia among outlier windows than among random windows. Cell color indicates the
154 similarity degree. Phu = *Ps. humilis*; Psu = *Po. superciliosus*; Ldi = *Lo. dichrous*; Pru =
155 *Pe. rubidiventris*; Pat_H = *Pe. ater* (HA); Pma_H = *P. major* (HA); Pmo_H = *Po.*
156 *montanus* (HA).

157 **Table S1. Summary for samples of parid and outgroup species used in this study.**

Species	Common names	No. of samples	No. of SNPs	Heterozygosity ($H, \times 10^{-3}$)	Nucleotide diversity ($\pi, \times 10^{-3}$)
<i>Cyanistes cyanus</i>	Azure Tit	3	12,123,996	0.247	0.256
<i>Machlolophus holsti</i>	Yellow Tit	2	12,126,871	0.0732	0.0729
<i>Machlolophus spilonotus</i>	Yellow-cheeked Tit	5	13,848,362	1.040	1.095
<i>Pseudopodoces humilis</i>	Ground Tit	10	14,925,296	0.508	0.538
<i>Parus major</i>	Great Tit	6	4,079,932	1.613	1.770
<i>Parus monticolus</i>	Green-backed Tit	4	9,107,223	1.053	1.060
<i>Lophophanes dichrous</i>	Grey-crested Tit	9	19,085,141	0.713	0.989
<i>Periparus ater</i>	Coal Tit	8	18,351,291	1.155	1.389
<i>Periparus rubidiventris</i>	Rufous-vented Tit	10	19,702,307	1.270	1.303
<i>Periparus rufonuchalis</i>	Rufous-naped Tit	1	16,219,882	0.310	0.316
<i>Pardaliparus venustulus</i>	Yellow-bellied Tit	5	17,790,733	1.588	1.768
<i>Poecile davidi</i>	Rusty-breasted Tit	1	15,575,825	0.216	0.219
<i>Poecile montanus</i>	Willow Tit	6	17,423,939	0.597	0.926
<i>Poecile palustris</i>	Marsh Tit	6	17,975,211	0.733	0.822
<i>Poecile superciliosus</i>	White-browed Tit	1	14,765,034	0.379	0.381
<i>Sittiparus varius</i>	Varied Tit	5	16,063,208	0.670	0.681
<i>Melanochlora sultanea</i>	Sultan Tit	2	12,733,744	0.272	0.280
<i>Sylviparus modestus</i>	Yellow-browed Tit	2	12,839,195	0.663	0.697
<i>Cephalopyrus flammiceps</i>	Fire-capped Tit	1	7,848,698	0.355	0.360
<i>Remiz consobrinus</i>	Chinese Penduline Tit	2	10,521,662	0.362	0.377
<i>Remiz coronatus</i>	White-crowned Penduline Tit	2	10,180,575	0.216	0.230

158

159

160 **Table S2. Statistics for the assemblies and protein-coding genes from 24 species or**
 161 **populations.**

Taxa	Individuals	Depth	Genome size (Gb)	Contig N50; Scaffold N50	No. of scaffolds	CDS (number; mean length)
<i>Cy. cyanus_WH</i>	XJ10088	22×	0.993	3.18K; 32.22K	87,857	12,086; 1.51K
<i>Ma. holsti_EL</i>	T1969	22×	0.998	6.04K; 48.73K	74,836	12,709; 1.61K
<i>Ma. spilonotus_EL</i>	GX09261	26×	1.165	0.75K; 3.60K	366,458	9,298; 1.18K
<i>Ps. humilis_WH</i>	2	20×	0.995	2.79K; 37.58K	68,825	12,497; 1.56K
<i>P. major_EL</i>	BS09166	17×	1.09	0.85K; 6.67K	253,321	10,019; 1.15K
<i>P. major_WH</i>	E8	20×	1.07	1.08K; 7.26K	250,750	9,417; 1.09K
<i>P. monticolus_EL</i>	SNJ08251	25×	1.05	1.70K; 11.77K	188,240	9,877; 1.25K
<i>Lo. dichrous_WH</i>	1271	22×	1.07	1.48K; 12.70K	179,838	11,080; 1.37K
<i>Pe. ater_WH</i>	XZ14251	22×	1.16	0.79K; 4.40K	359,243	9,434; 1.19K
<i>Pe. ater_EL</i>	a15	30×	1.25	0.56K; 2.07K	507,845	11,769; 0.97K
<i>Pe. rubidiventris_WH</i>	XZ15155	20×	1.10	1.01K; 6.73K	280,605	9,521; 1.14K
<i>Pe. rufonuchalis_WH</i>	TJK13097	16×	0.947	1.13K; 5.39K	268,236	9,200; 0.92K
<i>Pa. venustulus_EL</i>	14BJ05	21×	1.22	0.37K; 1.26K	619,453	10,522; 0.79K
<i>Po. davidi_WH</i>	SC13013	18×	0.994	1.72K; 21.13K	109,349	11,560; 1.4K
<i>Po. montanus_WH</i>	1208	20×	1.00	2.86K; 32.5K	92,400	12,162; 1.53K
<i>Po. montanus_EL</i>	NM09302	23×	1.08	1.34K; 11.19K	211,990	10,632; 1.31K
<i>Po. palustris_EL</i>	HC09195	19×	1.03	1.74K; 14.21K	165,215	10,157; 1.33K
<i>Po. superciliosus_WH</i>	1402	14×	0.981	1.37K; 14.86K	127,575	11,256; 1.32K
<i>Si. varius_EL</i>	LZS003	23×	1.11	1.18K; 7.61K	261,732	10,542; 1.27K
<i>Me. sultanea_EL</i>	GZ001	22×	1.07	1.70K; 12.68K	147,173	11,194; 1.34K
<i>Sy. modestus_WH</i>	SC14083	17×	1.12	0.72K; 4.17K	343,569	11,241; 0.99K
<i>Ce. flammiceps_WH</i>	SC14321	13×	1.07	1.1K; 9.13K	221,907	10,632; 1.31K
<i>R. consobrinus</i>	PJ09016	15×	0.986	1.69K; 21.6K	108,306	11,278; 1.36K
<i>R. coronatus</i>	TJK14022	14×	1.10	2.69K; 26.2K	119,391	10,896; 1.46K

162

163

164 **Table S3. Comparisons between effective population sizes (Ne) at the end and the
165 beginning of the glaciations.**

Taxa	Individuals	Identifiers	LGP_End vs. LGP Beginning	LGP_End vs. LGM Beginning
<i>Pe. rufonuchalis_WH</i>	TJK13097	a	$\Delta Ne = -150315$, $W = 0, P < 2.2 \times 10^{-16}$	
<i>Ps. humilis_WH</i>	QZ01086	b	$\Delta Ne = -65261$, $W = 311010, P < 2.2 \times 10^{-16}$	
<i>Lo. dichrous_WH</i>	1271	c	$\Delta Ne = -177759.57232504$, $W = 481, P < 2.2 \times 10^{-16}$	
<i>Pe. rubidiventris_WH</i>	XZ16432	d	$\Delta Ne = -534753$, $W = 508, P < 2.2 \times 10^{-16}$	
<i>Sy. modestus_WH</i>	SC14082	e	$\Delta Ne = -552073$, $W = 150560, P < 2.2 \times 10^{-16}$	
<i>Ce. flammiceps_WH</i>	SC14321	f	$\Delta Ne = -1230416$, $W = 0, P < 2.2 \times 10^{-16}$	
<i>Cy. cyanus_WH</i>	XJ10088	g		$\Delta Ne = -36909$, $W = 567402, P < 2.2 \times 10^{-16}$
<i>Po. superciliosus_WH</i>	1402	h		$\Delta Ne = -16454$, $W = 235123, P < 2.2 \times 10^{-16}$
<i>Po. davidi_WH</i>	SC13013	i		$\Delta Ne = -174013$, $W = 56955, P < 2.2 \times 10^{-16}$
<i>Po. palustris_EL</i>	HC09195	j		$\Delta Ne = 399570$, $W = 493123, P < 2.2 \times 10^{-16}$
<i>Pa. venustulus_EL</i>	HBXT001	k	$\Delta Ne = 777359$, $W = 997610, P < 2.2 \times 10^{-16}$	
<i>Si. varius_EL</i>	LZS003	l	$\Delta Ne = 149119$, $W = 137350, P < 2.2 \times 10^{-16}$	$\Delta Ne = 431689$, $W = 31008, P < 2.2 \times 10^{-16}$
<i>P. monticolus_EL</i>	SNJ08251	m	$\Delta Ne = 2350448$, $W = 162825, P < 2.2 \times 10^{-16}$	
<i>Me. sultanea_EL</i>	GZ001	n		$\Delta Ne = 146957$, $W = 29281, P < 2.2 \times 10^{-16}$
<i>Ma. spilonotus_EL</i>	FJ412	o	$\Delta Ne = -323771$, $W = 0, P < 2.2 \times 10^{-16}$	
<i>Pe. ater_WH</i>	XZ16532	p	$\Delta Ne = 98419$, $W = 699640, P < 2.2 \times 10^{-16}$	
<i>P. major_WH</i>	1-E8	q	$\Delta Ne = -344137$, $W = 0, P < 2.2 \times 10^{-16}$	
<i>Po. montanus_WH</i>	1221	r	$\Delta Ne = 56162$, $W = 5870039, P < 2.2 \times 10^{-16}$	
<i>Pe. ater_EL</i>	a16	s	$\Delta Ne = 320091$, $W = 191910, P < 2.2 \times 10^{-16}$	
<i>P. major_EL</i>	B041	t	$\Delta Ne = 812728$, $W = 67000, P < 2.2 \times 10^{-16}$	
<i>Po. montanus_EL</i>	NM09110	u	$\Delta Ne = 906868$, $W = 590037, P < 2.2 \times 10^{-16}$	
<i>Ma. holsti_EL</i>	T1969	tw	$\Delta Ne = 32875$, $W = 10151000, P < 2.2 \times 10^{-16}$	

166 Note: W indicates the Wilcoxon rank sum, P indicates the significant value. LGP: Last

167 Glacial Period; LGM: Last Glacial Maximum.

168 **Table S4. Enrichment statistics for 17 Gene Ontogeny (GO) terms associated with**
 169 **the oxygen transport cascade and hypoxia response in all HA–LA comparisons.**

GO IDs	GO terms	Phu	Psu	Ldi	Pru	Pat_H	Pma_H	Pmo_H
GO:0007585	respiratory gaseous exchange	2.11E-02	1.00E+00	5.00E-01	5.51E-01	1.00E+00	7.82E-01	1.00E+00
GO:0060541	respiratory system development	1.06E-01	4.31E-02	2.93E-02	1.37E-01	5.51E-01	1.00E+00	4.40E-01
GO:0072359	circulatory system development	1.29E-12	1.32E-03	4.01E-05	1.02E-04	5.78E-02	2.47E-03	2.18E-10
GO:0003013	circulatory system process	6.93E-14	2.25E-02	1.04E-03	6.28E-02	7.92E-04	6.17E-03	8.44E-02
GO:0019825	oxygen binding	1.00E+00	1.00E+00	1.00E+00	1.00E+00	8.18E-01	1.00E+00	1.19E-01
GO:0015671	oxygen transport	1.00E+00	1.00E+00	1.00E+00	1.00E+00	1.00E+00	1.00E+00	3.23E-02
GO:0034101	erythrocyte homeostasis	3.56E-01	6.89E-02	7.48E-04	2.31E-01	6.72E-03	4.05E-01	2.40E-01
GO:0003012	muscle system process	1.34E-15	8.83E-01	3.09E-04	1.53E-03	3.26E-02	1.84E-03	8.44E-01
GO:0055001	muscle cell development	6.93E-07	4.03E-01	9.92E-02	1.00E+00	1.00E+00	1.00E+00	1.00E+00
GO:0043292	contractile fiber	1.11E-08	8.37E-01	1.73E-01	3.15E-02	2.85E-04	1.62E-04	1.00E+00
GO:0051646	mitochondrion localization	4.80E-01	4.97E-01	3.86E-01	5.50E-02	5.81E-01	9.70E-03	4.40E-01
GO:0070584	mitochondrion morphogenesis	1.00E+00	3.41E-01	1.00E+00	2.90E-01	4.14E-01	4.26E-02	1.00E+00
GO:0003032	detection of oxygen	1.00E+00	1.00E+00	1.04E-01	1.00E+00	1.00E+00	1.00E+00	1.00E+00
GO:0046034	ATP metabolic process	5.16E-02	6.89E-02	1.02E-02	4.83E-02	6.72E-01	8.03E-03	5.47E-01
GO:0006629	lipid metabolic process	4.75E-09	1.47E-02	1.24E-08	1.02E-06	4.95E-06	6.47E-05	1.69E-02
GO:0005975	carbohydrate metabolic process	1.98E-13	5.54E-05	2.84E-03	1.70E-06	7.07E-03	1.11E-09	1.37E-02
GO:0036293	response to decreased oxygen levels	8.03E-06	2.45E-02	9.90E-05	3.39E-03	1.70E-02	1.62E-02	2.46E-01

170

171 Note: The filled colors indicate the four physiological stages of the oxygen cascade
 172 showed in Fig. 4b. The bolded *P* values indicate significant enrichment. Phu = *Ps.*
 173 *humilis*; Psu = *Po. superciliosus*; Ldi = *Lo. dichrous*; Pru = *Pe. rubidiventris*; Pat_H = *Pe.*
 174 *ater* (HA); Pma_H = *P. major* (HA); Pmo_H = *Po. montanus* (HA). HA: high altitude;
 175 LA: low altitude.

176

177 **Table S5. Mutation rates for each species calculated by PAML.**

Species	dN/dS	dN	N*dN	S*dS	dS	Mutation rate ($\times 10^{-9}$)	Generation time (Years)
<i>Cy. cyanus</i>	0.2971	0.004	598.6	793.6	0.0149	2.213	2
<i>Ma. holsti</i>	0.2684	0.002	266.4	391	0.0073	2.346	2
<i>Ma. spilonotus</i>	0.3049	0.002	268.8	347.3	0.0065	2.089	2
<i>Ps. humilis</i>	0.3084	0.004	470.7	601.2	0.0113	1.996	2
<i>P. major</i>	0.3317	0.002	310.2	368.4	0.0069	2.096	2
<i>P. monticolus</i>	0.2955	0.002	272.2	362.8	0.0068	2.066	2
<i>Lo. dichrous</i>	0.336	0.004	571	669.5	0.0125	1.848	2
<i>Pe. ater</i>	0.2782	0.003	348.1	492.8	0.0092	2.489	2
<i>Pe. rubidiventris</i>	0.2437	0.001	183.4	296.4	0.0055	1.971	2
<i>Pe. rufonuchalis</i>	0.3399	0.002	282.7	327.6	0.0061	2.186	2
<i>Pa. venustulus</i>	0.3231	0.004	506.4	617.2	0.0116	2.285	2
<i>Po. davidi</i>	0.2876	0.002	296.7	406.3	0.0076	2.169	2
<i>Po. montanus</i>	0.3283	0.002	297	356.3	0.0067	2.038	2
<i>Po. palustris</i>	0.2747	0.002	277.7	398.1	0.0075	2.281	2
<i>Po. superciliosus</i>	0.305	0.003	382.6	494.1	0.0092	2.065	2
<i>Si. varius</i>	0.306	0.003	465.1	598.6	0.0112	1.975	2
<i>Me. sultanea</i>	0.3063	0.007	915.7	1177	0.022	1.723	2
<i>Sy. modestus</i>	0.2962	0.008	1029.6	1369	0.0256	1.736	2
<i>Ce. flammiceps</i>	0.3218	0.021	2801	3428	0.0642	2.586	2

178

179

180 **Legends for data files S1 to S3**

181 **Data file S1.** Detail information for sequenced samples, including sources and tissue
182 types of samples, ecological data, quality and coverage of sequencing, NCBI accessions
183 of sequencing data, as well as heterozygosity of each individual.

184

185 **Data file S2.** List of 973 Gene Ontogeny (GO) terms (i.e. 17 parental-level GO terms and
186 their child terms) associated with the oxygen transport cascade and hypoxia response.

187

188 **Data file S3.** List of hypoxia-related genes found in F_{ST} outlier windows for each high
189 altitude (HA) and low altitude (LA) parids comparison, and the corresponding statistics
190 for McDonald-Kreitman test, including number of D_n , D_s , P_n , P_s sites and the significance
191 value of Fisher's exact test.

192

193